ABSTRACT

SUH, MINYOUNG. Static Generation and Dissipation on Textiles. (Under the direction of Dr. Abdel-Fattah M. Seyam and Dr. William Oxenham.)

Static charge has been a major source of problem in textile industry as well as consumers. During textile manufacturing process, there is a potential of static charge generation when fibers are extruded, and yarns are woven or knitted, and finished. This gives spinners and weavers much trouble in terms of productivity, and can lead malfunction of electronic equipments. Static problems in textile industry have become more serious as synthetic fibers and higher processing speeds are met. More or less, natural fibers are not as susceptible to static problems as synthetics. Synthetics such as nylon or polyester are so hydrophobic that they are easy to accumulate electrostatic charges.

This research was undertaken to gain better understanding of static generation and dissipation on continuous yarn surface in terms of environmental conditions (temperature and relative humidity), yarn tension, yarn speed, and fiber type. Four experiments were conducted: (1) effect of environmental conditions, yarn tension, and yarn speed on static generation/dissipation of continuous filament polyester yarn, (2) effect of charging pin material (stainless steel, nylon, polyester, polypropylene, and Teflon) on static generation/dissipation of continuous filament polyester yarn, (3) effect of fiber type (polyester, nylon, and polypropylene) on static generation/dissipation of finish free continuous filament yarns, and (4) effect of humidity, yarn tension, and yarn speed on yarns of different fiber types with different filament count. The assessment of static generation/dissipation was done by using a device equipped with winder, two potential probes, charge pin, tension and speed controllers, and data acquisition system. The device was housed in an environmental room where relative humidity and temperature can be

precisely controlled. Potentials collected by the two probes at two different positions on a running yarn in real time were used to calculate initial potential (at the point of separation of yarn and charge pin) and characteristic decay time. The independent parameters of the experimental designs were broad to include the conditions practiced by the textile industry.

The results of the first experiment indicated that temperature, humidity, yarn tension and speed had significant effects on static generation, while only temperature and yarn speed showed statistically significant effects on static dissipation. More charge was created with lower temperature and humidity, and higher yarn tension and speed. At a temperature of 35° the charge on the polyester yarn increased as the yarn moved from first probe to the second probe while at lower temperatures the charge was dissipated. It was also found that high yarn speed promoted the charge dissipation (shorter decay time).

The results of the second experiment showed that different charging materials affected static generation, but not static dissipation. The charge materials showed the following polarity categorized into three groups; stainless steel (gave negative charge on the polyester yarn), nylon (gave positive charge on the polyester yarn), and polyester (gave positive charge on the polyester yarn). The polypropylene and Teflon charge materials exhibited almost no polarity (charge on the yarn is almost zero). Charge polarity generated on the polyester sample yarn did not coincide with tribo-electric series due to the presence of spin finish.

The results of the third experiments, however, showed that finish-free yarn materials followed tribo-electric series. The stainless steel charge pin caused the polyester and polypropylene to be charged negatively, whereas nylon was positively charged. Finish-free yarns had potential as high as 8,000 volts. Polypropylene yarns showed relatively smaller

static charges than polyester and nylon yarns, and nylon yarns were characterized by the slowest charge decay.

The results of the last experiment exhibited that humidity, yarn tension and speed showed significant effect on static generation of multifilament yarns, while none of them were significant in case of monofilament yarns. For the multifilament yarns, more charge was generated with lower humidity, and higher yarn tension and speed. Static dissipation was influenced only by yarn speed for both multifilament and monofilament yarns. The effect of yarn speed on decay time for multifilament and monofilament yarns was the same in terms of trend, where high yarn speed promoted the charge dissipation (shorter decay time).

STATIC GENERATION AND DISSIPATION ON TEXTILES

by Minyoung Suh

A thesis submitted to the Graduate Faculty of
North Carolina State University
In partial fulfillment of the
Requirements for the Degree of
Master of Science

TEXTILES

RALEIGH

2008

Approved by:

Dr. Abdel-Fattah M. Seyam Chair of Advisory Committee	Dr. William Oxenham Co-chair of Advisory Committee
Dr. Jeff Thompson Minor Representative of Advisory Committee	Dr. Tom Theyson Member of Advisory Committee

DEDICATION

Dedicated to

My beloved great grand mother

Just a year before her hundredth birthday

BIOGRAPHY

Minyoung Suh was born on September 16th, 1980 in Seoul, South Korea. She received two Bachelor of Science degrees in Clothing & Textiles and Human Environment & Design on February, 2003 from Yonsei University. She worked for Inthef Company (an apparel producer), as a textile designer. She joined North Carolina State University, NC to start her master program in Textile Technology and Management in August, 2006. She expects to graduate in May, 2008.

ACKNOWLEDGEMENTS

The author wishes to thank her advisors, Dr. Abdel-Fattah M. Seyam and Dr. William Oxenham, for the opportunity to work with them and the guidance throughout the research. Appreciation is extended to the members of advisory committee, Dr. Tom Theyson who provides the yarns and Dr. Jeff Thompson who helped in statistical procedures. Gratitude is due to National Textile Center for providing financial support during graduate program.

Thanks to Dr. Yiyun Cai for training on using the static generation/dissipation equipment and mentoring. Appreciation is extended to Lu Liu and Brad James for their valuable discussion and sharing their research findings.

The author would like to extend her thanks to the technical staff Mr. Timothy Mumford, Mr. Dzung Nguyen, Mr. Hai Bui, and Ms. Birgit Andersen for providing help with sample preparation, machining of parts, analytical measurements, and troubleshooting of electrical and mechanical problems.

Thanks also to lovely friends, Kyunghye Jung and Sangwon Chung for entertaining the life in Raleigh with fun, and to many friends in Korea, Jihyun Kim, Song Kim, Soyeon Kim, Eunae Cho, Eunsan Shin, and Jungeun Shin, for being a big source of comfort.

Finally, the author wishes to express sincere appreciation and love to her parents, Sangsuhp Suh and Sunock Lee, for their constant support and encouragement during the entire study. Gratitude extends to her sister and brothers, Minhee, Junyong, and brand new brother-in-law Hyungsoo Kim. As the emotional prop throughout the life, her great grand mother, Sungnyeo Kim, deserves the most and best appreciation.

TABLE OF CONTENTS

LIST OF TABLES

LIST OF FIGURES

TERMS RELATED TO STATIC ELECTRICITY

This section provides definitions of parameters used in the field of static generation. When applicable, the symbol commonly used to abbreviate a parameter is given along with units.

Capacitance (Farad): the amount of electric charge stored for a given electric potential, (Symbol: C) [13]

Charge (Coulomb, C): a fundamental property of subatomic particles, determining electromagnetic interaction and producing electromagnetic fields (symbol: Q) [32]

Charge Density: the amount of electric charge in a line (C/m), surface (C/m^2), or volume (C/m^3)

Conductivity (Siemens/meter, S/m): the inverse of resistivity, a measure of electron mobility to flow through the object (symbol: σ)

Conductor: a material within which an electric current is produced by application of voltage between points on or within the material

Corona Discharge: a type of discharge occurring when the potential gradient exceeds a certain value, but conditions are not sufficient to cause complete electrical breakdown [32]

Current (Ampere or **Coulomb/sec**, **A** or **C/s)**: the flow of electric charge (symbol: I) [32]

Decay Time (second): the time required to decay to a fraction of the initial quantity

Half Decay Time: the time required to get half original quantity **[**35]

Characteristic Decay Time: the time required to get 1/e times of original quantity [13]

Direct Charging: by the contrast with triboelectric charging, the formation of electrostatic charges by means of a voltage generator and electrodes or corona charging.

Faraday Cage: an enclosure to block out external electric field causing electrical charges [32]

Electric Field (Volts/meter, V/m): the space established around an electric charge or in time-varying magnetic filed, exerting a force on other electrically charged objects (symbol: E) [32]

Electrification: the action or process of making a thing get charged with electricity [8]

Electrostatic Discharge (ESD): a sudden and momentary electric current that flows from or to the surroundings at different electrical potentials for neutralization

Insulator: a material in which a voltage applied between two points on or within the material produces a small or negligible current

Potential (Volts or **Joule/Coulomb, V** or **J/C)**: potential difference, the change in potential energy per unit charge associated with electric field (symbol: V) [32]

Resistance: the physical property of a material which is a measure of the ability of electrons to flow through it when a voltage is applied across two points on the material, function of physical geometry and resistivity (symbol: R) [5]

Surface Resistance (Ω): the ratio of a potential difference to the current flowing on the surface of the specimen [**7**]

Volume Resistance (Ω): the ratio of a potential difference to the current flowing through the specimen [**7**]

Resistivity: material property equal to the ratio of the voltage gradient to the current density, the degree to which a material opposes the flow of current (symbol: ρ) [4]

Surface Resistivity (Ω): the surface resistance multiplied by the ratio of electrode width

(the current path) to the distance between electrodes [4, **7**]

Volume Resistivity (Ω·m): the volume resistance multiplied by the ratio specimen cross-sectional area to distance between electrodes [4, **7**]

Triboelectric Charging: the formation of electrostatic charges, with or without rubbing, by the separation of contacting materials [18]

Work Function: the minimum energy needed to remove an electron from a solid surface to an outside point [12]

I. INTRODUCTION

Static generation of textiles can be explained as tribo-electricity which is caused by contact or rubbing operation between two surfaces. The tribo-electricity had been initially observed by a Greek philosopher, Thales, around B.C. 600 [34]. After rubbing amber with hemp clothes, he found the force on the amber attracting such things like bird feathers. Then, by late 16th century, an English physicist, William Gilbert, had distinguished the electricity and magnetism from this [9]. The term 'electricity' was originated from a Greek word referring amber.

Materials can be divided into two types in terms of flow of electric current, conductors and insulators. When two surfaces come into contact, they exchange electrons and get electrically charged. Due to their low surface resistance, conductive materials have high probability of charge exchange, while insulative materials tend to keep electrons because they possess high surface resistance. Metal and ceramic are good examples of conductor and insulator, respectively. Textile materials are usually defined as semi-conductors. They can transfer the electricity like conductors and also can hold electricity like insulators.

Low energy surfaces such as polymeric materials are characterized by their nature to collect electrostatic charge when rubbed against themselves, other polymeric surfaces, or metals [38]. Static shock occurs when relatively large charge built up on a person or low surface energy material due to charge tendency to pass over for neutralization. Static charge generated by friction may impair the properties of textile products, for example, it may cling to the body resulting in discomfort and attract dust from the air resulting in spoiling the

appearance of garments. Static shock, as a result of discharge, is commonly experienced especially in dry winter when walking on a carpet, touching a door knob, and putting on or taking off clothes. Static can be a matter of life and death when a parachute fails to open because of static problems or spark generation at a gas station that may cause fire [44].

Static has been a major source of problem in textile industry as well as consumers. During textile manufacturing process, there is a potential of static charge generation when fibers are extruded, and yarns are woven or knitted, and finished. Fibers, yarns, or fabrics are rubbed with guides, rollers or tension devices on the machinery and this operation of contact and separation continuously occur throughout the process. This gives many spinners and weavers much trouble in terms of productivity, and can lead malfunction of electronic equipments. Static problems in textile industry have become more serious as synthetic fibers and higher processing speeds are met. More or less, natural fibers are not as susceptible to static problems as synthetics. Synthetics such as nylon or polyester are so hydrophobic that they are easy to accumulate electrostatic charges.

Researchers studied static electricity for useful applications as well as for the prevention. Static charge has positive attributes in dust collectors, copiers, or laser printers. Copiers make use of static generated on projected images to copy them by attracting carbon powder. Additionally, static charge is used in fabric formation (flocking and fiberweb formation [11, 41]) as well as electrets filters.

By nature, material itself has own ranking of polarity which is relative tendency to gain or lose electrons. When materials get into contact, they exchange electrons according to the relative ranking of receiving and releasing electrons. According to Hersh and

Montgomery [29], wool is on the top of tribo-electric series in terms of ease of releasing electrons. The rank of textile materials in terms of releasing electrons (in descending order) is nylon, viscose rayon, cotton, silk, acetate, polyester, acrylic, polyethylene, and Teflon (nylon being the easiest among the list to release electrons). A study by Henniker [27] showed different tribo-charge series than shown by Hersh and Montgomery with the following order: nylon, wool, silk, cotton, polyethylene, and Teflon. Another study [1] indicated different order from Hersh and Montgomery with the order: nylon, wool, silk, cotton, polyester, acrylic, polyethylene, and Teflon. While Diaz and Felix-Navarro work revealed the order: nylon, wool, silk, cotton, acetate, polyester, acrylic, polyethylene, and Teflon.

Despite of accumulated research in this area, there is hardly any explanation in regards to the mechanism of static generation and dissipation agreed universally due to low reproducibility of tribo-electrification [8, 9, 12, 18]. Contradicting results in regards to the effect of material resistivity on static charge dissipation judged by decay time were published [14, 15, 28, 35]. According to Chubb [14, 15], it was asserted that electrical resistivity had no relation with charge decay property, whereas in Henry et al. [28] and Jonasssen **[**35] work, it was shown that there is proportionality between resistivity and charge decay time. Diaz and Felix-Navarro [18] pointed out that the contradiction may be explained by the complexity of measurement and the numerous parameters affecting the static generation/dissipation such as chemical composition, surface characteristics, nature of contact, experimental conditions, etc. Besides, charge transfer mechanism of insulators is still debatable.

This research was undertaken to gain better understanding of static generation and dissipation on continuous filament yarn surface in terms of environmental conditions

(temperature and relative humidity), yarn tension, yarn speed, fiber type, and filament count (monofilament and multifilament).

II. LITERATURE REVIEW

2.1. Electrostatic Standard

Compared to the increasing interest of scholars in researching the static charge generation/dissipation of materials, there are few standard methods addressing the measurement of such parameters. There are four major organizations publishing electrostatic standards; American Society of Testing and Materials (ASTM), Electrostatic Discharge (ESD) Association, American Association of Textile Chemists and Colorists (AATCC), and International Standard Organization (ISO). These organizations developed test methods to assess resistivity, and static charge generation and accumulation. In addition to the four organizations mentioned above, the Federal Test Method (FTM) developed a standard test concerning charge dissipation. Devices to charge and procedure to generate static charge using such devices are provided as standard to increase measurement accuracy and reproducibility.

2.1.1. Resistance/Resistivity

Test methods were developed to measure resistance and resistivity of yarns and films/fabrics. Electrical resistance can be calculated from measurement of current and voltage under known electrode dimensions. Resistance is determined by the properties of material and the dimensions of a specimen. Surface resistance is the ratio of a potential difference to the current flowing on the surface of the specimen, and volume resistance is the ratio of a potential difference to the current flowing through the specimen. Volume resistance is in inverse proportion to the specimen cross section area and proportional to the yarn length.

Resistivity for yarns (better known as volume resistivity) is defined as the resistance per unit yarn length (Equation 2.1). For films or fabrics, resistivity (better known as surface resistivity) is defined as the resistance per unit fabric area (Equation 2.2).

$$R_v = \rho_v \times \frac{D}{S} \quad \text{.... (2.1)} \qquad\qquad R_s = \rho_s \times \frac{D}{W} \quad \text{.... (2.2)}$$

where,

R_v = Volume Resistance (Ω)

R_s = Surface Resistance (Ω)

ρ_v = Volume Resistivity (Ω·m)

ρ_s = Surface Resistivity (Ω)

S = Cross-sectional Area of Specimen (m^2)

D = Distance between Electrodes (m)

W = Width of Specimen (m)

ASTM first set the standard for measuring resistance in 1999 (ASTM D257-99) [7]. The method is used to assess the resistivity of high resistance insulating and polymeric materials. The method describes an apparatus that consists of electrode system, power supply, guard circuit, and current-measuring devices used for measuring resistance. The method requires direct voltage application to the sample. The voltage level is 500 ± 5 volts and the electrification time is 60 seconds. For the electrodes, ASTM suggested 11 different systems according to types of materials, which are (1) Binding-Post and Taper-Pin Electrodes, (2) Metal bars, (3) Silver Paint, (4) Sprayed Metal, (5) Evaporated Metal, (6) Metal Foil, (7) Colloidal Graphite, (8) Mercury or Other Liquid Metal Electrodes, (9) Flat Metal Plate, (10)

Conducting Rubber, and (11) Water. The equations for the volume and surface resistivity/conductivity calculation and applications of the electrode systems for selected relevant materials are depicted in Table 2.1 and Table 2.2.

Table 2.1. Equations for the volume and surface resistivity / conductivity (ASTM) [**7**]

Electrode or Specimen types	Resistivity		Conductivity	
	Volume	Surface	Volume	Surface
Circular Electrodes	$\rho_v = \frac{A}{t} \times R_v$	$\rho_s = \frac{P}{g} \times R_s$	$\sigma_v = \frac{t}{A} \times G_v$	$\sigma_s = \frac{g}{P} \times G_s$
Square Electrodes	$\rho_v = \frac{2\pi L R_v}{\ln \frac{D_2}{D_1}}$	$\rho_s = \frac{P}{g} \times R_s$	$\sigma_v = \frac{\ln \frac{D_2}{D_1}}{2\pi L R_v}$	$\sigma_s = \frac{g}{P} \times G_s$

where, ρ_v = volume resistivity (Ω·cm)

σ_v = volume conductivity (Siemens/cm)

ρ_s = surface resistivity (Ω/cm^2)

σ_s = surface conductivity (Siemens/cm^2)

A = the effective area of the measuring electrode (cm^2)

P = the effective perimeter of the guarded electrode (cm)

R_v = measured volume resistance (Ω)

G_v = measured volume conductance (Siemens)

R_s = measured surface resistance (Ω)

G_s=measured surface conductance (Siemens)

t = average thickness of the specimen (cm)

D_1, D_2, = electrode diameter (cm)

g = distance between electrode$_1$ and electrode$_2$ (cm)

L = electrode length (cm)

Table 2.2. Electrode systems (ASTM) [7]

Electrode system	Applications
Binding-Post and Taper-Pin Electrodes	Rigid insulating materials
Metal Bars	Flexible, thin and solid materials
Sprayed Metal	When adhesion to the materials is needed
Evaporated Metal	When adhesion to materials is needed
Metal Foil	When the electrodes are needed on surface
Colloidal Graphite	Nonporous, sheet insulating materials
Liquid Metal Electrodes	Flat and solid specimens
Flat Metal Plate	Flexible and compressible materials
Conducting Rubber	When quick and easy application is needed

ESD Association suggested an apparatus for measuring surface resistance (ANSI/ESD STM 11.11) [19] and volume resistance (ANSI/ESD STM 11.12) [20] dedicated for planar materials that could be applied films and fabrics. ESD apparatus consists of electrode assembly, specimen support surface, instrumentation for charge measurement, and fixture for verification.

Electrode assembly has two concentric rings to establish contact with the material under test (Figure 2.1). The inner electrode is a solid disk whose diameter is 30.48 ± 0.64 mm. The outer electrode is a ring having 57.15 ± 0.64 mm inner diameter, and 3.18 ± 0.254

mm ring thickness. Additionally, for the volume resistance measurement, a bottom electrode is needed, which is a flat conductive metal plate. Two concentric rings are used as a top electrode, and a metal plate is used as a bottom electrode. The contact surface material of electrode assembly is a conductive material with hardness between 50 and 70 on the Shore-A Durometer scale and volume resistivity less than 10 ohm·cm. The expected total weight of electrode assembly is given to be 2.27 kg ± 56.79 g. Instrumentation includes an ammeter and power supply (10 ~ 100 volts). Verification fixture attaches to the electrode assembly in order to check whether the system works as it should. Different kinds of resistor are suggested for materials with low resistance and high resistance. With the verification fixture, the apparatus indicates about 5.0×10^{5} ohms for low resistant fixture and 1.0×10^{12} ohms for high resistant fixture.

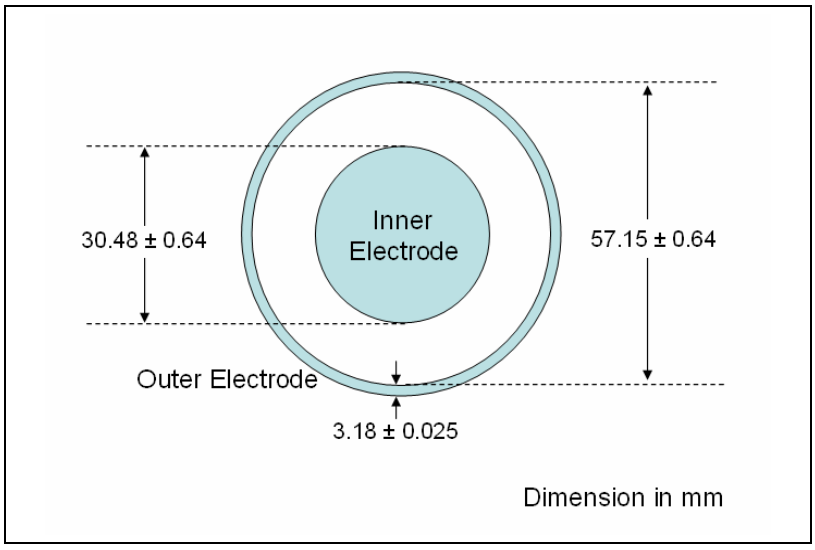

Figure 2.1. ESD Electrode [19, 20]

For both surface resistance [19] and volume resistance [20], 6 samples of test specimen with size of at least 76 mm × 127 mm should be prepared and conditioned for

minimum 48 hours but no greater than 72 hours in 23 ± 3°C and 12 ± 3% R.H. Resistance can be obtained after 10 volt power is supplied for the resistance below 1.0×10^6 ohms, and 100 volt power for measurement of higher resistance. An average, minimum and maximum values of resistance from 6 samples needed to be reported as a result with the conditioning period, relative humidity and temperature. For the volume resistance, the thickness of the samples is required additionally.

AATCC describes a test method for resistivity of fabrics (AATCC Test Method 76) [4], and yarns (AATCC Test Method 84) [5]. The methods assess surface resistivity for fabric materials and volume resistivity for yarn materials. The standards for fabrics [4] require using an electrical resistance meter between two parallel plate electrodes or concentric ring electrodes for measuring electrical resistivity of fabrics. For the parallel plate electrode, two sets of test are needed for resistivity in length direction and width direction. For concentric ring electrode, one set is enough because both length and width directions can be achieved simultaneously. The test specimen is placed in contact with the electrodes after conditioning in a chamber. Electrodes are located 25 mm away from each other. Current passed through the specimen is measured after supplying 80~100 volts of power to the electrode.

Resistivity of specimens is calculated from Equation 2.3 for parallel plate electrode and Equation 2.4 for concentric ring electrode. The result should be reported in forms of the logarithm of the resistance (log R) with the number of specimens tested, environment conditions, and the direction of testing (in case of using parallel plate electrodes).

$$\rho = \frac{R \times W}{D} \quad \text{....} \ (2.3)$$

$$\rho = \frac{2.73 \times R}{\log \frac{r_o}{r_i}} \quad \text{....} \ (2.4)$$

where, ρ = surface resistivity (Ω)

R = measured resistance (Ω)

W = width of specimen (m)

D = distance between electrodes (m)

r_o = outer electrodes radius (mm)

r_i = inner electrodes radius (mm)

AATCC developed a similar standard for electrical resistance of yarn (AATCC Test Method 84) [5]. The main principle is same to the fabrics [4]. The test yarn is placed between the parallel plate electrodes whose distance is not specified indication of user is allowed lengths as desired. Concentric ring electrode system is not applicable for testing yarns. The length of the yarn depends on the distance between electrodes. The specimen can be made of single strand or multiple strands. Every strand should be under same tension, and evenly spaced without overlap. Electrodes are located 10 mm away from each other. 30~40 volts of power is applied to the yarn and the current passed through the yarn is measured.

Equation 2.5 describes the yarn resistance calculation. Because resistance can be affected by the length of test yarns, 10 mm length was set for calculating resistance. The result should be reported in forms of the logarithm of the resistance (log R) with environmental conditions.

$$R = \frac{S}{D} \times \frac{r_1 + r_2 + r_3 + \cdots + r_n}{n} \times 10 \qquad \ldots. (2.5)$$

where, R = resistance per mm per strand of yarn (Ω)

S = number of strands per specimen

D = distance between electrodes (mm)

r = resistance of individual specimens containing S strands per specimen (Ω)

n = total number of specimens tested

Ambient condition can vary with purposes, but 24°C temperature and 65% relative humidity were given as a standard. In addition, AATCC recommended humidity in a testing chamber as 20% R.H. for the materials having critical electrostatic propensity and as 40% R.H. for the materials having less critical propensity.

2.1.2. Tribo-electrification

Standardization of electrification is a must because reliability and reproducibility of electrostatic experiments have been great impediments obstructing the development of universal theories. Driven by this fact, several ASTM and ESD standard methods to electrify materials and determine static charge were developed.

ASTM standard for electrification (ASTM D4470-97) [8] contains common criteria that should be considered in a general static electrification. It is describing the method of generating tribo-electric charge, and measuring the charge and associated electric field strength.

ASTM D4470-97 [8] introduced electrification methods for powder, liquids, web and sheet. In order to get charged, powder or liquids can pass through the tube so that the friction between the specimen and the wall inside of the tube create the charge on the specimen. For webs, contact against a charging roller surface is used to generating electricity. Sheet materials can be electrified by sliding down chutes, by vacuum platens, or by pinch rollers. Pinch rollers and sliding down chutes are considered to generate the largest amount of charge.

The method of measuring charge and electric field was also introduced. Measuring charges can be achieved by putting the electrified specimen in Faraday Cage connected to an electrometer. Faraday Cage is a device excluding the effect from external electric fields. For the measurement of electric field strength, which is the magnitude of the vector force on a point charge, Rotating Vane Field Meter and Vibrating Plate Field Meter were developed. The meters are shown schematically in Figure 2.2.

In addition, five test parameters that should be under control are given; (1) cleanliness of material surfaces, (2) contact area, (3) contact time, (4) rapidity of separation, and (5) external electric fields. Cleaning the material surfaces with solvents is not making the surfaces clean, but it creates evenly contaminated surfaces. Real area of contact can be controlled by keeping pressure, roughness of surfaces, and slip between surfaces constant. Time of contact and rapidity of separation can control additional charge flow into the bulk of the specimen or back to the origin. Elimination of electric fields in the vicinity can be achieved by removing all insulators from the test area or by shielding the area. Reporting test results should include average and standard deviation of charge amount/electric field strength, the conditioning and cleaning procedure, pressure between contacting surfaces, time of

contact, rapidity of separation, amount of rubbing, specimen identification, equipment description, and ambient conditions.

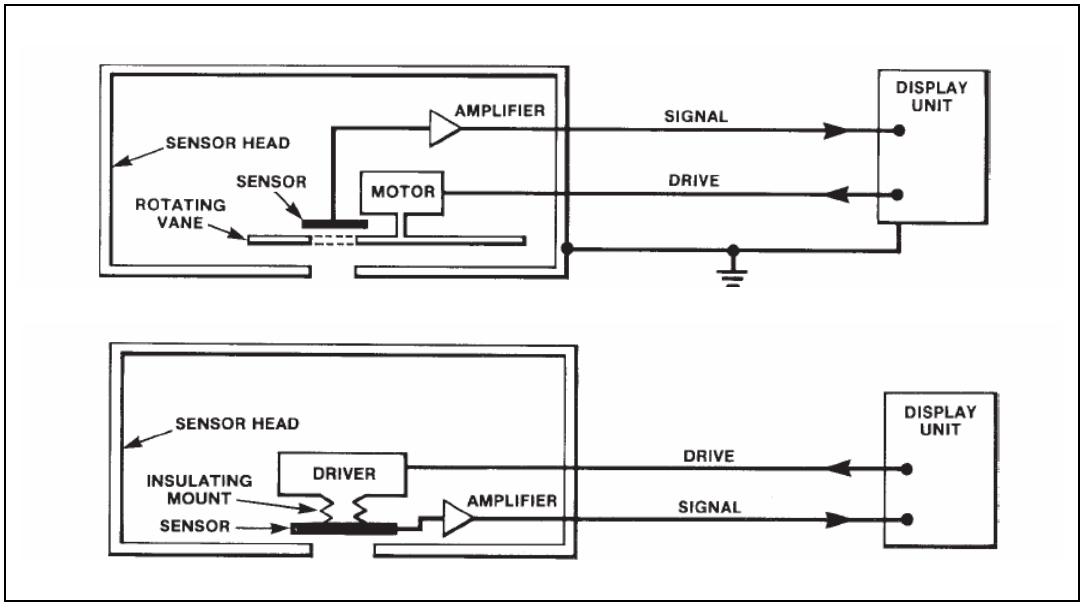

Figure 2.2. Rotating Vane (top) and Vibrating Sensor Field Meter (bottom) [8]

ESD association has a method for testing tribo-electric charge accumulation (ESD ADV 11.2) [21]. The methods for tribo-electrification are (1) Magazines, (2) Inclined Plane Method for Large Cylinders, (3) Inclined Plane Method for Small Cylinders, (4) Charging due to Transport or Handling in Packing Materials, (5) Hand Held Charging Test, (6) Card Pull Test, (7) Rolling Friction Tester, and (8) Adhesive Tape Pull Test. Among them, Hand Held Charging Test and Card Pull Test are for field application having manual operations, and the others are for laboratory use. Charging due to Transport or Handling in Packing Materials, Hand Held Charging Test and Card Pull Test are especially designed for packing process in the industries.

ESD association also pointed out the factors reducing repeatability in tribo-charging

tests. Theoretical factors of tribo-electrification are (1) surface contact effects, (2) material work function, (3) charge backflow, and (4) gaseous breakdown. Surface contact effects are the issues related to the changes of real contact area, pressure, and surface temperature by repetitive contact. Work function is defined as the minimum energy required removing an electron from a solid surface to an outside point. It is the subject of change with charge transfer. Charge backflow is the phenomenon that charges move back to the origin during separation. Gaseous breakdown refers to charge flow to the atmosphere after the separation. In order to overcome these factors, ESD association recommended to conduct tests in as many methods as possible, to have comparison values, to make as simple and consistent rubbing movements as possible, to treat independent testing groups, to use averages and distributions from repeated tests, and to control as many variables as possible.

2.1.3. Electrostatic Test Method for Textiles

A new approach developed by AATCC [6] and ISO [33] is applicable for an electrostatic experiment for textile products. They established similar standards, focused on the simulation of the charge accumulation on carpets. The static propensity of textiles on which a person walks is observed through laboratory simulation.

According to AATCC Test Method 134 [6], ambient condition is set as 21 ± 1°C in temperature and 20 ± 2 % in relative humidity. Test room should be big enough so that the operator comes no closer than 60 cm to extraneous objects such as walls or equipments. Two pairs of standard sandal with the soles of Neolite and suede leather are prepared. Neolite is most common shoe soles and suede leather is the material tending to give high values on the

carpet. Carpet specimens (70 cm × 90 cm) is put over the underlay of a cushion made of jute and hair (120 cm × 120 cm) which is laid on the grounded metal plate (120 cm × 120 cm).

The operator wearing the sandal mounts on the specimen avoiding any friction and contact with the test probe. Test is running with stepping and scuffing motions. Stepping is walking on the specimen with lifting sandals as close as possible to 8 cm above the specimen at the rate of 120 ± 10 steps per minute, while scuffing is wiping the specimen forward and backward with lifting the sandals as close as possible to 7 cm above the specimen at the rate of 60 ± 5 steps per minute. Analysis of test results is performed in terms of peak voltages, and they should be reported with averages.

Table 2.3. Standard Test Method Compared

	AATCC Standard [6]	ISO Standard [33]
Temperature	21 ± 1°C	23 ± 1°C
Humidity	20 ± 2 %	20 ± 1% or 25 ± 1%
Specimen Size	70 cm × 90 cm	200 cm × 100 cm
Underlay	Jute / Hair Cushion	Rubber Mat
Sandal Soles	Neolite / Suede leather	Neolite
Walking Manner	Stepping and Scuffing	Stepping
Walking Speed	120 ± 10 steps/min	120 steps/min
Sandal Lifting During Walk	8 cm	5 ~ 8 cm
Measurement	Potential in voltage	Potential in voltage

A standard of International Standard Organization (ISO) [33] is substantially identical to AATCC standard with negligible differences. They are compared in Table 2.3. The

principle is assessing the difference in electrical potential produced by a person walking on the textile floor in a prescribed manner with standardized footwear. Specimen size was specified to be 2,000 mm × 1,000 mm, and atmospheric condition was defined to be 23 ± 1°C and 20 ± 1% R.H. or 25 ± 1% R.H. Major apparatus consists of earthed metal base plate (2,000 mm × 1,000 mm), rubber mat (2,200 mm × 1,200 mm, thickness 4.5 ± 0.5 mm), sandals, and body voltage measuring system. Sandals should be cleaned using designated cotton fabric, ethanol, and sandpaper. Two standard reference carpets are given for setting the measuring system.

Prescribed walking manner is defined to walk on the specimen at the rate of 2 steps per second forward and backwards, but avoiding scuffing or pivoting. Stepping action continues for about 60 seconds with sandal lifting between 50 and 80 mm. After three sets of walks for each specimen, the individual body voltages for each walk, average of those voltages, and deviations are required to be reported.

2.1.4. Static Decay Measurement

Federal Test Standard (FTS) 101C Method 4046 [23] measures static decay property of materials in forms of film or sheet. The material must be homogeneous and free from defects such as holes, cracks, and tears. This method assesses the ability of material to dissipate a charge induced on the surface when grounded.

Test environment is defined as 73 ± 3.5 °F and 15% R.H. The test is performed on a sample specimen (5 inch × 3 inch) mounted between electrodes connected to a fieldmeter. The electrodes consist of outer electrode made of Teflon and inner electrode made of Teflon

and brass. Detailed description of the electrode system is not given. A voltage of 5000V is applied to the electrodes from a high voltage source until the fieldmeter observes no more increase in voltage, which means the specimen has received its maximum charge. After stopping supplying voltage, the specimen is earthed so that static charge can decay. The time from the point where the specimen is grounded to the point of complete dissipation of charge is recorded as a decay time. Three times of repetition is suggested.

2.2. Electrostatic Measurement Technique

2.2.1. Measurement Method

There have been three classes of method measuring electrostatic propensity of textile materials; (1) direct measurement, (2) indirect measurement, and (3) use of simulation [32]. The first class is measuring electrical property such as electrical field (E), potential (V), charge amount (Q), or electrostatic discharge rate after developing charges on the material by standard treatments. These properties can be replaced by other indicators like electrical resistance (R) or conductance for indirect measurement. Simulation method is observing the behavior of textiles in a situation simulating the end-use for which they are intended.

Electrostatic field meter and electrostatic voltmeter can be used for the measurement of electric field and potential on the surface of textile material, respectively. They can be converted to charge density, charges per unit area, which represents the probability of an electrical discharge. A field meter should be the only earthed object near the specimen, while a voltmeter requires the contact of specimen as a dominant earth. Due to additional charge generation, noncontact measurement system is preferred [32].

Resistance is the property of a substance indicating how it resists the flow of an electric current through it. Conductance is the reciprocal of resistance, and it refers the property how the material allows current to flow through it when a potential difference is applied. There has been a debate in previous research regarding the correct use of these indirect indicators for textile application [14, 15, 28, 35]. They were still generally believed to represent electrostatic properties [32].

Simulation tests have an approach focusing more on the end-use problems than electrostatic properties. The most common forms are cling test and walking test. The former observes cling behavior of textiles as an indicator of static property, and the latter is observing static charges caused by walking action mainly on carpets.

2.2.2. Tester Development

As research on electrostatic properties in textiles made steady progress, developing devices for electrostatic experiments became the focus of investigation. The limitations of resistivity stimulated researchers to develop their own devices for charging and assessing electrostatic. Resistivity, which had been accepted as an index of electric properties, was claimed not to be appropriate for textiles because: (1) resistivity does not have any information about the capacitance of the material, (2) textile material does not obey Ohm's Law, affected by residual voltages, (3) textile material is not homogeneous, especially for composite materials, and (4) charge transfer is affected by adjacent earthed surfaces [13, 15].

Several electrostatic devices dedicated for charging and assessing static on textiles materials have been developed. These include National Aeronautics and Space

Administration (NASA) Tribo-electric Tester [25], Shirley Method [48], John Chubb Instrumentation (JCI) Tribo-charging Tester [15], Linear Tester [40], and Rubbing Tester [40]. With different means of generating and dissipating charges on test specimens, the devices are measuring electric properties under controlled parameters which have influence on static characteristics of textiles.

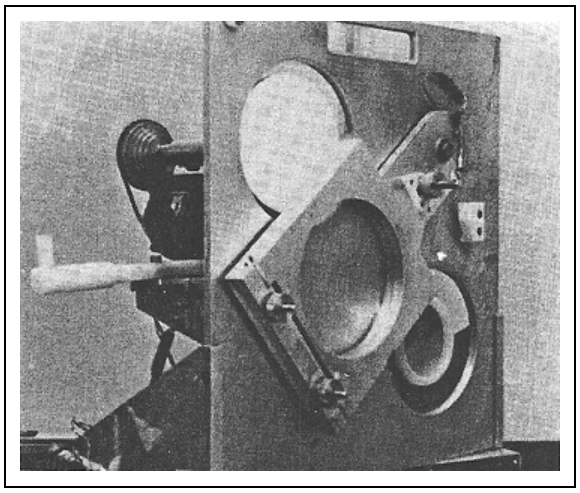

Figure 2.3. NASA Tester [25]

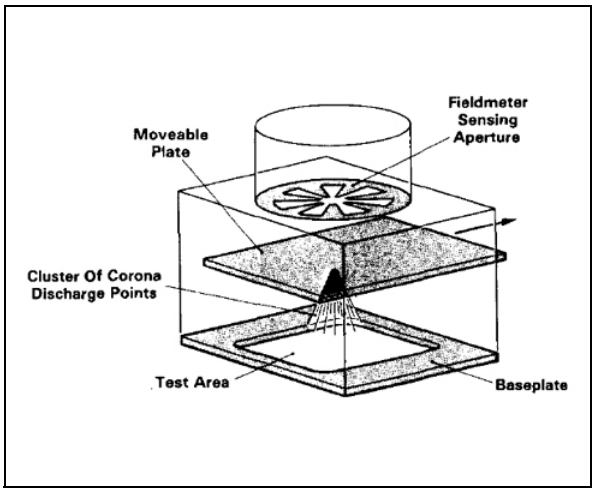

Figure 2.4. JCI Tester [15]

Gompf [25] described the tribo-electric method used at Kennedy Space Center by NASA, which was developed by Dr. Webster of Pan American World Airways in 1960s. The device, shown in Figure 2.3, basically consists of a grounded aluminum frame with two cutouts. Test specimens are arranged on the grounded aluminum sample holder. Through the upper left cutout, test specimens get charged by rubbing against soft wool, hard Teflon or Teflon felt, mounted on the rubbing wheels operated by electric drive motor. In the lower right cutout is the static detector head. Static detector head is expected to measure the electrostatic field and it is transferred to dc voltage in the electrometer.

A year later, Wilson [48] reported a new method, Shirley Method, used for measuring

electrostatic properties of textiles in British Textile Technology Group (BTTG). While NASA Tribo-electric Tester is designed only for measuring charge generated on the sample by rubbing, Shirley Method observes charge and discharge characteristics. Additionally, Shirley Method is concentrated upon the subject of spark and ignition caused by static electricity.

In Shirley Method [48], test samples are mounted on the ring-shaped Perspex holders. Sample holders are rested on Perspex table covered with the same materials that generate charge on the samples. Rubbing material is either woven nylon or woven Teflon because of their extreme positions in the tribo-electric series of textiles. Nylon and Teflon can generate positive and negative potential, respectively, on any kind of textile materials. Wilson, however, did not give enough explanation about how the charge generating process would be achieved in the system. Illustration of external figures of the system was neglected, as well. Figures presented are hardly recognizable and not helpful to understand the system.

Shirley Method [48] adopted a parameter of initial charge potential on the sample surface as a charge property, measured after inserting the charged sample into the Faraday cage. Discharging behavior is examined from the charge in a single spark and critical values of the charge released in sparks for the ignition. Discharging from the charged samples is inducted by bringing samples close to the electrode. The electrode system consists of various sizes of sphere electrode with various sizes of core and stainless steel rod.

Chubb's instrumentation [15], which is called as John Chubb Instrumentation (JCI) of Figure 2.4, was made up of a base plate for holding a test specimen, a field meter for monitoring potentials on the specimen surface and a moveable plate with corona discharging

cluster between the base plate and field meter. Below the base plate, there are either open-backing or earthed-backing. JCI Tribo-charging Tester was greatly innovative from extant testers above in terms of charge generation system. It raised charges on specimens by means of corona discharge, not a rubbing process. He used the corona discharge between two electrodes with high voltage for generating charge on test specimens and observed the initial peak voltage and decay behavior during self-dissipation of charged samples.

While a test specimen starts getting charged from the corona discharge cluster, moveable plate slides aside so that the charged specimen can be exposed to the field meter, which converts field meter signal into the surface voltage of the specimen. The moveable plate is withdrawn within 20 ms enough to prevent the charge redistribution on the specimen surface. Initial peak voltage is caught when the moveable plate is fully removed and then the specimen starts to discharge. Charge decay curve versus time can be obtained through microcomputer.

Two new devices, which termed “linear Tester” and “Rubbing Tester”, to measure static generation/dissipation on yarn and polymeric surfaces were developed at the College of Textiles, NC State University [40]. Linear Tester is especially designed for measuring potentials on linear type materials (yarn), and Rubbing Tester is for planar type materials such as fabrics and films.

A schematic illustration of Linear Tester is shown in Figure 2.5. A yarn flows in a path between the supply package and the winder (shown in the Figure 2.5) under controlled speed and tension. As the yarn moves, it gets tribo-charged by means of the charge pin. Static generation (surface potential) and decay behavior are examined by detecting the charges at

two spots on the yarn using two noncontact probes to prevent creating additional static charge by contact. Each probe is connected to a voltmeter, which in turn is interfaced to a standard data acquisition system.

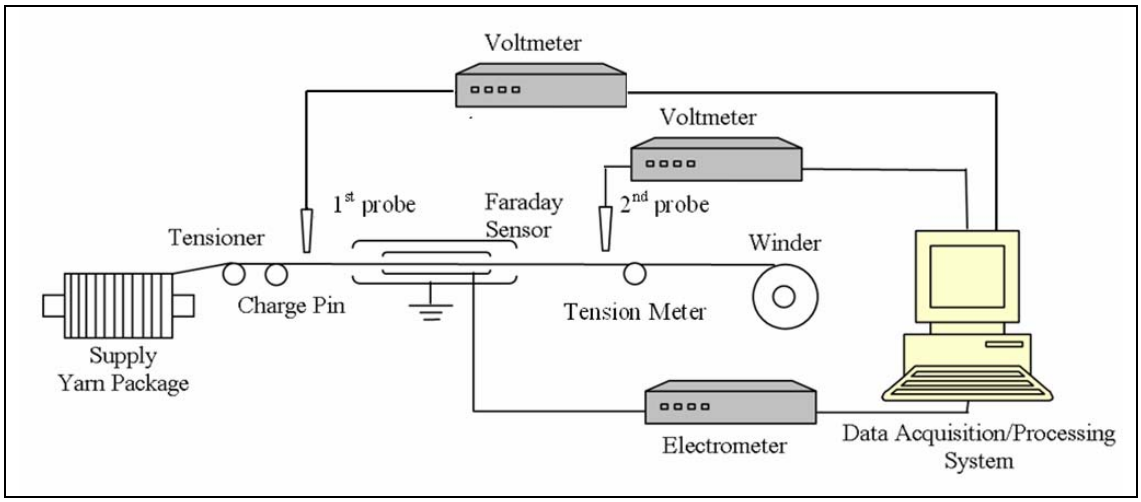

Figure 2.5. Linear Tester [40]

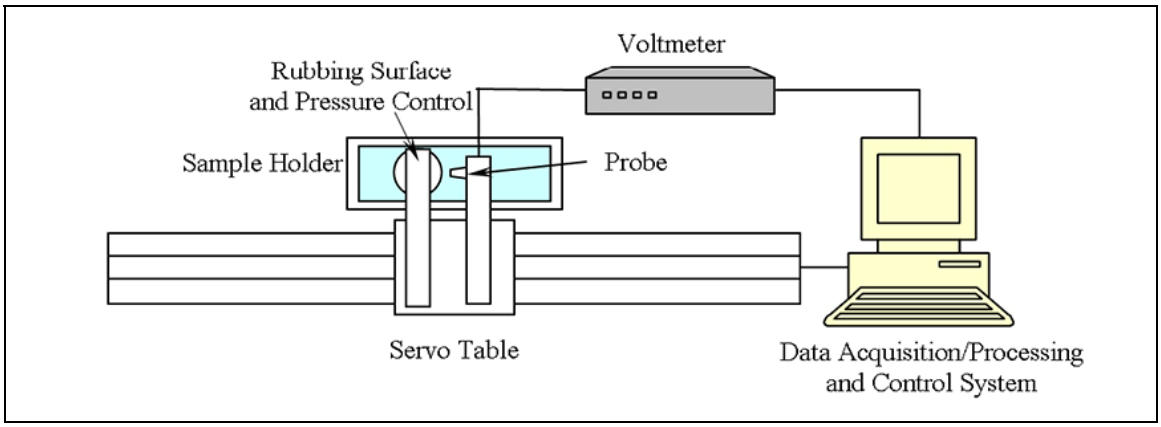

Figure 2.6. Rubbing Tester [40]

Figure 2.6 is depicting the Rubbing Tester. The device is equipped with a sample holder to mount the test sample. Rubbing material and noncontact probe are attached to a servo table. The rubbing material movement parameters (speed, stroke, number of cycles)

were controlled by a computer program. Tribo-electricity between sample and rubbing material is generated with the movement of servo table. The pressure between the rubbing surface and the test sample was controlled by vertical motion of the rubbing surface and the pressure is measured by a pressure transducer. The static generation/dissipation data were automatically collected by a standard data acquisition system that is connected to a voltmeter which is connected to the probe.

Electrostatic devices for textiles are compared in Table 2.4. NASA tester [25] is pretty simple in design compared to other testers because it is the earliest one. Following testers observe both charge and discharge characteristics, focused on unique parameters that can affect the electrostatic properties of textile materials. Shirley Method [48] and JCI Tester [15] are concentrating on the parameters related to the matter of sample size, while Linear Tester [40] and Rubbing Tester [40] are studying the variation of rubbing motion. Shirley Method is distinct from others in terms that it applies inducted charge dissipation, and so is JCI Tester in terms that it applies corona charge generation.

2.3. Experimental Studies

The previous research can be classified to methodological, experimental, and theoretical research. Methodological research is focused on comparing different apparatus or suggesting an appropriate index for assessing electrostatic properties of textiles. The experimental studies dealt with examination of how static properties of textiles are affected by some parameters (parametric studies). Experimental studies also dealt with the use of antistatic finishes and adding conductive yarns to reduce problems associated with static.

Theoretical research conducted to establish a universal tribo-electric theory by making plausible explanations on empirical observations of static charge transfer.

Table 2.4. Comparison between Capabilities of Electrostatic Devices

	NASA Tester [25]	Shirley Method [48]	JCI Tester [15]	Linear Tester [40]	Rubbing Tester [40]
Static Properties Measured	Surface Potential	Surface Potential, Spark Discharge	Surface Potential, Charge Decay	Surface Potential, Charge Decay	Surface Potential, Charge Decay
Charge Generation	Rubbing	Rubbing	Corona Charge	Rubbing	Rubbing
Charge Dissipation	N/A	Induction	Self Dissipation	Self Dissipation	Self Dissipation
Sample Type	Surface Type	Surface Type	Surface Type	Linear Type	Surface Type
Recommended Charging Material	Wool Teflon	Nylon Teflon	N/A	Variable	Variable
Controllable Parameters	N/A	Sample Size, Electrode Size, Core Size	Sample Size, Backing	Yarn Speed, Yarn Tension, Contact Angle, Charging Pin Speed	Rubbing Speed, Rubbing Pressure, Rubbing Length, Number of Rubbing Cycles

2.3.1. Development of Devices

Gompf et al. [24] analyzed the correlation of static properties measured using different electrostatic testers/methods. They compared NASA tribo-electric tester, the modified Shirley method, and the JCI tribo-charging tester. The testers use wool and Teflon as a charging material, except JCI tester which apply corona charging technique. The data generated from the three testers/methods of different materials were used to rank the materials from the highest generator to the lowest. Material ranking is shown in Table 2.5. Spearman ranking correlation coefficients between NASA tester and Shirley method were good (93%) with Teflon, but unacceptable (43%) with wool. The correlation coefficient between NASA tester and JCI tester was reasonable (73%) when Teflon was used as a charging material for NASA tester.

The lower correlation between the tests using wool might be owing to unexpected variability of natural fibers. For a given test material, Teflon was found to raise more electricity than wool. Additionally, test results reproducibility was higher in case of using Teflon than wool. From the data, Gompf et al. [24] believed that it was possible to reliably rank textile materials in their static properties. However, the fact that experimental results from different devices are not exactly matched (Table 2.5) still represents the dependence of static generation on instrument used.

Chubb [13] also compared eight kinds of charge decay measurement methods in use for charge decay measurement. They were Corona Charge Decay, Federal Test Standard (FTS) 101C, ITV-TEV method, NASA tester, Shirley Method 20, Scuff-charging method, STFI method, and Charge Plate Monitor (CPM) method. Four of those (FTS 101C, Shirley

Method 20, STFI, and CPM) were judged not to be appropriate for assessing charge decay property. NASA tester, Scuff-charging, and ITV-TEV method, which are based on tribo-electrification, were hard to control the charge generation and not available for commercial use. Only corona charging decay gave results matched with tribo-charging and had commercial availability.

Table 2.5. Material Ranking for Each Test Method at 25% Relative Humidity [24]

Material	NASA Tester		Shirley Method		JCI Tester
	Wool	Teflon	Wool	Teflon	
PPC8*	6	4	7	4	2
PPC11*	7	6	4	6	3
PPC12*	5	5	3	5	5
PPC17*	8	8	5	8	8
PPC20*	9	9	9	9	7
PPC24*	4	7	8	7	3
PPC27*	1	1	6	3	1
XP1*	2	2	2	2	No Data
XP2*	3	3	1	1	6

*PPC8 Polyester clean-room fabric with 20mm conductive stripe
*PPC11 Polyester/cotton fabric with 10mm conductive grid
*PPC12 Polyester/cotton fabric with blend of conductive fibers
*PPC17 100% cotton with flame retardant finish
*PPC20 100% aramid
*PPC24 Aramid with ore conductive fiber
*PPC27 Polyurethane coated fabric with antistatic finish
*XP1 Black plastic storage bag
*XP2 Transparent plastic document wallet

2.3.2. Previous Studies on Yarns and Fibers

Nidonova et al. [37] studied the effect of yarn speed and preload on frictional and electrostatic properties of Capron® yarns. Yarn speed was varied in the range of 0~30 m/min, and preload range was 0~30 gf. The experiments ran under a standard condition of 20 ± 0.5 °C and 62 ± 1% R.H. was used. Frictional coefficient and static charge increased with the speed of the yarn, while the influence of preloads was negligibly small.

Ukraintseva et al. [47] dealt with polyamide yarns coated with electrically conducting component of carbon black. Sample yarns were different in terms of linear density (10 tex and 25 tex), and carbon black content (15%, 35%, 60%). Electrical potential and current was monitored. It was reported that the thinner was the yarn and the more conductive particles were on the yarn surface, the lower was the potential which meant possibility of the static risk became less.

Berberi [10] investigated the dependency of electrical resistivity on the form of textile structure and manufacturing process. Electrical resistivity of fabric, yarn, and cut yarn were compared and found to be about the sa3me value regardless of the form. Measurement of electrical resistivity of fibers and yarns was assessed after each process for fibers and yarns from Greek cotton, USA cotton, and un-dyed and black-dyed wool. USA cotton which was affected by sugar disease appeared to have a lower resistivity than Greek cotton. Cotton got higher resistivity as the processing went on. Especially, the resistivity appeared to have a rapid increase during opening and carding. The reason of increasing resistivity of cotton is the layer of wax on the surface, which was damaged during processing. Wool was getting resistive during the process, as well. For the dyed wool sample, dyeing was conducted after

washing and cleaning. For both dyed and un-dyed wool, spin finishing, which have antistatic effect, was applied after dyeing and for un-dyed wool the spin finish was applied before blending. Un-dyed wool lost the effectiveness of spin finish during blending (which was done after application of spin finish), while dyed wool lost the effect of spin finish gradually as it moved from process to another. Therefore, it was proved that spin finish was not necessary for un-dyed wool. However, Berberi did not explain whether blending would be difficult as a result of skipping spin finish.

2.3.3. Previous Studies on Material Surfaces

Chubb [14] introduced 'charge decay time' and 'capacitance loading' as a new index replacing resistivity for assessing electrostatic properties of textile material. Charge decay time is how quickly charge can migrate away, whereas capacitance loading indicates how the surface potential is limited by the nature and structure of materials. Electrostatic-safe materials are supposed to have short decay time and high capacitance loading. Charge decay time and capacitance loading were calculated from tribo-charging test and corona charging test (JCI tester). Tribo-charging test is operated by scuffing the center of a round sample (200 mm in diameter) with a charge neutral Teflon rod. Tribo-charging can be used to validate charge decay time and capacitance loading based on corona charging. Charge decay time was measured by the time from the initial peak voltage (V_{pk}) to V_{pk}/e. Capacitance loading was obtained from the ratio of the field meter observation without test material to the observation with the test material for tribo-charging test, and by comparing voltage measurements of the test material to those of a very thin layer of dielectric for corona charging test.

In tribo-charging test, capacitance loading was independent from the quantity of charge generation. Also, in corona charging test, capacitance loading values and decay times did not vary much with the quantity of charge. As relative humidity increased, capacitance loading showed an increase, but charge decay times decreased with different degrees according to sample types. When comparing tribo-charging tests to corona charging tests, ranking orders for capacitance loading and charge decay time were very similar, although capacitance loading often showed higher values in corona charging.

Diaz et al. [18] combined four tribo-electric series from literatures [1, 16, 27, 29]. Common materials in each series were lined up for comparison, and results of charge were incorporated to support the rank. In tribo-electric series, materials at higher positions get positive charges after the contact with a material at a lower position. Diaz et al tribo-electric series and charge data of textile materials are given in Table 2.6. Natural fibers got charged in the range 0.6 - 1.1 pC, whereas synthetic fibers were charged with wider ranges. How functional groups in polymer structures might have affected electrostatic properties was speculated. The nitrogen containing polymers developed the most positive charges, and halogenated polymers established the most negative charges. Polymers with oxygen functional groups were charged positive, but lower than those with nitrogen groups. Hydrocarbons generated almost no charge.

Ohara et al. [38] constructed a tribo-electric series of atomic groups with the view that atomic groups in the molecules can affect the polymers' electrification properties. Polymer films such as nylon 6 (Ny), polycarbonate (PC), polypropylene (PP), polystyrene (PS), polyethylene terephthalate (PET), polymethyle methacrylate (PMMA) and

polyvinylchloride (PVC) were studied. The Langmuir-Blodgett method enabled a specific polar group to be bonded to the same kind of hydrocarbon chain. Three Langmuir-Blodgett films such as stearic acid (ST) with COOH group, stearylamine (SAN) with CH_2NH_2 group, and stearamide (SAD) with $CONH_2$ group were constructed. Triboelectric series is shown in Table 2.7. Langmuir-Blodgett films were observed to have higher charge than the polymer films with corresponding polar groups because of higher molecular density. For example, ST having same atomic group (−COO) to PMMA showed larger electrification voltage than PMMA. Due to the influence of oxygen in SAD, opposite polarity was observed on SAD and SAN, although they share amino groups (NH_2) which electrifies a material positively. It was possible to make a tribo-elecric series of atomic groups for –$CONH_2$, –COOH, and –CH_2NH_2, but this issue needed to be studied more in terms of interactions between inside atomic groups.

Table 2.6. Summarized Tribo-electric Series [18]

Fiber Type	Charge (pC) against Gold	Functional Group
Polyamide (Nylon)	+1.2	Nitrogen
Wool, Silk	+0.6 ~ +1.1	Nitrogen, Oxygen
Cotton	+0.15 ~ +0.19	Oxygen
Acetate, Rayon	+0.14	Oxygen
Polyester (Dacron)	+0.1	Oxygen
Polyethylene, Polypropylene	~ 0	Hydrocarbons
PTFE (Teflon)	−2.8	Halogenated

Table 2.7. Tribo-electric Series (against Glass) [38]

	(+) Positive	Negative (−)
For Polymer Films	Ny, PMMA, PC, PP, PS, PET, PVC	
For Langmuir-Blodgett Films	SAN, ST, SAD	
For Atomic Groups	− COOH, − CH_2NH_2, − $CONH_2$	

Akande and Adedoyin [3] tried to explain contact charge transfer between polymers and metals using metal work function. Work function is the minimum energy needed to remove an electron from a solid surface to an outside point. Charge density and the metal work function were observed between metals and three polymer films (UV-radiated polystyrene, polymethyl-methacrylate, and poly(2-vinylpyridine)). Experimental results indicated that charge transfer was influenced by the metal work function, but there was no simple universal relationship between charge transfer and work function. This was coincided with Elsdon and Mitchell's research [22] claiming that metal work function has no systematic effect on charge transfer. This was confirmed once more by a later study by Akande [2].

2.3.4. Fabric containing Conductive Yarns

Paasi et al. [39] studied an appropriate test method for evaluating electrostatic discharge protective garments. Evaluation was achieved by measuring peak current and transferred charge during the dissipation because damage caused by electrostatic is usually originated from charge dissipation energy. Three protective fabrics with carbon core-

conducting, carbon surface-conducting, and stainless steel threads were evaluated with different probes and charging methods. Two electrostatic discharge probes from different manufacturers and charging method (tribo-charging / direct charging) showed no significant differences in experimental results. Protective fabrics were placed in the order of increasing charge and peak current at given surface voltage as follows: carbon core-conductive, carbon surface-conductive, and stainless steel conductive fabrics.

Coletti et al. [17] analyzed the effect of charge dissipation modes. Two types of specimens were used; one was polyester and cotton blend hosting a surface conductive grid, and the other was pure polyester hosting a core conductive grid. Static decay behavior was observed, depending on three different charge dissipation modes: touching a center of the specimen with a grounded stick, touching a side of the specimen with a grounded stick, and letting the specimen alone (self-dissipation). Surface conductive textiles showed a clear difference as charge dissipation modes changed. Touching a side of the specimen was the fastest, and self-dissipation was the slowest. For core conductive textiles, however, the difference was not as much significant as surface conductive textiles. There was little difference in charge dissipation behavior.

This research was limited in terms of sample preparation having two variables at once. One was 50%/50% polyester/cotton cloth hosting a surface conductive grid, and the other was 100% polyester hosting a core conductive grid. Investigators' intention to compare the effect of surface/core conductive grids would be disturbed by the effect of fiber types. In addition, manual operation restricted the accuracy of experiments even though the authors took preliminary tests to check up the consistency. Manual task was done by rubbing fabrics

for charge generation and touching them by a Teflon rod for discharge. The reproducibility of such test results is questionable.

Tabata's research [45] intended to understand charge densities and discharge energy of antistatic fabrics containing electrically conductive yarns. The conductive yarns, which were not fully described, are core textile yarns coated with conductive material. The electrically conductive materials were coated carbon, silver, and copper. The conductive yarns were woven in striped and checkered patterns with various distances between the conductive yarns (2 ~ 30 mm). The woven pattern and distance between electrically conductive yarns influenced charge density and discharge energy, whereas the effect of material type was slight. Less charge density was observed as electrically conductive yarns were located close and checkered patterns exhibited lower charge density compared to striped patterns. Maximum discharge energies of the fabrics examined were below 100 μJ, which was safe enough to avoid the electrostatic risk. Checkered fabrics with 10 mm or less distance of electrically conductive yarns showed the best antistatic effect. Tabata also found that charge generation depended on the direction of separating samples after rubbing in case of striped fabrics. Parallel separation of the sample fabric to the conductive threads showed less charge density than perpendicular separation because of the corona discharge caused by electrostatic difference between the electrically conductive yarn and surroundings.

Ukraintseva et al. [47] investigated experiments to find out the effect of the conductive yarns woven in fabrics. Electrically conducting yarns were set in the fabric specimens with different intervals (1.5 cm and 3 cm). Surface charge density and potential were measured. In common with Tabata's [45], antistatic effect was strong when electrically

conducting yarns was located closer.

In a similar investigation, Guastavino et al. [26] evaluated the tribo-electric performances of composite textiles in electrostatic discharge protective garments by observing charge decay behavior. Three different conductive grids of stainless steel, surface conductive, and hybrid core conductive grids (which were not fully described) were woven in polyester and polyester/cotton blend fabrics in 5mm × 5mm and 10mm × 10mm squares. Fabric surface potentials on the center of a square and the cross position of 4 squares were recorded at the initial time and 2 seconds later. Charge generation on 5×5 grid samples showed less significant difference between center and cross position than 10×10 grid samples. In general, cross position tended to have fast charge dissipation than center. In eight fabric samples observed, parameters were not controlled. For example, a fabric with 5×5 surface conductive grid was compared to a fabric with 10×10 hybrid core conductive grid. Another sample with 5×5 stainless steel grids on a fabric of 65%/35% polyester/cotton was compared to a sample with 5×5 surface conductive grids on a fabric of 60%/40% polyester/ cotton. In the former case the effect of grid size and conductive yarn type is coupled, while in the latter case the fiber blend level and type of conductive yarn are coupled. Since static generation/dissipation is very sensitive to these parameters, it is hard to assess the effects of blend, grid size, and type of conductive yarn.

Holdstock et al. [31] studied experimentally the effect of static charge on bedding items as a result of removal from a bed in a hospital. Bedding items were given one wash cycle and four rinse cycles, and treated with fabric commercial conditioners (active agent of quaternary ammonium compound and cationic surface) by adding the appropriate amount in

the final rinse cycle. The experiment dealt with different fibers, fabric conditioners, and removal methods. Three bedding combinations (flame retardant cotton blanket + standard cotton sheet, flame retardant polyester blanket + flame retardant polyester sheet, and modacrylic blanket + standard polyester sheet) were used in each bedding assembly. Removal method of bedding items was achieved by pulling and folding. The experiments were conducted by an insulated human operator on insulated bed frameworks.

In all cases, folding method generated less potential than pulling. Also, the beddings having same fiber type in the blanket and the sheet generated less potential. The bedding assembly with highest static generation was between modacrylic blanket and standard polyester sheet. Minimum static potential generation was obtained when flame retardant cotton blanket was removed from standard cotton sheet by folding. Even in minimum static potential generation, the magnitude of potential induced was high enough to cause shocks or equipment damage in hospital environment. Fabric conditioners helped reduce static generation, but there was no significant difference between fabric conditioners from different manufacturers. The authors recommended single fiber type bedding items with the treatment of fabric conditioner and removal by folding in order to minimize the static problems. Necessity of the ground was emphasized because the experiments were done with insulated bed frameworks and operators. Generally, no bed framework in a hospital is completely insulated. Experiments with proper flooring materials should be conducted.

2.4. Electrostatic Theory

The mechanism of charge transfer is often explained with energy levels of electrons

[36]. Charge transfer is occurred between two metals in contact due to contact potential difference. For example, electrons at the highest energy level in Metal A can flow to the vacant level in Metal B until they have equal electron energy levels (Figure 2.7). By contrasts, insulators are characterized by forbidden bands. Accordingly, electrons in an insulator are limited in their energy levels unless they have enough energy to jump up into the vacant bands (Figure 2.7). It is possible for electrons in the insulator to pass into the metal if they have higher energy level than electrons in the metal. However, the opposite is not always possible because of forbidden bands in the insulator. That is why the charge transfer between a metal and an insulator is complicated.

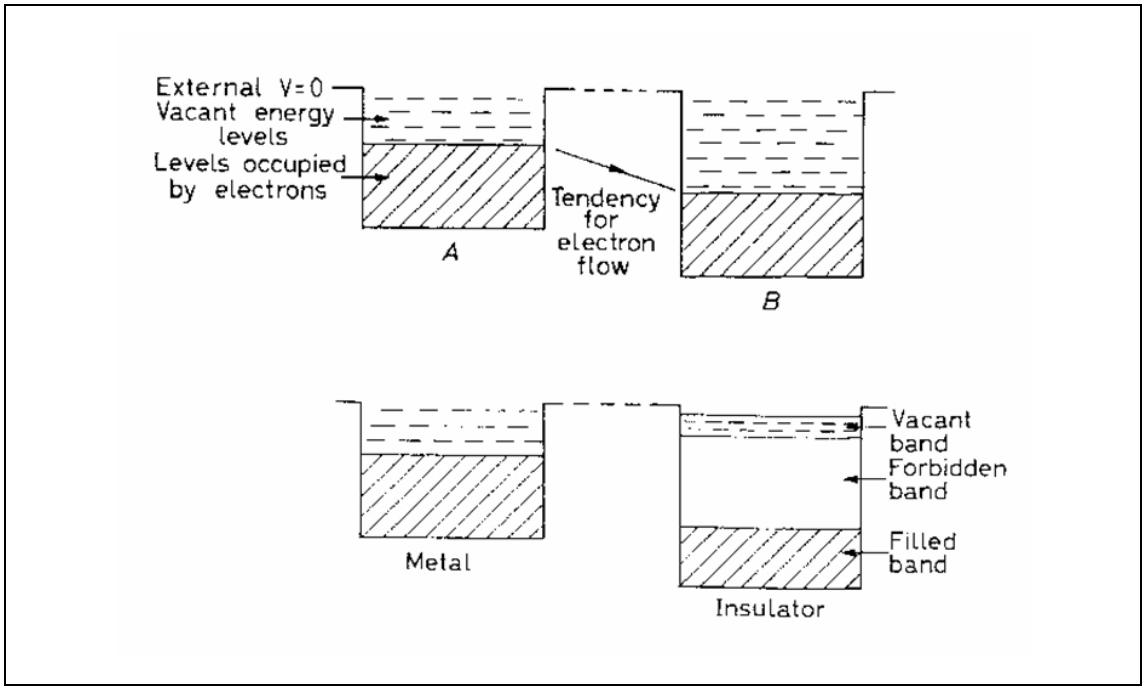

Figure 2.7. Energy Levels in Metals (top), and in Metal and Insulator (bottom) [36]

Castle [12] introduced the surface state theory with comments on low reproducibility of static experiments. Five possible responsibilities for many contradictory data existing in

the literature were given; (1) surface variability, (2) experimental variability, (3) nature of contact, (4) charge species, and (5) effect of charge back flow. The surface state theory explains the charge exchange with the difference of surface work functions between two surfaces. It is assumed that electron states exist within the large band gaps, and this state relate to a material's pseudo or effective work function. The density of theses states controls the surface charge density. According to Castle [12], charges were exchanged so that electrostatic energy could offset the difference in work functions at the interface.

III. OBJECTIVES

The literature review indicated that despite of accumulated research in this area, there is hardly any explanation in regards to the mechanism of static generation and dissipation agreed universally due to low reproducibility of tribo-electrification. Researchers' results disagreed in regards to the effect of material resistivity on static charge dissipation judged by decay time. For example, Chubb [13, 15] results indicated that electrical resistivity had no relation with charge decay property, whereas in Henry et al. [28] and Jonasssen et al. [35] work, it was shown that there is proportionality between resistivity and charge decay time. Diaz and Felix-Navarro [18] pointed out that the contradiction may be explained by the complexity of measurement and the numerous parameters affecting the static generation/dissipation such as chemical composition, surface characteristics, nature of contact, experimental conditions, etc. Besides, charge transfer mechanism of insulators is still debatable. The contradiction of results and the discrepancy between different methods and devices are the reason behind undertaken the current research. It is believed that with the advances in instrumentation, data acquisition systems, control systems, and implementation of correct procedure provide tools needed to carry out research in the area of static generation/dissipation of polymeric materials.

This research was undertaken to gain better understanding of static generation and dissipation on continuous filament yarn surface in terms of environmental conditions (temperature and relative humidity), yarn tension, yarn speed, and fiber type. Four experiments were conducted: (1) effect of environmental conditions, yarn tension, and yarn speed on static generation/dissipation of continuous filament polyester yarn, (2) effect of

charging pin material (stainless steel, nylon, polyester, polypropylene, and Teflon) on static generation/dissipation of continuous filament polyester yarn, (3) effect of fiber type (polyester, nylon, and polypropylene) on static generation/dissipation of finish free continuous filament yarns, and (4) effect of humidity, yarn tension, and yarn speed on yarns of different filament count. The assessment of static charge generation/dissipation was done by using a device equipped with winder, two potential probes, charge pin, tension and speed controllers, and data acquisition system. Potentials collected by the two probes at two different positions on a running yarn in real time were used to calculate initial potential (at the point of separation of yarn and charge pin) and characteristic decay time. The independent parameters of the experimental designs were broad to include the conditions practiced by the textile industry.

IV. EXPERIMENTAL

4.1. Materials

4.1.1. Continuous Filament Yarns

Table 4.1 lists all the yarns used in this work. As the table indicates, all the yarns are of flat (no twist) continuous filament yarns of multifilament and monofilament. The table also shows the surface treatment of each yarn indicated by the finish compound and % finish. All yarns had spin finish. 200 denier yarns got only spin finish and other yarns got spin finish in addition to finish on yarn. Analytical results on the extract of yarns for finish compound identification are given in Appendix G.

Table 4.1. List of Yarns

	Linear Density (denier)	No. of Filaments	Finish Compound	Finish On Yarn (%)
Polyester	1,000	140	No data	0.625
Nylon	420	72	Propylene Glycol Dilaurate	0.666
Polypropylene	300	144	Jim Walter Resources Foamstab 210	2.119
Polyester	200	60	Oleamide	0.015
Nylon	200	60	No data	0.042
Polypropylene	200	60	Eastman CP-343-1	0.914
Polyester	878	1	N/A	0
Nylon	393	1	Henkel Corp. Dehymuls E	0.008
Polypropylene	1,590	1	Trans-Chemco Inc. Trans-166	0.373

4.1.2. Charge Pins

The linear tester (Figure 2.5) was used to measure static generation/dissipation of each of the yarns of Table 4.1. Charge pins (Figure 4.2) of different material were acquired. These are stainless steel, nylon, polyester, polypropylene, and Teflon. All charge pins are of identical dimensions of 6mm in diameter and 50mm long (Figure 4.1 and Figure 4.2).

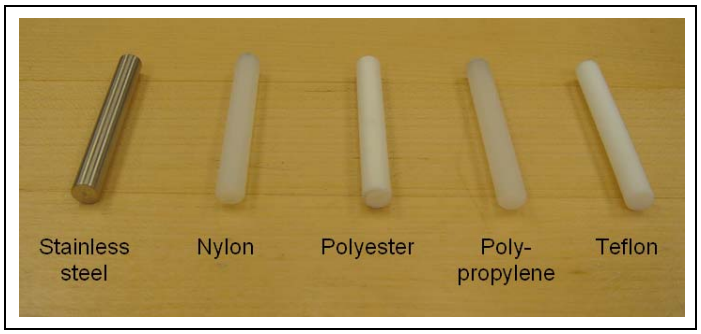

Figure 4.1. Charge Pins

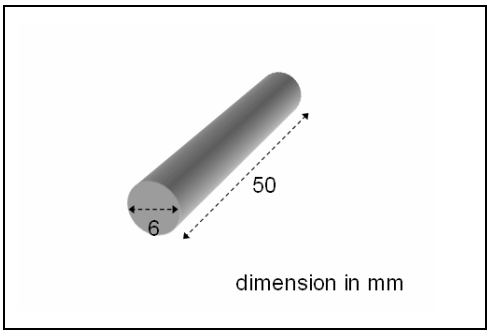

Figure 4.2. Charge Pin Dimension

4.2. Linear Tester

An image of the Linear Tester is shown in Figure 4.3. It consists of a CTT (Constant Tension Transport) machine, a charge pin, two potential probes connected to voltmeters, and computer system for automatically acquiring the output of the two potential probs. Important dimensions are given in Figure 4.4. More details on the Linear Tester were given in section 2.2.2 and elsewhere [40].

4.3. Environmental Room

The Linear Tester is hosted inside an environmental room. Environmental room is a walk-in chamber equipped with air controller (by Generation and Control, Inc.) and insulated panels (by Kysor Panel Systems). Dimension of the room is 3.25m (width) × 2.64m (height)

× 2.64m (depth). The environment which can be reached is in the range of 7~60°C temperature and 10~95% relative humidity.

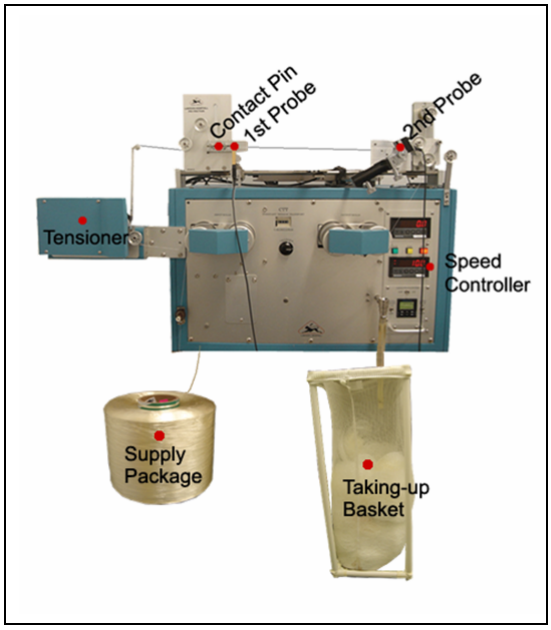

Figure 4.3. Linear Tester

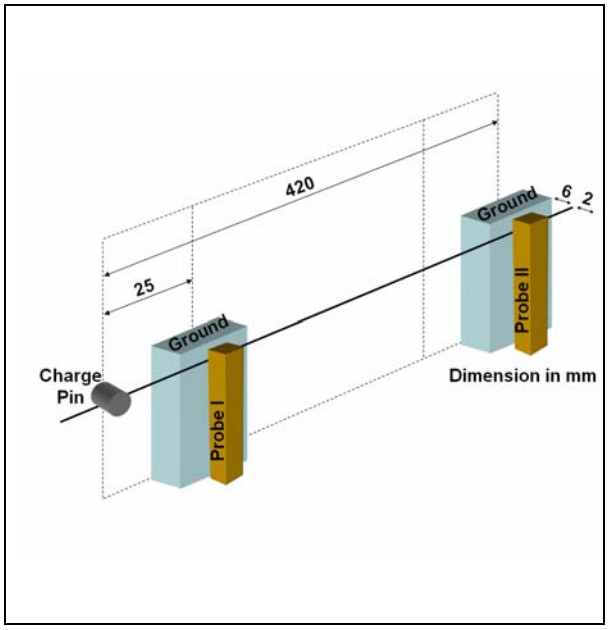

Figure 4.4. Dimensions between charge pin and probes

4.4. Experimental Designs

4.4.1. Experimental Design I

Experimental design I aimed at investigating the effect of temperature, relative humidity, yarn tension and speed on static generation and dissipation. Parameters and levels are described in Table 4.2. Four levels of temperature, relative humidity, yarn tension, and yarn speed were applied. 20°C temperature was replaced by 21°C, and 60% relative humidity was replaced by 65% in order to have the "standard atmospheric condition" (21°C, 65% R.H.) in common used in testing laboratories. In addition, two environmental conditions (21°C, 30% R.H. and 25°C, 30% R.H.) were excluded because relative humidity as low as

30% could not attainable under low temperatures. Accordingly, 14 environmental conditions and 16 contact conditions were used for total experiments. Responses were initial potential and characteristic decay time. Calculations of responses are shown later in section 4.6.

Table 4.2. Experimental Design I

Parameters	Levels
Temperature	21, 25, 30, 35 (°C)
Humidity	30, 40, 50, 65 (%)
Yarn Tension	0.45, 0.68, 0.90, 1.35 (gf/tex)
Yarn Speed	10, 50, 100, 300 (m/min)
Total Run	$\{(4 \times 4) - 2\} \times 4 \times 4 = 224$
Constant Parameters	Sample Yarn = 1000/140 Polyester Charge Pin = Stainless Steel Contact Angle = 120°

The parameters levels were selected to reflect the working environment in the textile industry. Polyester has a bad reputation for generating and accumulating static charges, and is the most widely used man-made fibers throughout the world. Static charge on the polyester yarn is created against a charge pin made of stainless steel, which is a surface material commonly used on textile machine.

4.4.2. Experimental Design II

The second experimental design was structured to study the effect of charging material on static generation and dissipation. As shown in Table 4.3, five different charge

pins made of stainless steel, nylon, polyester, polypropylene, and Teflon were used to compare and contrast different charging materials. Yarn tension was reduced to two levels, and yarn speed was limited to three levels to have manageable number of runs and still maintain meaningful study in regards to the range of each parameter. Responses were initial potential and characteristic decay time. Calculations of responses are shown later in section 4.6.

Table 4.3. Experimental Design II

Parameters	Levels
Humidity	30, 65 (%)
Yarn Tension	0.68, 1.35 (gf/tex)
Yarn Speed	50, 100, 300 (m/min)
Charge Pin	Stainless Steel, Nylon, Polyester, Polypropylene, Teflon
Total Run	2 ×2 × 3 × 5 = 60
Constant Parameters	Temperature = 30 °C Sample Yarn = 1000/140 Polyester Contact Angle = 120°

4.4.3. Experimental Design III

The third experiment (Table 4.4) was designed to study the static generation/dissipation behavior of different polymeric finish-free yarns. Finish-free yarns made of polyester, nylon, and polypropylene were investigated after rubbing against stainless steel. All yarns have the same linear density of 200 denier. Yarn tension was adjusted for lower linear density of finish-free yarn. 0.68 gf/tex was replaced by 2.00 gf/tex because 0.68

gf/tex was too low to support the yarn on the device. Actual tension amount applied to 200 denier (22 tex) sample yarns were 30 and 45 gf, respectively. Other parameters such as humidity and yarn speed were kept constant to former settings. Responses were initial potential and characteristic decay time. Calculations of responses are shown later in section 4.6.

Table 4.4. Experimental Design III

Parameters	Levels
Fiber Type	PET, Nylon, PP
Humidity	30, 65 (%)
Yarn Tension	1.35, 2.00 (gf/tex)
Yarn Speed	50, 100, 300 (m/min)
Total Run	3 × 2 × 2 × 3 = 36
Constant Parameters	Temperature = 30 °C Yarn Linear Density = 200 denier Number of filaments = 60 Charge Pin = Stainless Steel Contact Angle = 120°

Yarn surface area of the yarns was in cm^2 per one meter long yarn calculated. Filament radius is estimated from linear density of the yarn (Equation 4.1), and used to calculate surface area (Equation 4.2). Surface area of finish-free yarns is given in Table 4.5.

$$\frac{tex}{n} = \rho \times \pi \times \left(\frac{r \times 10^{-3}}{2} \right)^2 \times 10^{12} \qquad (4.1)$$

$$Surface \cdot Area = 2\pi r \times n \times 10^{-3} \qquad (4.2)$$

where, *tex* = linear density (g/km)

n = number of filaments

ρ = fiber density (g/cm^3)

r = filament radius (mm)

Table 4.5. Surface Area of Finish-free Yarn

Yarn	Surface Area (cm^2/m)
Polyester	1.5518
Nylon	1.7145
Polypropylene	1.9294

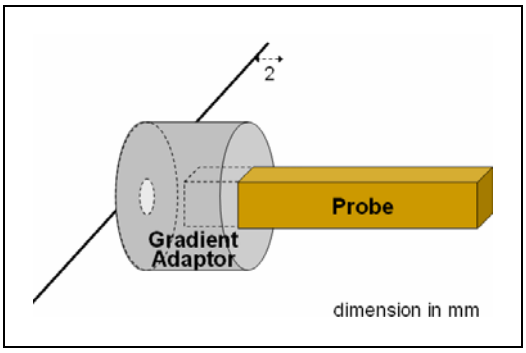

Figure 4.5. Gradient Adaptor

The charge pin, rollers, and guides having contact with the sample yarn on the device were cleaned with alcohol before experiments. Due to the higher potentials over 3,000 volts generated on finish-free yarns, gradient adaptors (by Monroe Electronics) were attached to both first and second probes as shown in Figure 4.5. These devices reduced the potential signals to one tenth of the actual values so that the signal would not exceed the voltmeter capacity.

4.4.4. Experimental Design IV

Six different yarns were used for this experimental design, which is shown in Table 4.6. As the table indicates, the yarns are multifilament and monofilament made of polyester, nylon, and polypropylene. Detailed description on sample yarns used in this experimental design is given in Table 4.1. Tension was kept at 0.68 gf/tex and 1.35 gf/tex, and the actual

tension given to each sample yarn depending on its linear density is displayed in Table 4.7. Responses were initial potential and characteristic decay time. Calculations of responses are shown later in section 4.6.

Table 4.6. Experimental Design IV

Parameters	Levels
Fiber Type	PET, Nylon, PP
Yarn Type	Multi-filament, Mono-filament
Humidity	30, 65 (%)
Yarn Tension	0.68, 1.35 (gf/tex)
Yarn Speed	50, 100, 300 (m/min)
Total Run	3 × 2 × 2 × 2 × 3 = 72
Constant Parameters	Temperature = 30 °C Charge Pin = Stainless Steel Contact Angle = 120°

Table 4.7. Yarn Tension and Surface Area Specification

Sample Yarn	Number of Filament	Linear Density (denier)	Yarn Tension (gf)		Surface Area (cm^2/m)
			1.35 gf/tex	0.68 gf/tex	
Polyester	140	1000	150	75	5.3227
Nylon	72	420	63	32	2.7216
Polypropylene	144	300	45	22	3.6607
Polyester	1	878	132	66	9.425
Nylon	1	393	60	30	6.283
Polypropylene	1	1590	239	120	15.708

4.5. Testing Procedures

Test procedures consist of:

1. Set the environmental room (Figure 4.6) to the required temperature and relative humidity using control pad (Figure 4.7) at the entrance.

Figure 4.6. Environmental Room

Figure 4.7. Control Pad

2. Condition the yarns to be tested by leaving them in the environmental room for at least 12 hours.
3. Turn on the CTT, voltmeters, and computer. A voltmeter's manufacturer recommends warm it up for an hour prior of running the test.
4. It is required to clean the rollers and guides of the Linear Tester with alcohol thoroughly before testing new yarns. This cleaning step is important when starting the test of new yarn (when switching from yarn to another).
5. Start the software for recording voltmeter measurements (LJStream software, which is a product of LabJack Corporation). The screen for input and output, shown in Figure 4.12,

will show up.

Figure 4.8. Zero and Balance Knob of the Voltmeter

6. Zero the voltmeter by adjusting ZERO knob and BALANCE knob (Figure 4.8) and moving the probe forward and backward to the ground. Verify the voltmeter indicating zero with the absence of the yarn regardless of the distance between the probe and the ground. (Voltmeter needs to be calibrated every year. Calibration procedure is given in Appendix B.)
7. Check the probe location for the distance from a charge pin, between two probes, and between probe and ground. These should be the same for all runs as shown in Figure 4.4. In addition, make sure the inlet of each probe is facing the yarn.
8. For measuring potentials exceeding the capacity of the voltmeter (3,000 volt), the gradient adaptor (by Monroe Electronics) was used. The gradient adaptor reduces the potential signal with certain scales. One tenth scale was used as manufacturer recommends so that reading on the voltmeter can be one tenth of the actual measured

potential.

9. Set the yarn tension by adjusting the tension knob (Figure 4.9). Confirm the input tension between the tensioner and a charge pin using a tension meter (Figure 4.10).
10. Set the yarn speed using control pad on the CTT (Figure 4.11).
11. Set the rate of data collection by changing scan rate on LJstream (Figure 4.12).

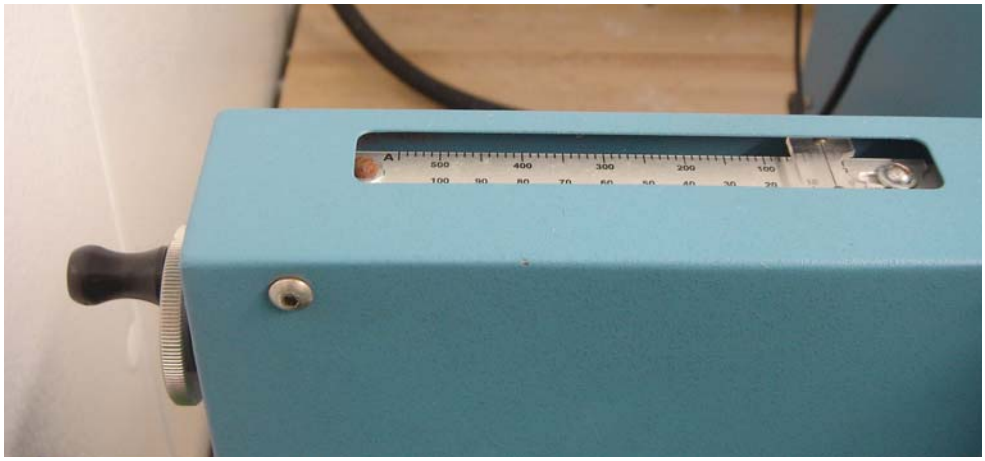

Figure 4.9. Tensioner of CTT

Figure 4.10. Tensionmeter

Figure 4.11. CTT Speed Control Pad

12. Start CTT so that the yarn flows through. Make sure that the yarn runs in the designated path.
13. After 5~10 seconds, start recording measurements by clicking 'Enable Stream' button, shown in Figure 4.12. It takes 5 ~ 10 second for the yarn to reach its set speed.
14. After completing the set length of yarn and collecting the corresponding data, stop CTT and stop recording observations.

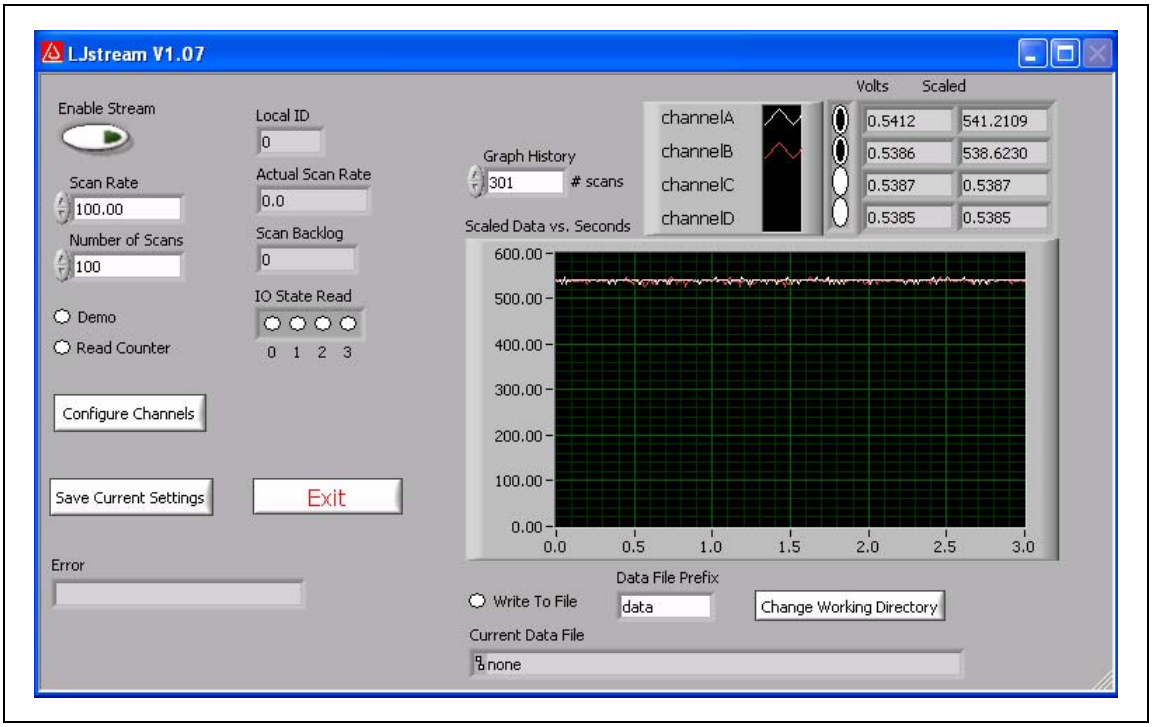

Figure 4.12. Input/output screen of LJstream software

15. If the temperature and humidity are same for the next run, repeat the procedures from step 7.
16. If the experiment needs to be end up, turn off the CTT, voltmeters, and computer. In case that temperature and humidity should be changed for next experiments, set environmental room to the new required condition.

4.6. Responses

4.6.1. Potential

Electric potential is defined as the energy needed for shifting a charge from one standard point to the other in the electric field. Technically, potential refers to potential difference between a certain point and the standard point which is electrically neutral. The noncontact probes are the products of Monroe Electronics, named Miniature Electrostatic Voltmeter Probes 1017A (Figure 4.13). The compatible voltmeter, Monroe Electronics ISOPROBE® Electrostatic Voltmeter 244A (Figure 4.14), are capable of measuring up to ±3,000 volts. This instrumentation was designed to make potential measurements without physical contact since contact creates additional charges.

As shown in Figure 4.4, two probes detecting potentials were located at different points whose distance from the charge pin is 25 mm and 420 mm, respectively. An inlet on the probe was facing the grounded metal plates with 8 mm distance. The sample yarn ran between the probes and the ground plate keeping a distance of 6 mm from the ground and 2 mm from each probe.

Figure 4.13. Electrostatic Probe 1017A
Monroe Electronics

Figure 4.14. Electrostatic Voltmeter 244A
Monroe Electronics

Since there was a time gap between two measurements of running yarn by the first probe and the second, a number of observations at the beginning of second probe measurements were removed in order to match up each measurement from two probes. The number of elimination was determined after calculating the time difference between two probes according to yarn speed (Table 4.8).

Table 4.8. Time (in seconds) from Charge Pin to Probes

	300 m/min	100 m/min	50 m/min	10 m/min
First Probe	0.005	0.015	0.030	0.150
Second Probe	0.084	0.252	0.504	2.520
Time Difference	0.079	0.237	0.474	2.370

4.6.2. Initial Potential

Initial potential refers to the charge on the yarn right after the yarn separates from the charge pin. The potential signal observed at the first probe is the static after some decay since the yarn travels 25mm from the charge pin to the probe. Therefore, the initial potential needs to be estimated in order to find out the true potential generated by the charge pin to the exclusion of any static decay. Initial potential can be predicted using two potential measurements and the time difference between two probes.

4.6.3. Characteristic Decay Time

Characteristic decay time is defined as the time needed for the potential to reduce to the 1/e of initial potential [14]. It is a useful index representing static dissipation properties.

Equation 4.3 expresses the empirical relationship between residual potential at a certain point (V_t) and the initial potential (V_0) using characteristic decay time (t^*). This allows us to calculate the potential at any desired time (t) based on the assumption that charges were decayed exponentially [46].

$$\text{Potential} = V_t = V_0 \times e^{-\frac{t}{t^*}} \qquad (4.3)$$

where, V_t = potential at time t (volt)

V_0 = initial potential (volt)

t = time at certain point (sec)

t^* = characteristic decay time (sec)

Equation 4.1 can be converted to Equation 4.4 representing ratio of residual potential to the initial potential. In this way, we can compare the charge dissipation property regardless of initial potential. Residual potential, described in Equation 4.4, would be visualized with a function of time in a decay curve by putting the retained potential on y-axis and time on x-axis.

$$\text{Retained Potential (\%)} = \frac{V_t}{V_0} \times 100 = e^{-\frac{t}{t^*}} \times 100 \qquad (4.4)$$

4.6.4. Rate of Data Collection

Because yarn speed is an independent variable in the experiments, the measurement needs to be adjusted to high resolution under high speed so that the number of data points collected for a certain yarn length is constant for fair comparison. Table 4.9 shows the

measurement frequency taken for each yarn speed, and consequent observation duration, number of measurement, and yarn length used for the observation.

Table 4.9. Rate of Data Collection

	300 m/min	100 m/min	50 m/min	10 m/min
Time Duration (second)	5	15	30	150
Number of Observations	1,501	1,501	1,501	1,501
Yarn Length (m)	25	25	25	25
Data Collection Rate (per second)	300	100	50	10

4.6.5. Calculation of Responses

Two potential measurements (1,501 different points at each probe) of the yarn were used to calculate the initial potential and characteristic decay time. Equation 4.5 and Equation 4.6 were obtained from the potential data collected from the first probe and second probe and plugged in Equation 4.3. There are two unknown parameters (V_0 and t^*) with two equations. Therefore, initial potential and characteristic decay time can be calculated for 1,501 different points on the yarn.

$$V_{t_1} = V_0 \times e^{-\frac{t_1}{t^*}} \quad \text{.... (4.5)} \qquad\qquad V_{t_2} = V_0 \times e^{-\frac{t_2}{t^*}} \quad \text{.... (4.6)}$$

where, V_{t1} = potential at time t_1 (volt)
V_{t2} = potential at time t_2 (volt)
t_1 = time at the first probe (sec)
t_2 = time at the second probe (sec)
V_0 = initial potential (volt)
t^* = decay time (sec)

4.7. Statistical Analysis

4.7.1. Analysis of Variance and Pair-Wise Multiple Comparison

Analysis of Variance (ANOVA) was conducted on average initial potentials and characteristic decay times using SAS 9.1 software package. They were compared for the effect of independent parameters in each experimental design described in Table 4.2, Table 4.3, Table 4.4, and Table 4.6. Scheffe's method was chosen for pair-wise multiple comparisons. Confidence level of 5% was used in assessing whether the effects of parameters and their interactions are statistically significant.

4.7.2. Spectrum Analysis

Spectrum analysis was done on the signals collected from the potential probes. R 2.5.1 software (which is a product of Free Software Foundation) was used for this time series analysis. Potential signals were fairly stable and had periodical peaks. The peaks showed up more clearly with polymer charge pins than a stainless steel pin. Figure 4.15 shows the potential signal observed in time domain and its raw periodogram in frequency domain. Theoretically, periodogram tends to converse to zero when there is no periodicity at a given frequency [43]. Consequently, downward peaks reveal nothing about the periodicity.

Dominant times and frequencies (peaks) are indicated on Figure 4.15. For the frequency domain, only the first peaks on raw periodograms were pointed out because all other frequencies were the multiples of these peaks, which indicated that periodic peak repeated with multiple cycles. Peaks repeated in 0.45 seconds when the yarn was traveling 300 m/min. The peak intervals were 1.3 seconds for 100 m/min, and 2.7 seconds for 50

m/min. Frequency is the reciprocal of peak interval time (frequency = 1/1.3). Yarn length corresponding to peak interval can be calculated from the time of peak interval and yarn speed. This was found to be approximately 2.2 meters. Polyester, polypropylene, and Teflon pins had the time difference in the similar range between the peaks, and the yarn length was 2.1 meters (Figure 4.16).

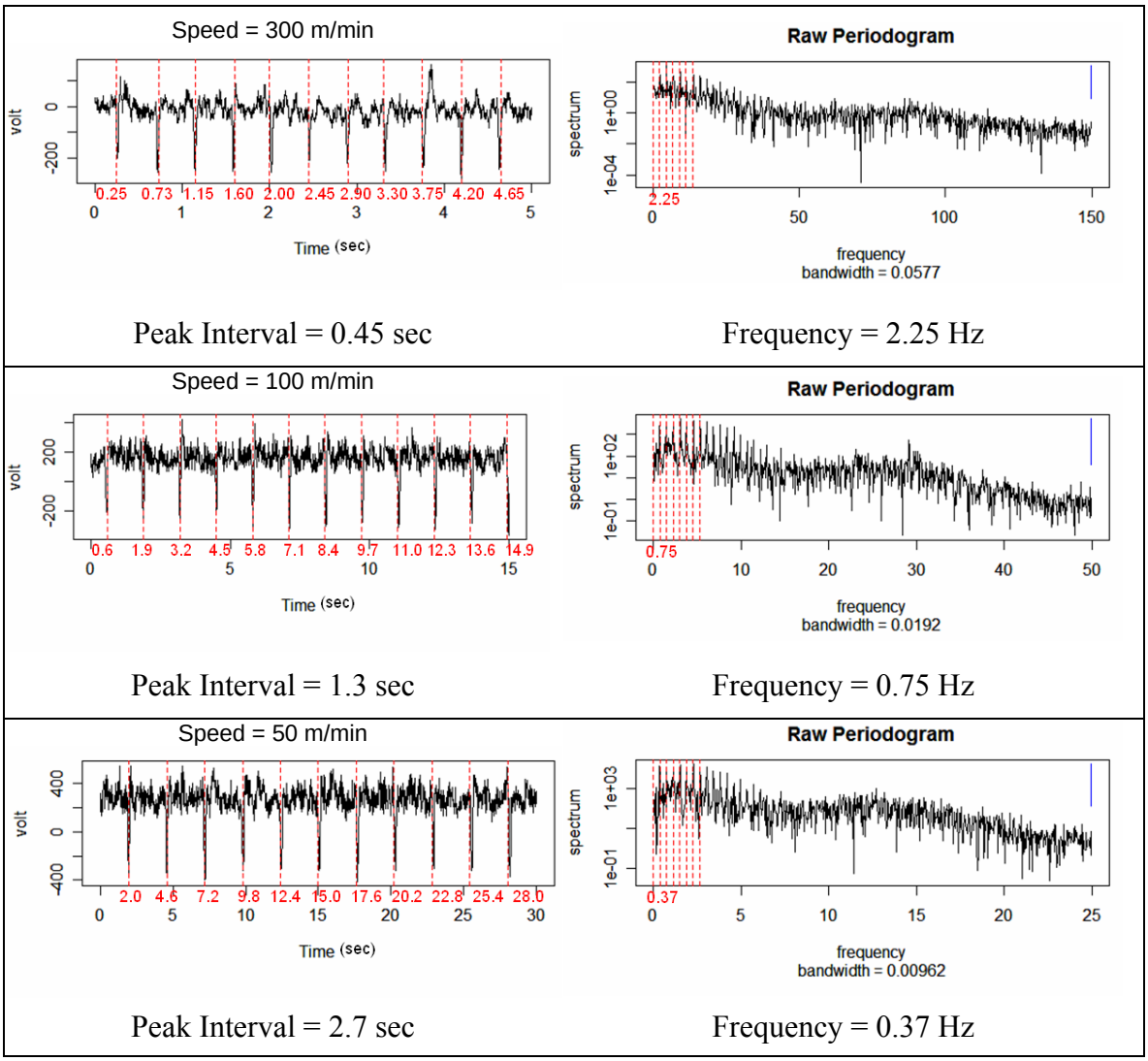

Figure 4.15. Spectrum analysis for nylon charge Pin
for 1000/140 polyester yarn with 1.35 gf/tex tension rubbed against a nylon charge pin at 30°C temperature and 30% humidity

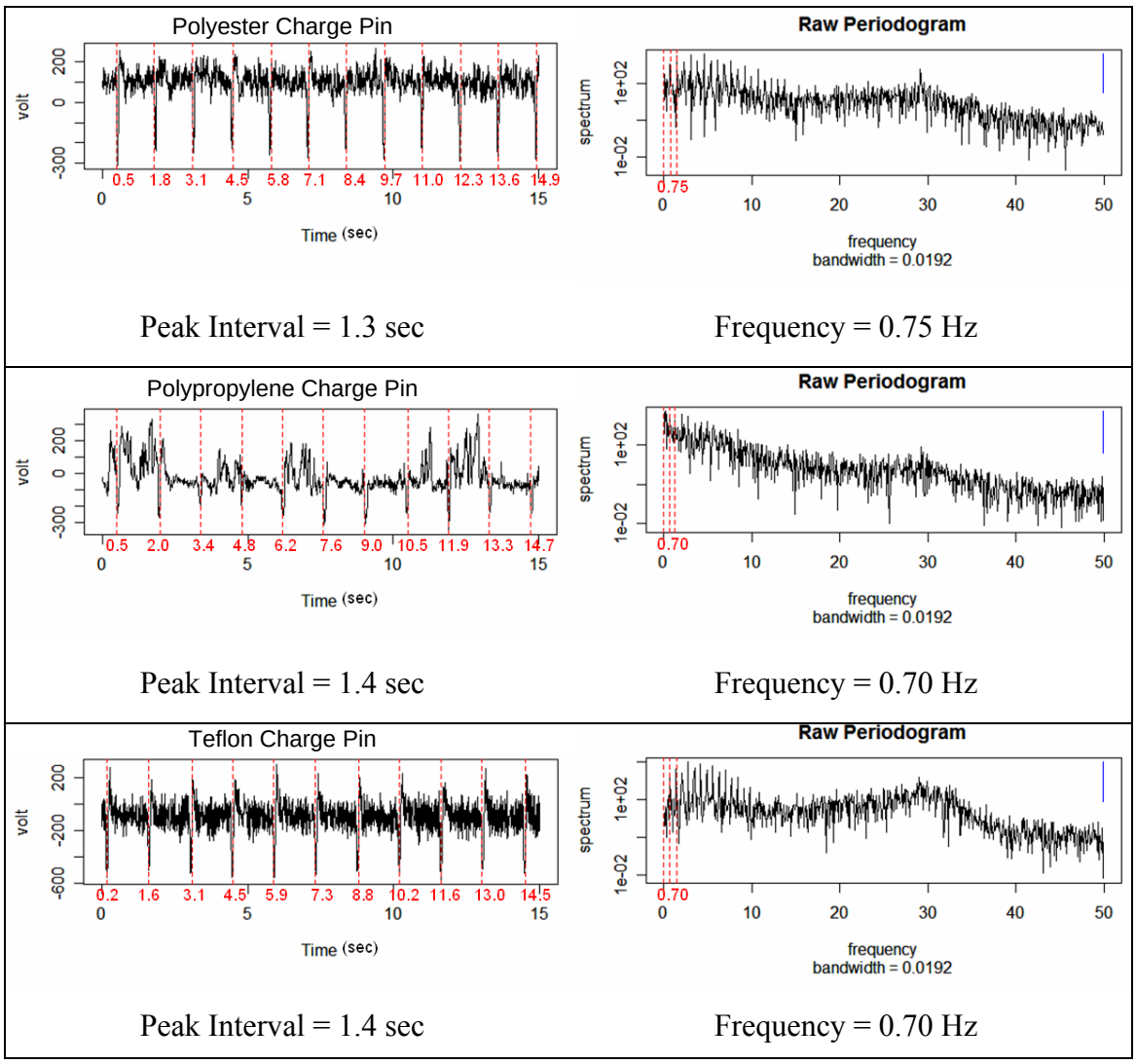

Figure 4.16. Spectrum Analysis with Other Polymer Pins at 100 m/min Speed for 1000/140 polyester yarn with 1.35 gf/tex tension and 100 m/min speed rubbed at 30°C temperature and 30% humidity

The source causing this periodicity was found to be the traverse of yarn during unwinding from the supply package (Figure 4.17). The yarn length per traverse is 2.1 meter (measured). After each traverse the traverse motion direction changes every 2.1 m of yarn. The yarn experiences sudden acceleration/deceleration at the points of direction change and

this caused high tension peaks. Potential peaks were resulted from tension variation. As it will be shown later in the results section, increase in tension causes increase in the potential.

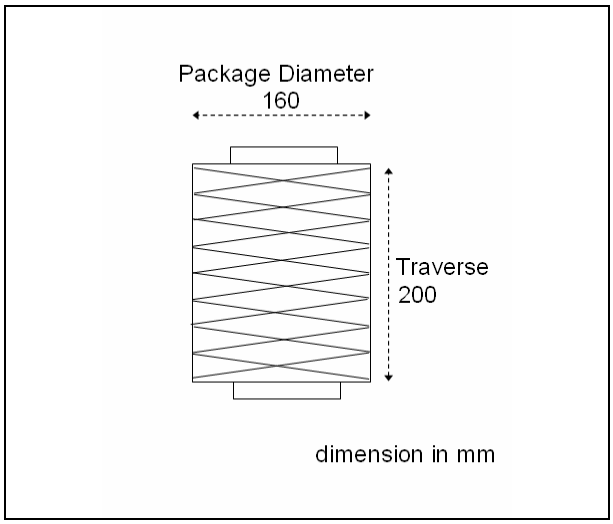

Figure 4.17. Supply package diameter at the time of test and traverse length

V. PRELIMINARY TEST

5.1. Charge Amount Measurement

Static generation happens when electrons are transferred between the surfaces in contact. Generally, an electron is believed to carry -1.6×10^{-19} coulombs of charge. Charge is defined as a fundamental property of subatomic particles, determining electromagnetic interaction and producing electromagnetic fields. Electric charge generates an electrical field around it, and the field strength is a measure of the amount of charge. Electric field strength can be evaluated by both charge amount (Q) and potential (V). They indicate the amount of static charges although they are different in concept. Charge is representing the amount of charges (or electrons) exchanged, while potential is measuring potential energy generated by electron exchange.

5.1.1. Charge Amount vs. Potential

A Faraday Tube is designed to isolate the outer environment and enable the assessment of the charge present inside. A Faraday Tube consists of two concentric cylindrical vessels, inner and outer, measuring voltage (V). Then, the voltage is converted to charge amount (Q) using the formula Q = CV, where C is the known capacitance of the tube [32].

The Faraday Tube was installed between the two potential probes (Figure 5.1 and Figure 5.2) in order to simultaneously measure charge amount as well as potentials on dynamic yarns. A coulometer and a voltmeter simultaneously made 100 and 1500 measurements during 30 seconds. These two measurements were compared (Table 5.1).

Overall correlation coefficient was as high as 0.9819, and the coefficients tended to decrease as relative humidity increased. Positive charges observed under the low yarn speed implied that there was no actual charge generation because the potential signal was observed to have random oscillations between -10 and +10 volts after zeroing voltmeter. As a result, we could conclude that both charge amount and potential measurements were good indicators for static charge observation.

5.1.2. Faraday Tube Length

Two Faraday Tubes having different length were tried in order to compare the accuracy of the charge amount measurement as a function of tube length. A shorter tube was 10 cm long, and a longer tube was 25 cm long, which meant they are measuring charge amounts on the 10cm yarn and 25 cm yarn, respectively. Dimensions on the device are given in Figure 5.1 and Figure 5.2, respectively. For the comparison, charge amount captured in shorter and longer Faraday Tubes was converted to average charge per 1 cm yarn.

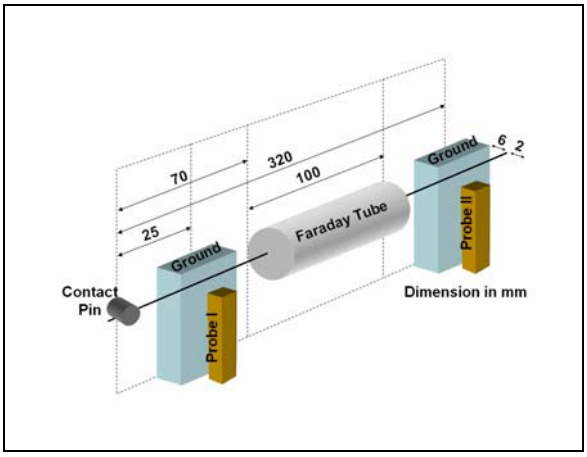

Figure 5.1. Dimensions with Shorter Tube

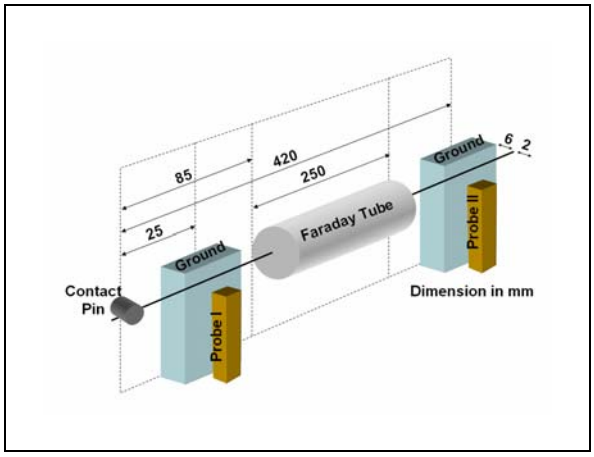

Figure 5.2. Dimensions with Longer Tube

Table 5.1. Static Charge Comparison between Charge Amount and Potential

		25°C, 40% R.H.		25°C, 50% R.H.		25°C, 65% R.H.	
tension (gf)	speed (m/min)	Charge (nC)	Potential (volt)	Charge (nC)	Potential (volt)	Charge (nC)	Potential (volt)
150	300	-1.2092	-1602.9	-1.0977	-1421.6	-0.8462	-1248.0
100	300	-0.8122	-1125.0	-0.7232	-1185.2	-0.4161	-683.9
75	300	-0.5351	-806.3	-0.4771	-683.1	-0.0856	-538.9
50	300	-0.2803	-466.8	-0.2376	-414.6	-0.2078	-329.2
150	100	-0.9952	-1587.6	-0.8570	-1314.4	-0.5230	-755.4
100	100	-0.6529	-1142.2	-0.5818	-817.7	-0.3659	-604.5
75	100	-0.4011	-728.3	-0.3863	-661.2	-0.1967	-378.5
50	100	-0.1630	-407.9	-0.1641	-341.8	-0.0705	-204.2
150	50	-0.6655	-983.5	-0.4808	-704.2	-0.0819	-173.4
100	50	-0.4222	-724.3	-0.3430	-566.3	-0.0648	-172.1
75	50	-0.2909	-554.2	-0.1590	-343.1	0.0280	-87.0
50	50	-0.0898	-273.1	-0.0282	-195.9	0.0796	-40.0
150	10	0.2408	-18.2	0.3980	-1.3	0.2143	1.0
100	10	0.2075	-1.6	0.2401	2.3	0.1215	2.0
75	10	0.1522	3.5	0.1829	6.1	0.1142	1.8
50	10	0.1518	6.5	0.1687	8.8	0.1628	1.7
Correlation Coefficient		0.9899		0.9809		0.9693	
Overall Coefficient		0.9819					

Static charge and charge per cm measured with the shorter tube and the longer tube did not show any significant difference (Table 5.2 and Table 5.3). One measurement with the shorter tube was omitted because a serious measurement error was found in that experimental run. Overall correlation coefficient was high. As relative humidity increased, the correlation

coefficients were observed to decrease just as those between charge amount and potential measurements did. Positive charge polarity was observed again under the low yarn speed, which meant no charge generation.

Table 5.2. Charge Amount Comparison between Short and Long Tubes unit : pC

tension	speed	25°C 40% R.H.		25°C 50% R.H.		25°C 65% R.H.	
(gf)	(m/min)	10cm	25cm	10cm	25cm	10cm	25cm
150	300	-120.6	-94.0	-110.0	-84.0	-84.9	-75.2
100	300	-81.0	-66.4	-72.2	-61.2	-41.3	-52.8
75	300	-53.4	-50.0	-47.7	-44.4	-8.6	-36.9
50	300	-28.0	-31.2	-23.8	-27.8	-20.6	-21.1
150	100	-99.5	-83.2	-84.6	-70.8	-53.0	-51.2
100	100	-64.9	-54.4	-58.4	-50.4	-37.0	-38.7
75	100	-39.6	-42.8		-36.8	-19.0	-22.8
50	100	-16.2	-25.6	-16.1	-21.6	-7.0	-8.4
150	50	-68.0	-64.0	-48.3	-45.6	-8.1	-15.0
100	50	-42.5	-41.2	-35.0	-32.1	-6.1	-9.0
75	50	-29.1	-28.2	-15.2	-21.5	2.6	-5.7
50	50	-8.7	-14.8	-2.7	-11.3	8.0	0.6
150	10	24.1	-1.4	39.7	2.5	21.4	8.6
100	10	20.7	1.7	24.0	2.4	12.2	4.4
75	10	15.2	4.7	18.3	1.6	11.4	3.8
50	10	15.3	5.5	16.9	0.9	16.3	5.2
Correlation Coefficient		0.9931		0.9925		0.9630	
Overall Coefficient		0.9816					

Table 5.3. Charge Amount per Unit Length unit :pC/cm

tension	speed	25°C 40% R.H.		25°C 50% R.H.		25°C 65% R.H.	
(gf)	(m/min)	10cm	25cm	10cm	25cm	10cm	25cm
150	300	-12.1	-3.8	-11.0	-3.4	-8.5	-3.0
100	300	-8.1	-2.7	-7.2	-2.4	-4.1	-2.1
75	300	-5.3	-2.0	-4.8	-1.8	-0.9	-1.5
50	300	-2.8	-1.2	-2.4	-1.1	-2.1	-0.8
150	100	-9.9	-3.3	-8.5	-2.8	-5.3	-2.0
100	100	-6.5	-2.2	-5.8	-2.0	-3.7	-1.5
75	100	-4.0	-1.7	0.0	-1.5	-1.9	-0.9
50	100	-1.6	-1.0	-1.6	-0.9	-0.7	-0.3
150	50	-6.8	-2.6	-4.8	-1.8	-0.8	-0.6
100	50	-4.2	-1.6	-3.5	-1.3	-0.6	-0.4
75	50	-2.9	-1.1	-1.5	-0.9	0.3	-0.2
50	50	-0.9	-0.6	-0.3	-0.5	0.8	0.0
150	10	2.4	-0.1	4.0	0.1	2.1	0.3
100	10	2.1	0.1	2.4	0.1	1.2	0.2
75	10	1.5	0.2	1.8	0.1	1.1	0.2
50	10	1.5	0.2	1.7	0.0	1.6	0.2
Correlation Coefficient		0.9931		0.9925		0.9630	
Overall Coefficient		0.9816					

5.2. Data Collection Rate

Potential measurements were tried with and without the adjustment of data collection rate, and they were compared. The adjustment implies to have an observation with high

resolution for fast yarn speed, so that there could be equal intervals of yarn length between the measurements. Without adjustment, uniform rate of data collection was applied for all kinds of speed for the purpose to have equal intervals of time between measurements. Data collection rate for each yarn speed, consequent time durations, number of observation, and yarn lengths are in Table 5.4 and Table 5.5.

Table 5.4. Rate of data collection in terms of speed

	300 m/min	100 m/min	50 m/min	10 m/min
Time Duration (second)	5	15	30	150
Number of Observations	1,501	1,501	1,501	1,501
Yarn Length (m)	25	25	25	25
Data Collection Rate (per second)	300	100	50	10

Table 5.5. Constant rate of data collection

	300 m/min	100 m/min	50 m/min	10 m/min
Time Duration (second)	15	15	15	15
Number of Observations	1,501	1,501	1,501	1,501
Yarn Length (m)	75	25	12.5	2.5
Data Collection Rate (per second)	100	100	100	100

Table 5.6 is comparing the measurements with and without the adjustment of data collection rate. Potential signals from both potential probes were highly correlated. Correlation coefficients of initial potentials and decay times calculated from each experimental result were high (Table 5.7). Therefore, we could conclude that rate of data

collection did not affect the potential signals on continuous filament yarns. This conclusion is only valid for the range of yarns used. Spun yarns are inherently irregular and may require same number of data points/unit yarn length for fair comparison. Additionally, more data points may need to be acquired since long term variation in mass/unit length of the yarn may exist.

Table 5.6. Measurement Comparison unit : volt

Yarn Speed	First Probe		Second Probe	
(m/min)	Adjusted Rate	Unadjusted Rate	Adjusted Rate	Unadjusted Rate
300	-758.4	-729.1	-378.6	-366.1
100	-545.8	-562.6	-282.3	-288.0
50	-308.4	-318.1	-163.3	-170.9
Correlation Coefficient	0.9985		0.9970	
Overall Coefficient	0.9977			

Table 5.7. Calculation Comparison unit : volt

Yarn Speed	Initial Potential		Decay Time	
(m/min)	Adjusted Rate	Unadjusted Rate	Adjusted Rate	Unadjusted Rate
300	-792.7	-761.8	0.1167	0.1173
100	-569.3	-587.3	0.3666	0.3624
50	-321.2	-331.0	0.7648	0.7762
Correlation Coefficient	0.9969		0.9999	

5.3. Friction Coefficient Measurement

As shown in Equation 5.1, the friction coefficient is defined as the ratio of the friction force between surfaces to the normal force. It is determined by a pair of surface property in contact, regardless of their dimensional property. When a sample yarn passes around a charge pin (Figure 5.3), output tension must be increased in order to overcome the frictional resistance between the yarn and the pin. Equation 5.2 describes how to get kinetic friction coefficient on a yarn.

$$\mu = \frac{N}{F} = \frac{mg}{F} \qquad (5.1)$$

where, μ = coefficient of friction

m = mass (g)

g = acceleration of gravity (g/sec)

N = normal force (N)

F = friction force (N)

$$e^{\mu\theta} = \frac{T_2}{T_1} \qquad (5.2)$$

where, μ = coefficient of friction

θ = angle of contact (rad)

T_1 = incoming tension (gf)

T_2 = leaving tension (gf)

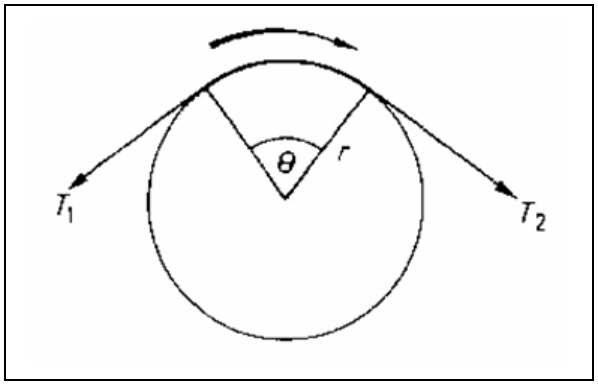

Figure 5.3. Friction in Yarn [36]

Output tension on the polyester sample yarn was measured with changes of input tension and yarn speed for five different kinds of charge pin. Input tension was measured on the yarn approximately 5cm before the charge pin, and output tension was measured on the yarn approximately 10cm after the charge pin. A tensionmeter, described in Figure 4.10, was used. Tension was monitored during 10 seconds, and average value was used. Contact angle on linear tester was kept as 120°. Output tension data are given in Table 5.8. Friction coefficients, calculated from the Equation 5.2, are given in Table 5.9.

The effects of input tension and yarn speed on friction coefficients were illustrate in Figure 5.4 for five different charge pins. Growing input tension seemed to lead to a reduction in friction coefficients, but friction increased with yarn speed increase. The effect of input tension was relatively greater on the Teflon pin, and smaller on the Nylon and PET pins. Teflon and polypropylene pins showed higher friction, while Nylon and polyester had lower friction. Stainless steel was located in the middle. From repeated measurements of friction coefficient, polypropylene appeared to have outliers compared to other polymer pins, which means yarn tension was hard to be controlled on it (Figure 5.5).

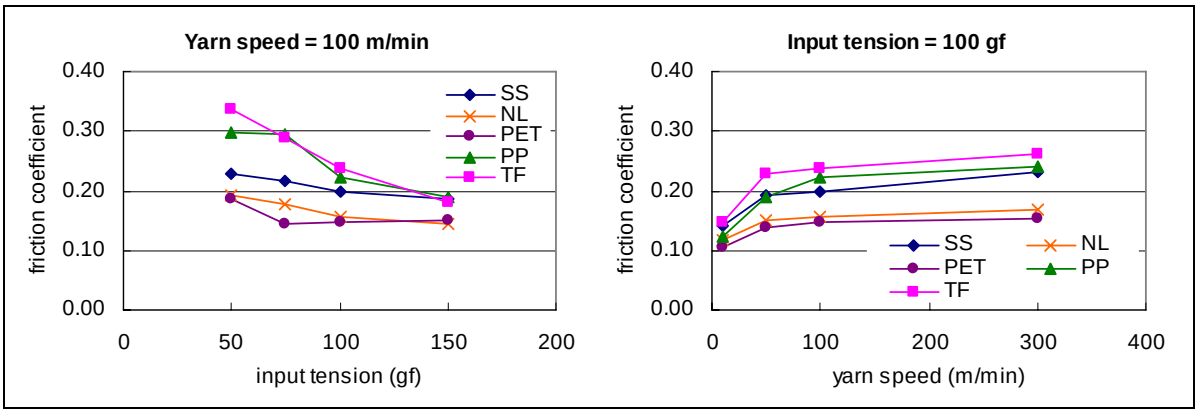

Figure 5.4. Effect of Tension and Speed on Friction Coefficient
(Abbreviations: SS=stainless steel, NL=nylon, TF=Teflon)

Table 5.8. Output Tension of 1000/140 PET yarn against Different Charge Pins

unit : gf

input tension (gf)	yarn speed (m/min)	Stainless Steel	Nylon	Polyester	Poly Propylene	Teflon
150	300	222.5	206.0	208.9	295.1	229.3
100	300	162.1	142.0	138.1	165.5	173.2
75	300	126.1	111.3	105.4	144.5	140.3
50	300	86.0	75.8	76.6	98.8	103.9
150	100	221.9	203.4	205.0	223.4	219.4
100	100	151.4	139.0	136.4	159.2	164.7
75	100	118.1	108.7	101.5	138.8	137.1
50	100	80.7	74.9	74.1	93.3	100.9
150	50	212.2	197.8	196.3	214.8	215.8
100	50	150.0	137.2	133.5	149.1	161.4
75	50	115.3	107.6	97.6	118.3	133.8
50	50	78.2	73.7	71.3	81.0	96.4
150	10	193.5	189.7	189.2	188.2	187.1
100	10	134.3	127.7	124.6	129.4	135.8
75	10	101.0	99.2	89.4	103.3	110.5
50	10	66.5	66.3	63.3	76.9	76.9

Table 5.9. Friction Coefficient of 1000/140 PET yarn against Different Charge Pins

input tension (gf)	yarn speed (m/min)	Stainless Steel	Nylon	Polyester	Poly Propylene	Teflon
150	300	0.1884	0.1515	0.1582	0.3233	0.2027
100	300	0.2308	0.1675	0.1542	0.2407	0.2624
75	300	0.2482	0.1886	0.1626	0.3133	0.2992
50	300	0.2591	0.1988	0.2038	0.3254	0.3494
150	100	0.1871	0.1455	0.1492	0.1903	0.1817
100	100	0.1981	0.1573	0.1483	0.2221	0.2384
75	100	0.2169	0.1773	0.1445	0.2941	0.2882
50	100	0.2287	0.1931	0.1879	0.2980	0.3354
150	50	0.1657	0.1321	0.1285	0.1715	0.1738
100	50	0.1937	0.1511	0.1380	0.1908	0.2287
75	50	0.2054	0.1724	0.1258	0.2177	0.2765
50	50	0.2137	0.1853	0.1695	0.2305	0.3136
150	10	0.1216	0.1122	0.1109	0.1084	0.1056
100	10	0.1409	0.1168	0.1051	0.1231	0.1462
75	10	0.1422	0.1336	0.0839	0.1529	0.1851
50	10	0.1362	0.1348	0.1127	0.2056	0.2056

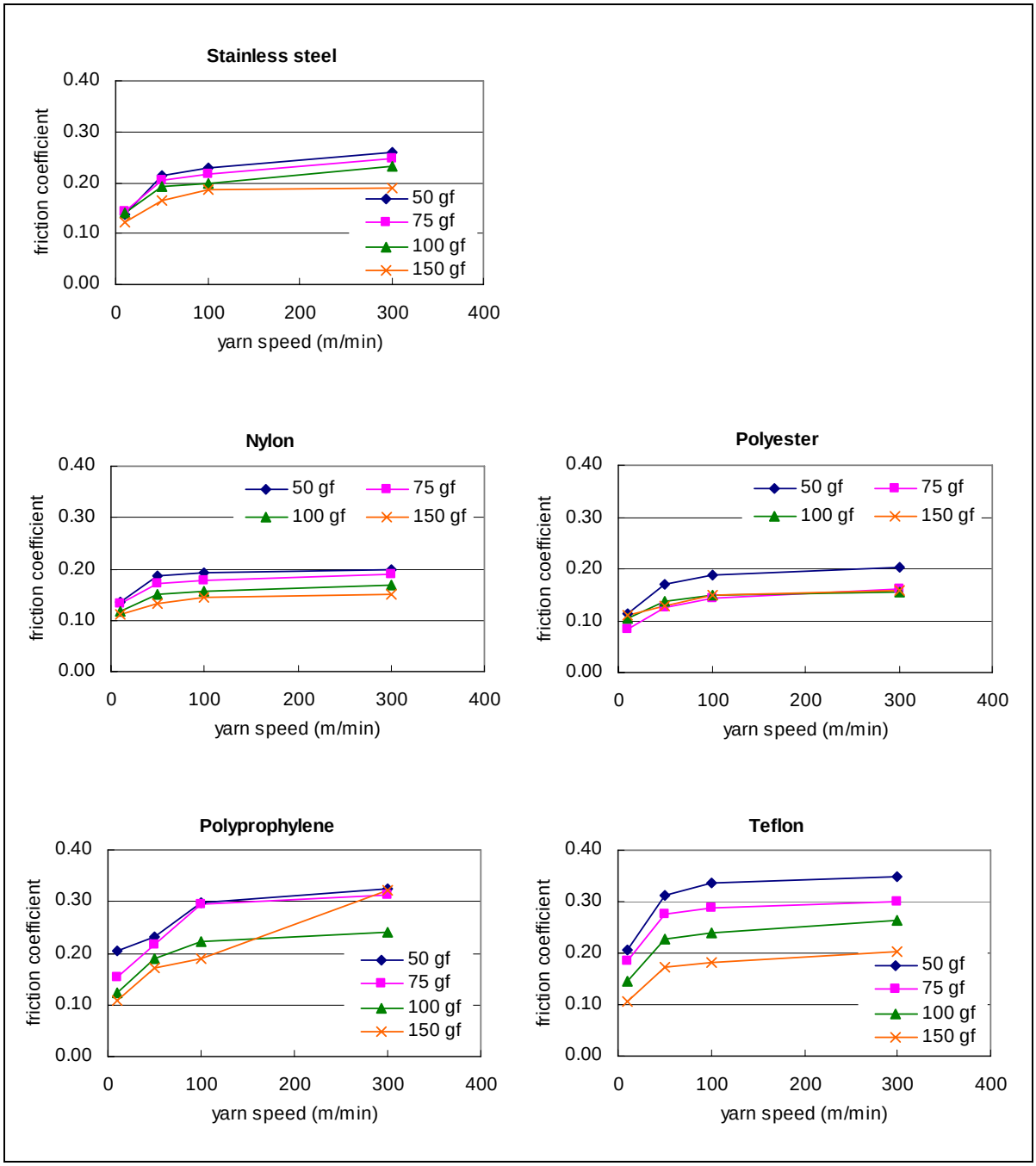

Figure 5.5. Friction Coefficients of PET yarns running against Polymer Charge Pins

VI. RESULTS AND DISCUSSION

6.1. Experimental Design I

6.1.1. Statistical Analysis

Data of 119 runs (out of 224) of initial potentials and decay times were examined with analysis of variance and Scheffe's multiple mean comparison. Data of runs with 35°C (64) were not included to the statistical analysis because response calculation was not possible with charge increase at the second probe compared to first probe at such temperature level. The initial potential and characteristic decay time are calculated from Equation 4.3 and data collected from the two probes (Figure 4.3). The equation is based on charge decay (reduction) as a function of time. Since the data at 35°C exhibited charge increase (not decay), the Equation 4.3 is not valid.

Additionally, data of 41 runs were excluded from statistical analysis because for some runs charges at first probe and second probe are of different polarity, which does not follow Equation 4.3 (charge reaches to zero value after extremely long time). For other runs the charge at the first probe and/or the second probe was extremely low. They were 1 set with 50 m/min yarn speed, and 40 sets with 10 m/min yarn speed. Under the low yarn speed, no static charge was generated, or static charge was almost dissipated before the yarn reached the second probe. Experimental responses input to ANOVA are given in Appendix A-1.

The results compared the initial potentials and decay times in terms of temperature, humidity, yarn tension, yarn speed, and their interactions. ANOVA results are given in Table 6.1 for initial potential and in Table 6.4 and for decay time, respectively. All the parameters and interactions appeared to be significant for initial potential model (Table 6.2 and Table

6.3), while decay time model was significant with only 3 parameters and 2 parameter interactions, which were temperature, humidity, speed, temperature*humidity, and humidity*tension (Table 6.5 and Table 6.6).

Table 6.1.Overall ANOVA for Initial Potential

Source	DF	Sum of Squares	Mean Square	F-value	Pr > F
Model	45	16601649.45	368925.54	58.99	<.0001
Error	73	456528.93	6253.82		
Corrected Total	118	17058178.38			

Table 6.2. Type I ANOVA for Initial Potential

Source	DF	Type I SS	Mean Square	F-value	Pr > F
temperature	**2**	**1772779.175**	**886389.588**	**141.74**	**<.0001**
humidity	**3**	**2181573.892**	**727191.297**	**116.28**	**<.0001**
tension	**3**	**6849127.224**	**2283042.408**	**365.06**	**<.0001**
speed	**2**	**3834316.491**	**1917158.246**	**306.56**	**<.0001**
temp.*hum.	**4**	**440107.719**	**110026.930**	**17.59**	**<.0001**
tension*speed	**6**	**482982.508**	**80497.085**	**12.87**	**<.0001**
temp.*tension	**6**	**435044.461**	**72507.410**	**11.59**	**<.0001**
temp.*speed	**4**	**86706.806**	**21676.701**	**3.47**	**0.0120**
hum.*tension	**9**	**354613.248**	**39401.472**	**6.30**	**<.0001**
hum.*speed	**6**	**164397.924**	**27399.654**	**4.38**	**0.0008**

Table 6.3. Type III ANOVA for Initial Potential

Source	DF	Type III SS	Mean Square	F-value	Pr > F
temperature	**2**	**2219548.990**	**1109774.495**	**177.46**	**<.0001**
humidity	**3**	**2253689.625**	**751229.875**	**120.12**	**<.0001**
tension	**3**	**5712109.024**	**1904036.341**	**304.46**	**<.0001**
speed	**2**	**2700157.060**	**1350078.530**	**215.88**	**<.0001**
temp.*hum.	**4**	**459479.083**	**114869.771**	**18.37**	**<.0001**
tension*speed	**6**	**516974.384**	**86162.397**	**13.78**	**<.0001**
temp.*tension	**6**	**459884.760**	**76647.460**	**12.26**	**<.0001**
temp.*speed	**4**	**78716.511**	**19679.128**	**3.15**	**0.0192**
hum.*tension	**9**	**338660.743**	**37628.971**	**6.02**	**<.0001**
hum.*speed	**6**	**164397.924**	**27399.654**	**4.38**	**0.0008**

Table 6.4. Overall ANOVA for Decay Time

Source	DF	Sum of Squares	Mean Square	F-value	Pr > F
Model	45	37.35549421	0.83012209	16.17	<.0001
Error	73	3.74798468	0.05134226		
Corrected Total	118	41.10347889			

Table 6.5. Type I ANOVA for Decay Time

Source	DF	Type I SS	Mean Square	F-value	Pr > F
temperature	**2**	**2.44635885**	**1.22317943**	**23.82**	**<.0001**
humidity	**3**	**1.67998741**	**0.55999580**	**10.91**	**<.0001**
tension	3	0.17272535	0.05757512	1.12	0.3461
speed	**2**	**25.97917785**	**12.98958892**	**253.00**	**<.0001**
temp.*hum.	**4**	**2.59372030**	**0.64843008**	**12.63**	**<.0001**
tension*speed	6	0.08337425	0.01389571	0.27	0.9489
temp.*tension	6	0.26654410	0.04442402	0.87	0.5246
temp.*speed	4	0.21519588	0.05379897	1.05	0.3886
hum.*tension	9	0.47249593	0.05249955	1.02	0.4305
hum.*speed	**6**	**3.44591429**	**0.57431905**	**11.19**	**<.0001**

Table 6.6. Type III ANOVA for Decay Time

Source	DF	Type III SS	Mean Square	F-value	Pr > F
temperature	**2**	**1.38034473**	**0.69017237**	**13.44**	**<.0001**
humidity	**3**	**1.67846046**	**0.55948682**	**10.90**	**<.0001**
tension	3	0.13511829	0.04503943	0.88	0.4570
speed	**2**	**17.51274489**	**8.75637245**	**170.55**	**<.0001**
temp.*hum.	**4**	**2.64484017**	**0.66121004**	**12.88**	**<.0001**
tension*speed	6	0.13550374	0.02258396	0.44	0.8498
temp.*tension	6	0.14937032	0.02489505	0.48	0.8176
temp.*speed	4	0.23652580	0.05913145	1.15	0.3393
hum.*tension	9	0.54497517	0.06055280	1.18	0.3210
hum.*speed	**6**	**3.44591429**	**0.57431905**	**11.19**	**<.0001**

For further investigation, multiple comparison analyses were conducted using Scheffe's method. Pair-wise multiple comparisons are displayed in Table 6.7, Table 6.8, Table 6.9, and Table 6.10. According to Scheffe, initial potentials at 21° and 25°C were not significantly different (Table 6.7). Significant difference was found only at 30°C (lower potential). Decay time was the longest at 25°C, and shortest at 30°C (Table 6.8). For the effect of humidity, initial potentials under 30% R.H. and 50% R.H. were not significantly different (Table 6.9). No significant difference in decay time was found between 40% R.H. and 50% R.H. (Table 6.10). Other multiple comparisons of significant parameters, not mentioned, were statistically different or identical for all pair-wise comparisons.

Table 6.7. Scheffe's Multiple Temperature Comparisons for Initial Potential

Temperature Comparison	Difference Between Means	Simultaneous 95% Confidence Limits		
21-25	36.49	-10.08	83.07	
21-30	-229.74	-273.51	-185.97	***
25-30	-266.23	-310.00	-222.47	***

*** indicates the difference is significant

Table 6.8. Scheffe's Multiple Temperature Comparisons for Decay Time

Temperature Comparison	Difference Between Means	Simultaneous 95% Confidence Limits		
21-25	-0.15309	-0.28655	-0.01963	***
21-30	0.19028	0.06487	0.31568	***
25-30	0.34336	0.21796	0.46877	***

*** indicates the difference is significant

Table 6.9. Scheffe's Multiple Humidity Comparisons for Initial Potential

Humidity Comparison	Difference Between Means	Simultaneous 95% Confidence Limits		
30-40	178.98	103.54	254.42	***
30-50	-12.03	-87.47	63.41	
30-65	-137.43	-213.14	-61.73	***
40-50	-191.01	-244.35	-137.67	***
40-65	-316.42	-370.14	-262.69	***
50-65	-125.41	-179.13	-71.68	***

*** indicates the difference is significant

Table 6.10. Scheffe's Multiple Humidity Comparisons for Decay Time

Humidity Comparison	Difference Between Means	Simultaneous 95% Confidence Limits		
30-40	-0.46653	-0.68269	-0.25038	***
30-50	-0.47073	-0.68689	-0.25458	***
30-65	-0.26233	-0.47925	-0.04540	***
40-50	-0.00420	-0.15704	0.14864	
40-65	0.20421	0.05028	0.35814	***
50-65	0.20841	0.05448	0.36234	***

*** indicates the difference is significant

6.1.2. Effect of Temperature

The effect of temperature on initial potential is shown in Figure 6.1. In general, the initial potentials decreased as temperature went up. Scheffe's comparisons (Table 6.7) showed that there is no significant difference between temperature 21°C and 25°C on the initial potential. However, the initial potential at 30°C was significantly lower. The effect of temperature on decay time was not gradual. Generally, decay time was the longest at 25°C, and shortest at 30°C (Figure 6.2).

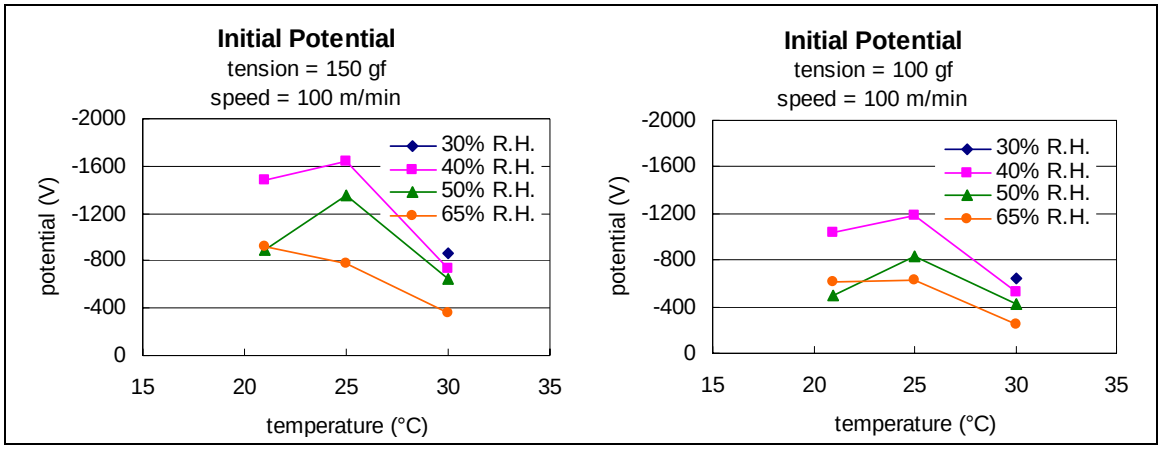

Figure 6.1. Effect of Temperature on Initial Potential

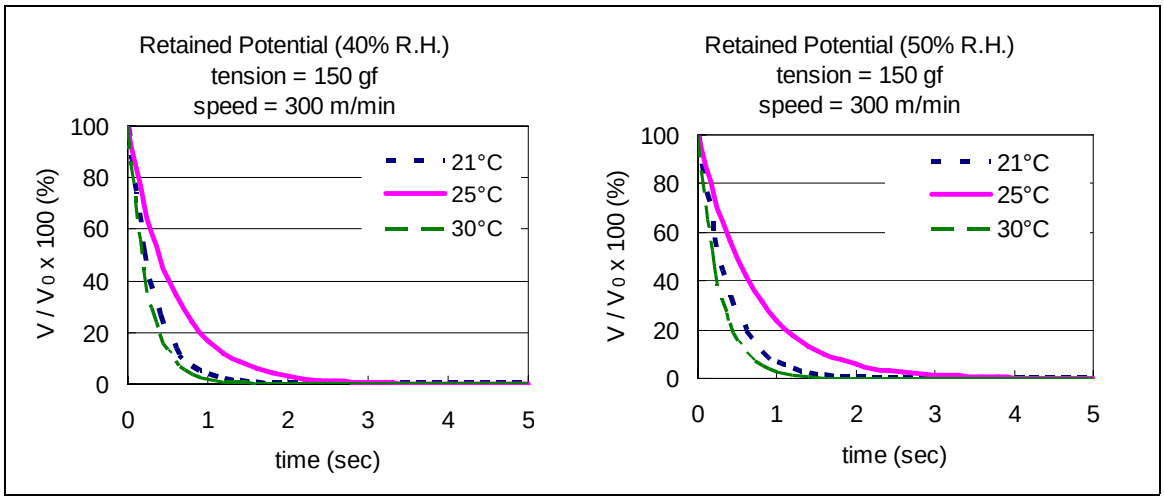

Figure 6.2. Effect of Temperature on Decay Time
(Calculated and visualized from Equation 4.1 and Equation 4.2)

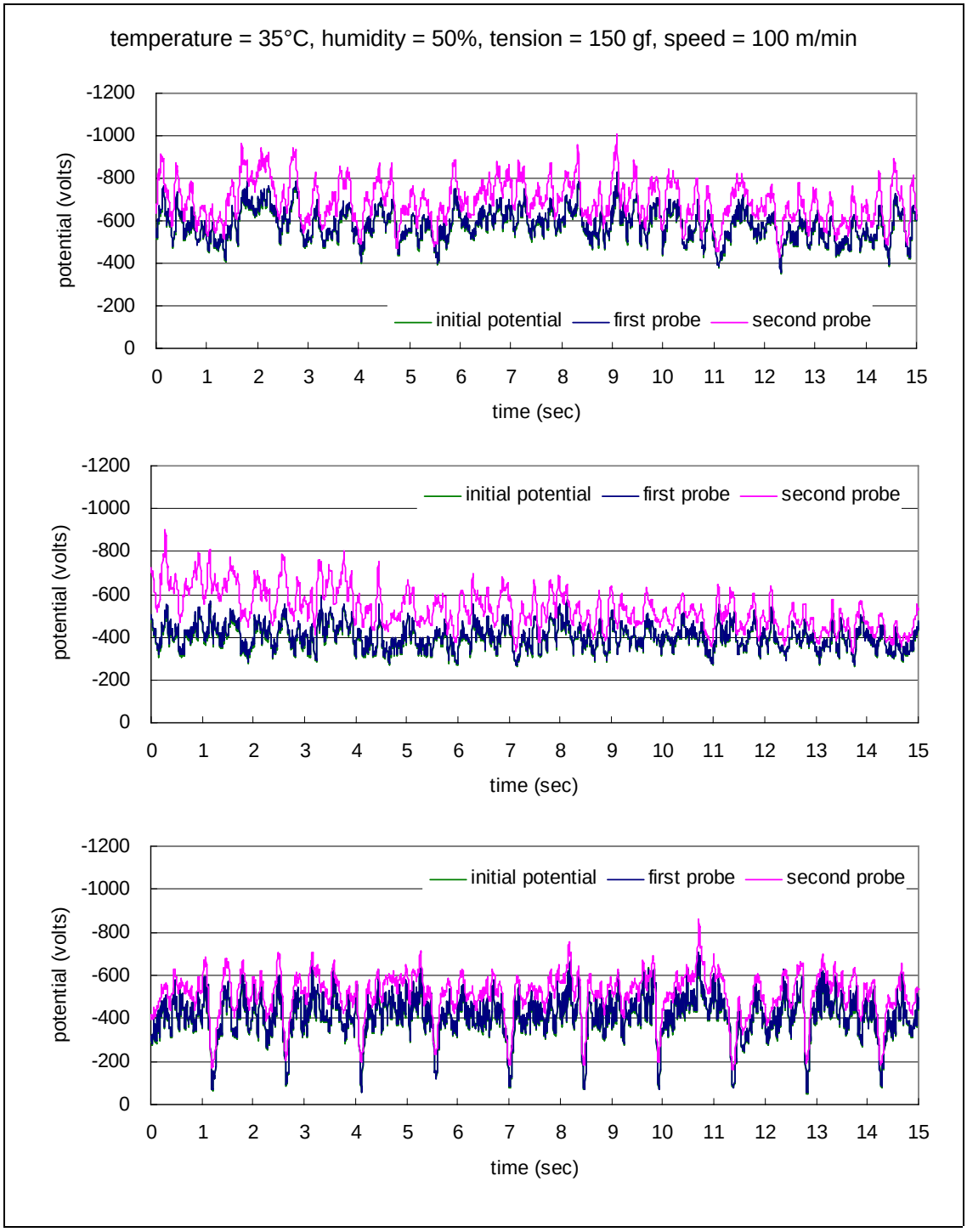

Figure 6.3. Potential Signals from Two Probes at Repeated Experiments

Charge decay behavior did not follow the trend at 35°C. Higher voltages were observed at the second probe than the first probe, which meant potential did not decease with time but increased. It was thought that the runs with this temperature are related to hidden reason. The runs were repeated twice at different times and the results were consistently same (Figure 6.3). Further investigation is required to figure out how the charge on the yarn increases as the yarn is moving due to yarn contact with air at such level of temperature. Observation on the stationary sample yarn supported this idea as it can be seen from Figure 6.4 and Figure 6.5, which display the potential measurements acquired from the first and second probes after stopping. The figures show the charge decayed with time as expected.

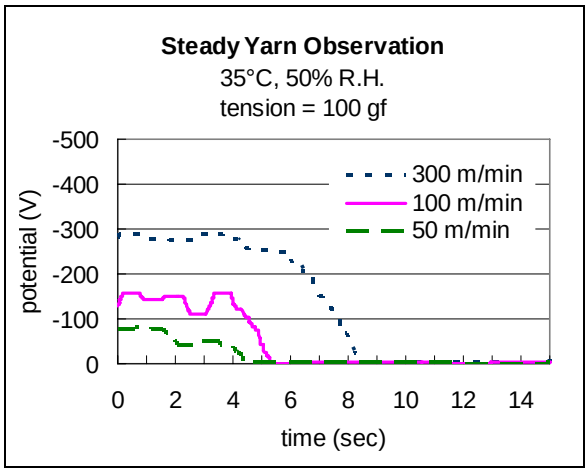

Figure 6.4. Steady Yarn Observation from the first probe

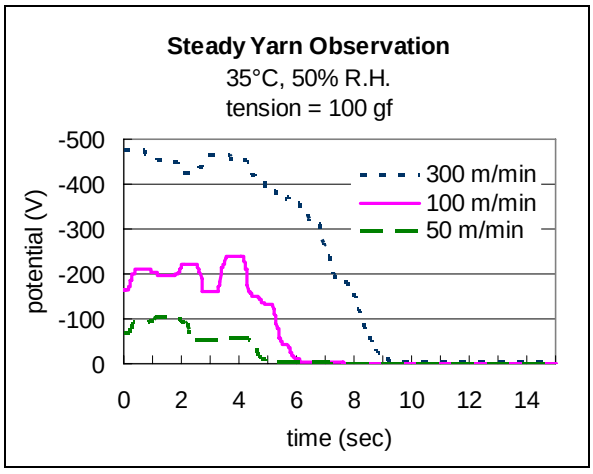

Figure 6.5. Steady Yarn Observation from the second probe

6.1.3. Effect of Humidity

It must be emphasized that the effect of temperature is confounded by the effect of humidity because, theoretically, the amount of moisture existing in the air is more under higher temperature than lower temperature at a given relative humidity. In general, potentials fell down as humidity increased (Figure 6.6). The fact that less static was generated under

higher humidity was clearly distinguished and is in concordance the great store of knowledge accumulated by previous studies. There was statistical evidence (Table 6.5 and Table 6.6) that humidity affects static decay time. Generally, decay time was the shortest at 30% R.H., but there was no significant difference between 40% R.H. and 50% R.H. (Figure 6.7) and Schefffe's analysis supports this fact (Table 6.10).

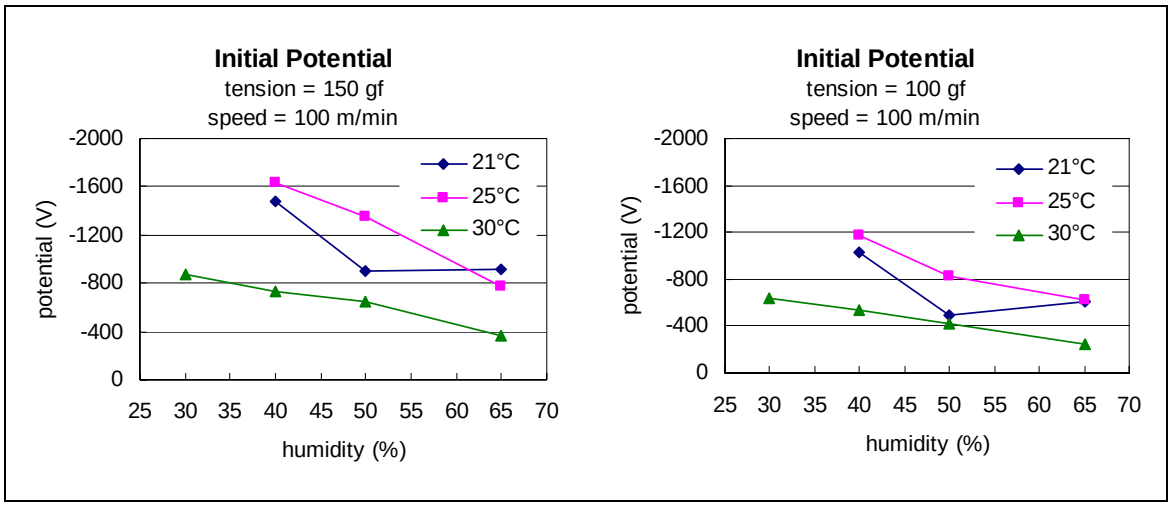

Figure 6.6. Effect of Humidity on Initial Potential

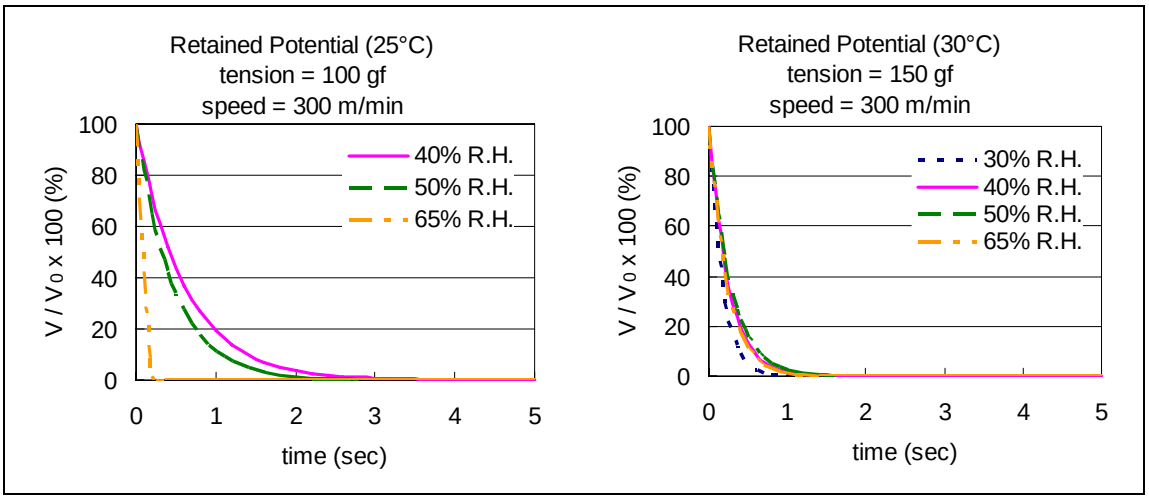

Figure 6.7. Effect of Humidity on Decay Time

6.1.4. Effect of Yarn Tension

Figure 6.8 and Figure 6.9 show the effect of yarn tension on initial potential at different temperature, humidity, and speed. The yarn tension and its interactions with temperature, humidity, and yarn speed can be seen clearly from the figures. The data of the figures support the ANOVA results of Table 6.2 and Table 6.3. Higher tension on the sample yarn resulted in more potential, and the magnitude of this effect was systematically influenced by the temperature, humidity, and speed. Effect of yarn tension was more pronounced when temperature and humidity were lower, and yarn speed was higher.

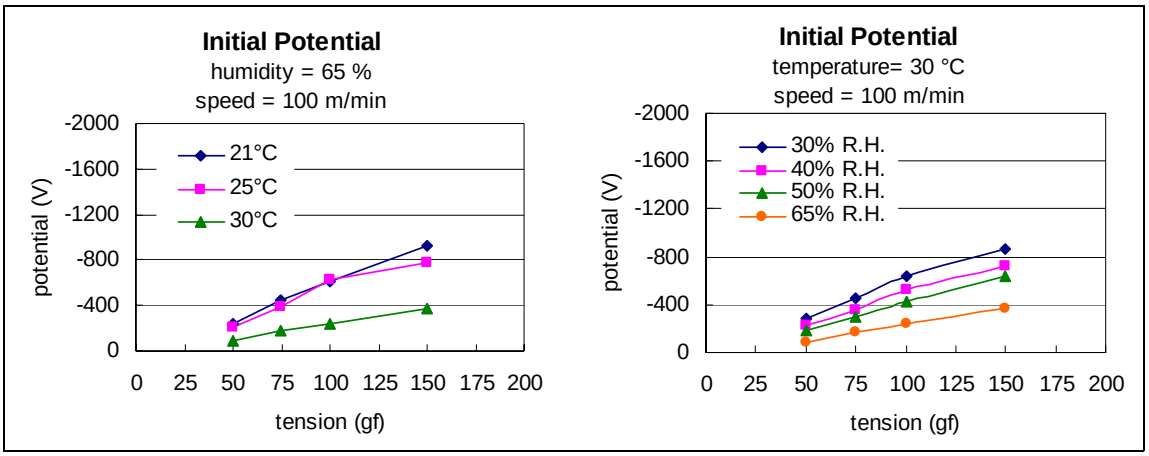

Figure 6.8. Effect of Yarn Tension on Initial Potential

These findings are supported by former studies [22]. Contact area is known to be proportional to the normal contact force [36]. Increase in yarn tension enlarged the contact area between a charge pin and the yarn due to yarn flattening as a result of spreading the filaments on the charge pin. Minor flattening of individual filament may also have taken place by tension increase. The degree of yarn flattening increases with yarn tension. Increased contact area gives the yarn more chance to exchange charges. This explanation is

supported by the former study of Elsdon and Mitchell [22], who worked on charge of polymeric surfaces. They found that transferred charge was proportional to the real area of contact and the normal force.

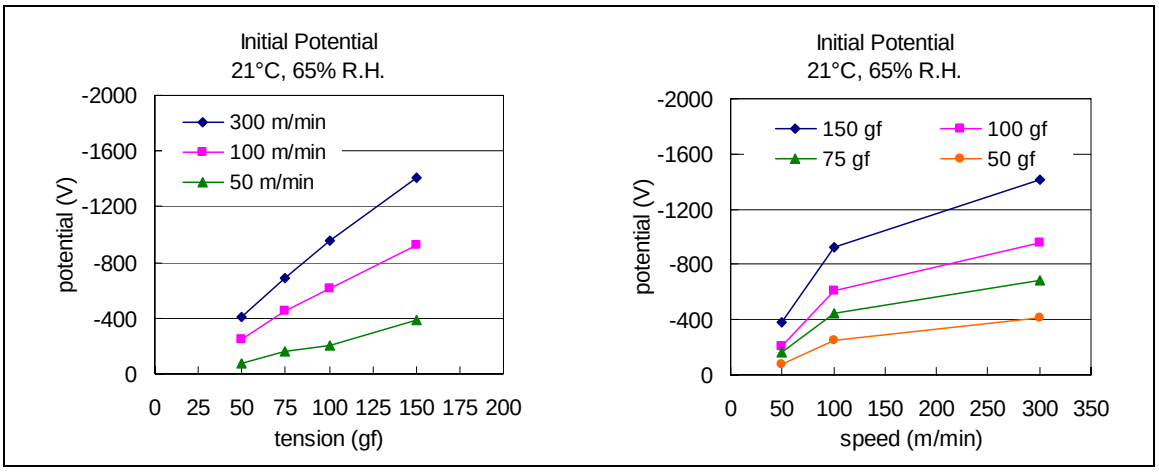

Figure 6.9. Interactions between Yarn Tension and Speed

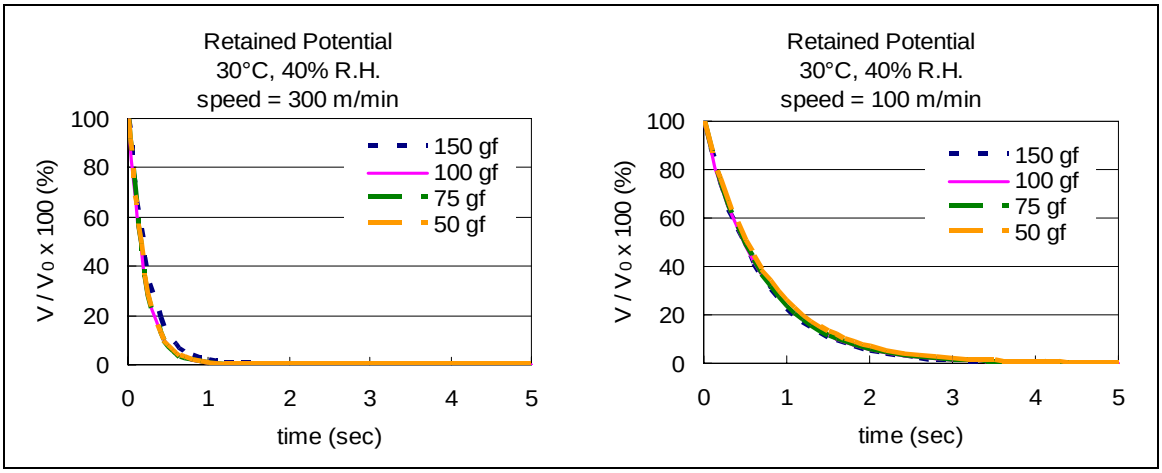

Figure 6.10. Effect of Yarn Tension on Decay Time

For the static dissipation, Figure 6.10 shows that yarn tension did not have any effect on decay time. We can assume that tension applied to the yarn enlarged the contact area between the yarn and a charge pin, generating more static charge, but it lost its effect soon

after the yarn left the pin. Larger yarn area due to flattening is subjected to larger surrounding environment and the rate of charge loss is larger than the un-flattened yarn. Percentage of potential retained on the yarn to the initial potential stayed same regardless of the yarn tension level.

6.1.5. Effect of Yarn Speed

The experimental design included the yarn speeds of 10, 50, 100, and 300 m/min, but data with 10 m/min were not included in the analysis because it was found impossible to calculate initial potential from two potential measurements. The reason for this deficiency was that the charge completely dissipated before the yarn arrived at the second probe. This could be remedied by using shorter spacing between the two probes.

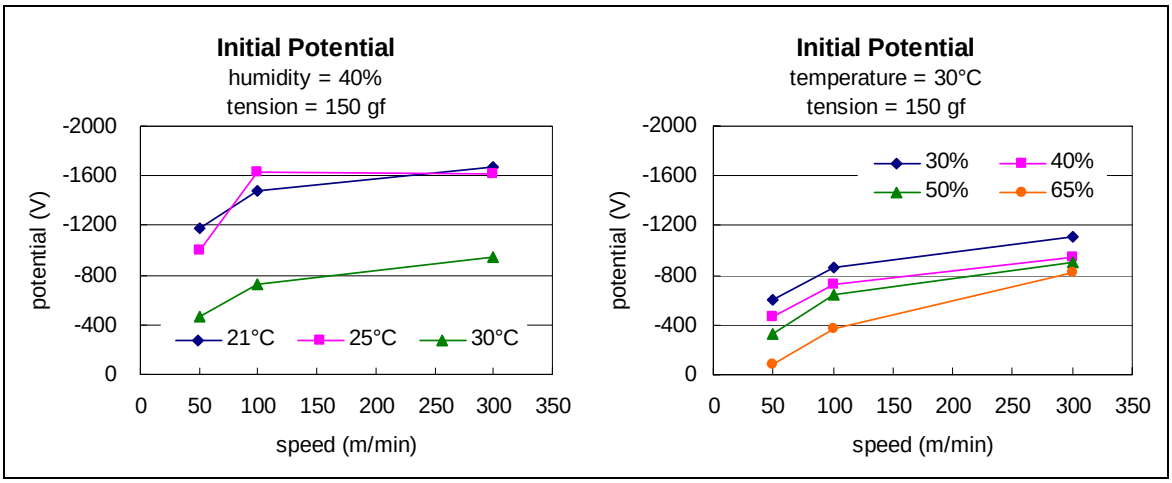

Figure 6.11. Effect of Yarn Speed on Initial Potential

Initial potential increased with yarn speed, and there were interactions with temperature, humidity, and yarn tension. The effect of yarn speed was larger at the low temperature and humidity and smaller at the high temperature and humidity (Figure 6.11).

Also, it was larger with high tension, and smaller with low tension (Figure 6.9). The effect of yarn speed could be explained by the frictional behavior between the yarn and the charge pin. The fiber friction was reported to increase as sliding speed increases at higher speed more than 1 m/min [36]. This was also confirmed with preliminary test where increasing friction coefficient depended on yarn speed (Figure 5.4 and Figure 5.5). Indeed the shapes of the effect of speed on friction coefficient and the effect of speed on initial potential are very similar, and their correlation is shown in Figure 6.12.

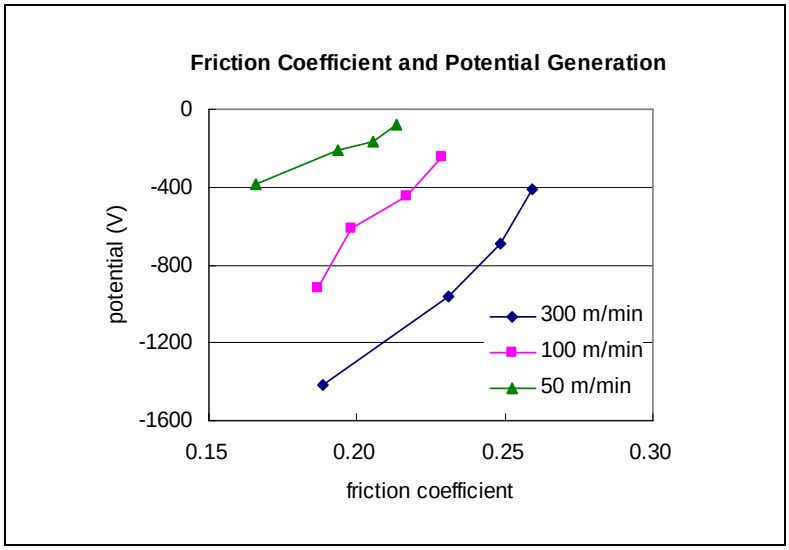

Figure 6.12. Friction Coefficient and Potential Generation

For decay time, it took approximately one second for the yarn moving with 300 m/min to loose charges completely, and characteristic decay time was shorter than 0.5 second (Figure 6.13). Decay time was shorter when the yarn was moving faster, and this meant static charge decayed faster. The effect of yarn speed for static generation seems to be only caused by the change in contact between a yarn and the surrounding air. This indicates that static charge was diffused effectively throughout the air as the yarn ran faster. This is a point that

obviously warrants further investigation, but was beyond the scope of the current thesis.

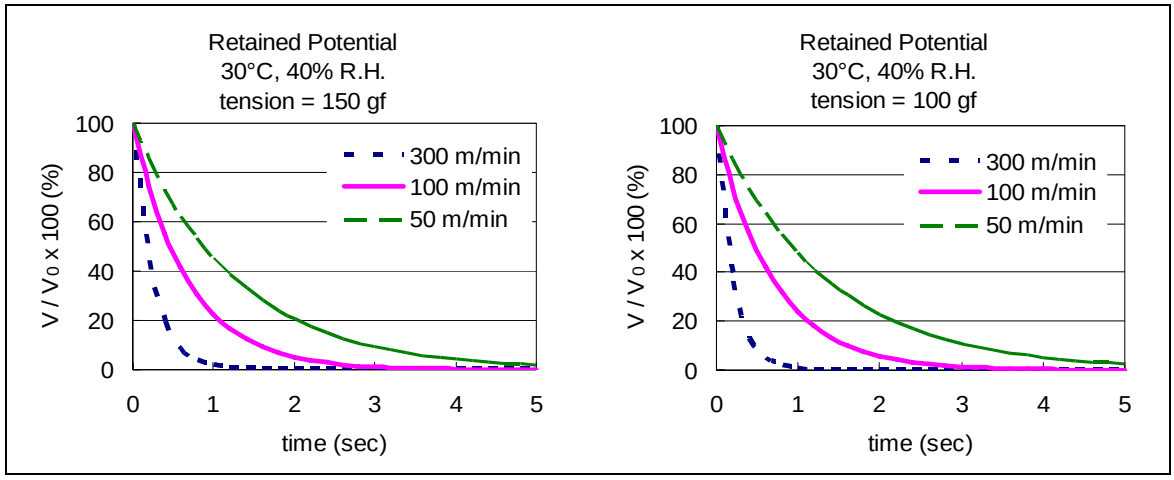

Figure 6.13. Effect of Yarn Speed on Decay Time

6.2. Experimental Design II

6.2.1. Statistical Analysis

Through 60 experimental runs shown in Table 4.3, 57 initial potentials and 45 decay times were successfully obtained and used for statistical analysis. Under the 65% relative humidity, the polypropylene and Teflon charge pin did not generate any static charges on the yarn. There were three more cases in which potential signals changed their polarity from the first probe to second probe. This made it impossible to calculate meaningful initial potentials as well as decay times. Experimental responses input to ANOVA are given in Appendix A-2.

Initial potentials and decay times were compared for the effect of charge pin material. ANOVA test is shown in Table 6.11 for initial potential and in Table 6.13 for decay time, respectively. The model for initial potential was highly significant which meant charge pin type affected static generation. Effect of charge pin type on initial potential was highly significant, but the model for decay time was not significant.

Table 6.11. Overall ANOVA for Initial Potential

Source	DF	Sum of Squares	Mean Square	F-value	Pr > F
Model	4	3562569.362	890642.340	22.56	<.0001
Error	52	2052648.219	39474.004		
Corrected Total	56	5615217.580			

Table 6.12. Type I and Type III ANOVA for Initial Potential

Source	DF	Type I SS	Mean Square	F-value	Pr > F
Charge Pin	4	3562569.362	890642.340	22.56	<.0001

Table 6.13. Overall ANOVA for Decay Time

Source	DF	Sum of Squares	Mean Square	F-value	Pr > F
Model	4	1.05841008	0.26460252	2.30	0.0750
Error	40	4.59236359	0.11480909		
Corrected Total	44	5.65077367			

Table 6.14. Type I and Type III ANOVA for Decay Time

Source	DF	Type I SS	Mean Square	F-value	Pr > F
Charge Pin	4	1.05841008	0.26460252	2.30	0.0750

Table 6.15 depicts multiple comparisons between initial potentials caused by stainless steel (SS), Nylon (NL), polyester (PET), polypropylene (PP), and Teflon (TF) charge pins. Stainless steel was different (highest potential in negative) from all other pins. Nylon and polyester showed similar level of positive charge, and polypropylene and Teflon pins showed almost no charge (Table 6.15).

Table 6.15. Scheffe's Multiple Charge Pin Comparisons for Initial Potential

Charge Pin Comparison	Difference Between Means	Simultaneous 99% Confidence Limits		
SS-NL	-734.74	-1006.42	-463.06	***
SS-PET	-622.93	-887.79	-358.07	***
SS-PP	-451.78	-710.82	-192.75	***
SS-TF	-423.00	-682.04	-163.96	***
NL-PET	111.81	-165.43	389.04	
NL-PP	282.96	11.28	554.63	***
NL-TF	311.74	40.06	583.42	***
PET-PP	171.15	-93.71	436.01	
PET-TF	199.93	-64.93	464.79	
PP-TF	28.78	-230.25	287.82	

*** indicates the difference is significant

6.2.2. Effect of Charge Pin Material

Effect of charge pin materials on initial potential is depicted in Figure 6.14. The polyester multifilament sample yarn charged negatively after rubbed against a stainless steel

charge pin. Static polarity turned to positive with nylon or polyester charge pins. Polypropylene and Teflon caused little charges under the 30% humidity, and no charge under the 65% humidity. Charge pin materials could be categorized by three groups in terms of charge polarity and magnitude; (1) Stainless Steel (negative), (2) Nylon-Polyester (positive), and (3) Polypropylene-Teflon (almost zero).

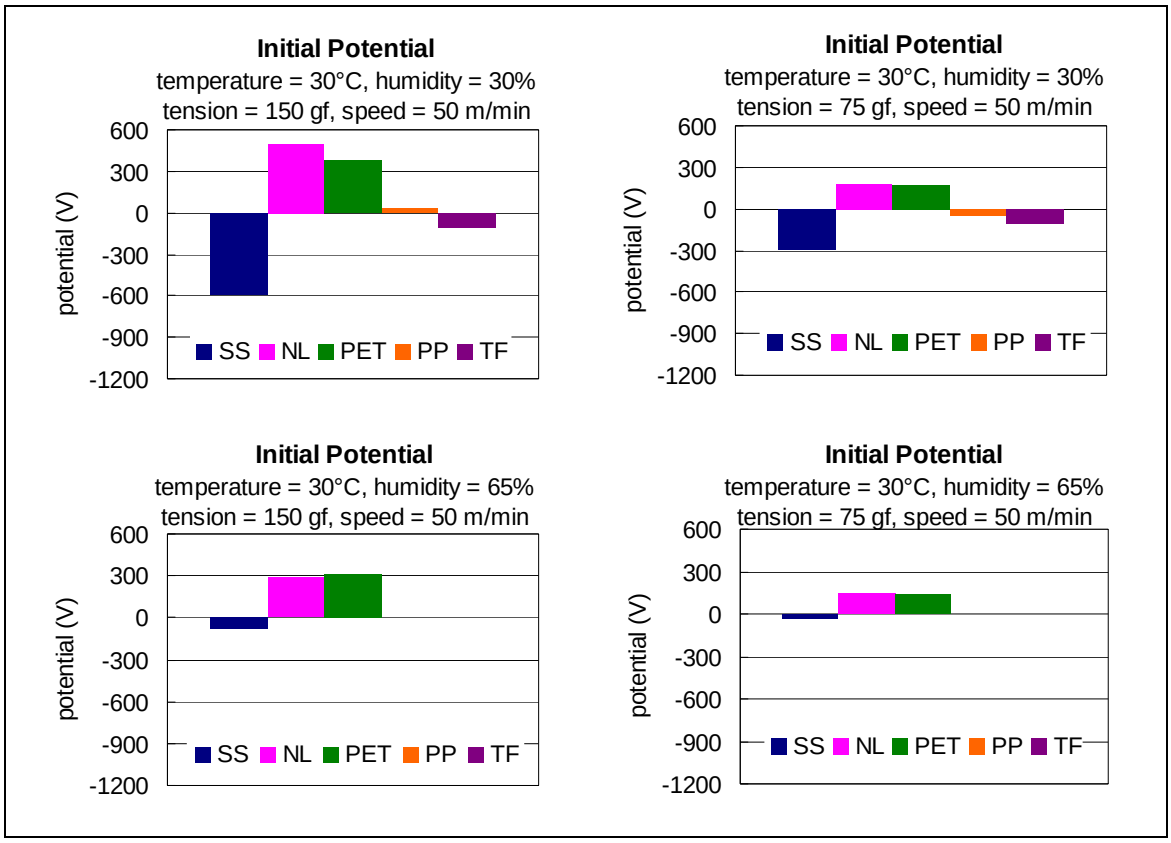

Figure 6.14. Effect of Charge Pin Type on Initial Potential
(Abbreviations: SS=stainless steel, NL=nylon, TF=Teflon)

Comparison between the charge pins was described in Figure 6.14, and they did not follow the tribo-electric series. According to the tribo-electric series developed by Hersh and Montgomery [29], polyester yarn gets negative charge against stainless steel and nylon, and positive charge against polypropylene and Teflon. Charge polarity conversion depending on

yarn speed was observed in some cases (Figure 6.15). Finishes on the sample yarn might be responsible for this. For nylon and polyester charge pin, potential changed polarity as yarn speed changed. Unfortunately, it was hard to say exactly what happened in finishes on the sample yarn after the friction against a charge pin. This occurred obviously under the 30% humidity, but it was less obvious under the 65% humidity. Finish-free yarns made of polyester, nylon, and polypropylene were studied in following experiments in order to eliminate yarn finishing effect.

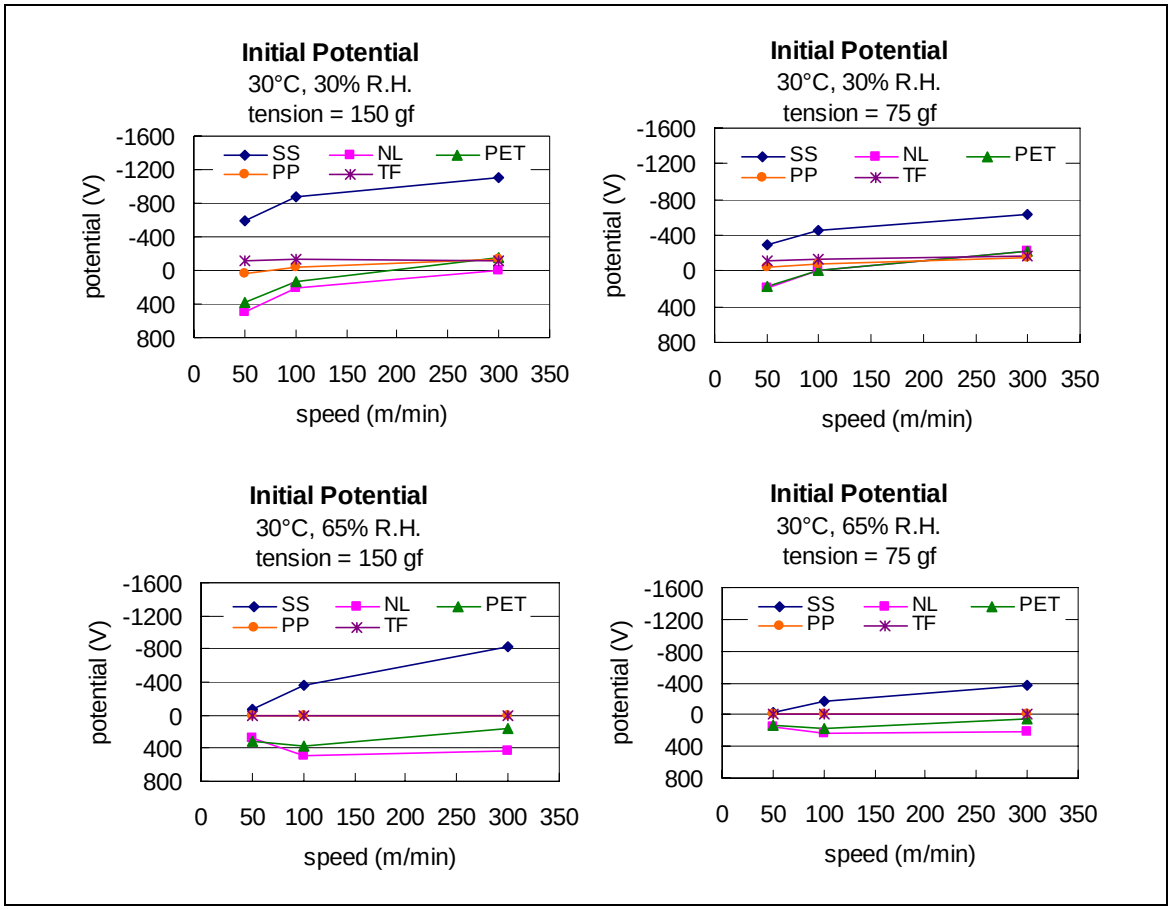

Figure 6.15. Effect of Yarn Finishing on Initial Potential
(Abbreviations: SS=stainless steel, NL=nylon, TF=Teflon)

6.3. Experimental Design III

6.3.1. Statistical Analysis

A total of 36 runs of experiment were conducted for finish-free sample yarns. Initial potentials and decay times in two runs could not be obtained because no charge was observed on first, second, or both probes. Experimental responses input to ANOVA are given in Appendix A-3. Data of 34 runs of initial potential and decay time were used for ANOVA analysis, and results are shown in Table 6.16, Table 6.17 (for initial potential), Table 6.18, and Table 6.19 (for decay time). The effect of material type of the finish-free yarn was statistically verified for static generation, but not for static dissipation. Multiple comparisons revealed that initial potentials were significantly different in all pairs of polyester, nylon, and polypropylene finish-free yarn (Table 6.20).

For additional analysis, potential per unit yarn surface area is given in Appendix C-1, and ANOVA results with those responses are in Appendix C-2.

Table 6.16. Overall ANOVA for Initial Potential

Source	DF	Sum of Squares	Mean Square	F-value	Pr > F
Model	2	4070731.435	2035365.718	84.97	< .0001
Error	31	742550.000	23953.226		
Corrected Total	33	4813281.435			

Table 6.17. Type I and Type III ANOVA for Initial Potential

Source	DF	Type I SS	Mean Square	F-value	Pr > F
Yarn Material	2	4070731.435	2035365.718	84.97	< .0001

Table 6.18. Overall ANOVA for Decay Time

Source	DF	Sum of Squares	Mean Square	F-value	Pr > F
Model	2	0.25544166	0.12772083	2.78	0.0777
Error	31	1.42531914	0.04597804		
Corrected Total	33	1.68076081			

Table 6.19. Type I and Type III ANOVA for Initial Potential

Source	DF	Type I SS	Mean Square	F-value	Pr > F
Yarn Material	2	0.25544166	0.12772083	2.78	0.0777

Table 6.20. Scheffe's Multiple Yarn Material Comparisons for Initial Potential

Charge Pin Comparison	Difference Between Means	Simultaneous 99% Confidence Limits		
PET-NL	-859.74	-1029.40	-690.07	***
PET-PP	-403.44	-569.53	-237.34	***
NL-PP	456.30	290.21	622.39	***

*** indicates the difference is significant

6.3.2. Effect of Yarn Material

According to Diaz et al. (2004) [18] and Hersh and Montgomery (1955) [29], the generally agreed tribo-electric series between materials studied in this research is (+) Nylon,

Stainless Steel, Polyester, Polypropylene, and Teflon (−). Yarns exactly followed the tribo-electric series in the absence of finishes. Against stainless steel charge pin, polyester and polypropylene got charged negatively, whereas nylon charged positively (Figure 6.16). Polyester had more charges under lower humidity, but nylon and polypropylene did so under higher humidity. Polypropylene always showed the lowest static generation (initial potential). Yarns with finish-free surface had much higher charges than those with finish. Finish-free polyester was recorded the highest initial potential (over 8,000 volts).

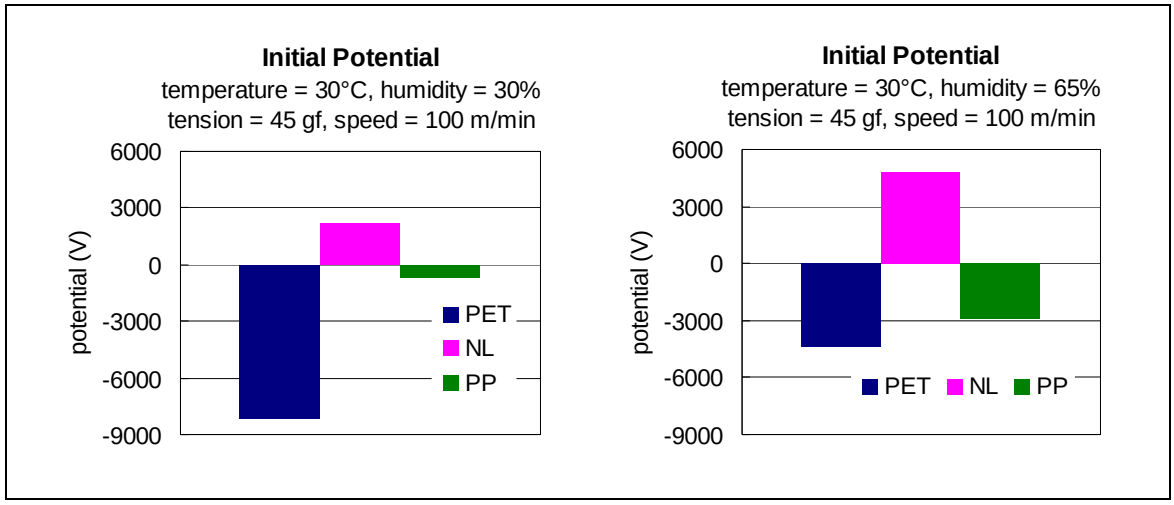

Figure 6.16. Effect of Yarn Material on Initial Potential
(Abbreviations: NL=nylon)

6.4. Experimental Design IV

6.4.1. Statistical Analysis

Analysis of variance was conducted on 36 experimental runs using multifilament yarns and 36 experimental runs using monofilament yarns. For multifilament yarns, 22 initial potentials and 22 decay times was used for ANOVA analysis. All experimental data from the polypropylene multifilament yarn were excluded because of no charge generation.

Additionally, two decay times on nylon multifilament yarns were not obtained due to measurement errors (charge increase at the second probe compared to first probe was observed). For monofilament yarns, 30 initial potentials and 30 decay times were used for ANOVA analysis because under the 65% relative humidity, the nylon monofilament yarn did not generate any static charges and it was impossible to calculate responses. Experimental responses input to ANOVA are given in Appendix A-4.

Initial potentials and decay times were investigated for the effect of humidity, yarn tension, and speed. ANOVA models were significant both for initial potential (Table 6.21) and decay time (Table 6.24). For initial potential, yarn type and humidity had significant effect, but the effect of yarn tension and speed was not clear (Table 6.22 and Table 6.23). They were significant only in type III ANOVA (Table 6.23). It was because the effect of yarn tension and speed was different on multifilament and monofilament yarns. ANOVA conducted separately on multifilament and monofilament yarns (Table 6.28, Table 6.29, Table 6.34, and Table 6.35) supports this. For decay time, yarn type, tension, and speed showed significance (Table 6.25 and Table 6.26).

Table 6.21. Overall ANOVA for Initial Potential

Source	DF	Sum of Squares	Mean Square	F-value	Pr > F
Model	14	10222973.72	730212.41	6.98	<.0001
Error	37	3872867.17	104672.09		
Corrected Total	51	14095840.89			

Table 6.22. Type I ANOVA for Initial Potential

Source	DF	Type I SS	Mean Square	F-value	Pr > F
type	1	7952352.741	7952352.741	75.97	<.0001
humidity	1	567963.687	567963.687	5.43	0.0254
tension	1	300496.299	300496.299	2.87	0.0986
speed	2	602934.089	301467.044	2.88	0.0688
type*hum.	1	110697.554	110697.554	1.06	0.3104
tension*speed	2	20513.437	10256.718	0.10	0.9069
type*tension	1	139919.647	139919.647	1.34	0.2550
type*speed	2	516318.719	258159.360	2.47	0.0987
hum.*tension	1	5725.363	5725.363	0.05	0.8164
hum.*speed	2	6052.182	3026.091	0.03	0.9715

Table 6.23. Type III ANOVA for Initial Potential

Source	DF	Type I SS	Mean Square	F-value	Pr > F
type	1	7087459.024	7087459.024	67.71	<.0001
humidity	1	783013.763	783013.763	7.48	0.0095
tension	1	446356.463	446356.463	4.26	0.0460
speed	2	775423.963	387711.982	3.70	0.0342
type*hum.	1	147011.508	147011.508	1.40	0.2435
tension*speed	2	11711.023	5855.511	0.06	0.9457
type*tension	1	159673.682	159673.682	1.53	0.2246
type*speed	2	519016.956	259508.478	2.48	0.0976
hum.*tension	1	5704.815	5704.815	0.05	0.8167
hum.*speed	2	6052.182	3026.091	0.03	0.9715

Table 6.24. Overall ANOVA for Decay Time

Source	DF	Sum of Squares	Mean Square	F-value	Pr > F
Model	14	9.16166499	0.65440464	9.89	<.0001
Error	37	2.44750626	0.06614882		
Corrected Total	51	51	11.60917125		

Table 6.25. Type I ANOVA for Decay Time

Source	DF	Type I SS	Mean Square	F-value	Pr > F
type	1	0.35996018	0.35996018	5.44	0.0252
humidity	1	0.13522465	0.13522465	2.04	0.1612
tension	1	0.42966727	0.42966727	6.50	0.0151
speed	2	7.58426970	3.79213485	57.33	<.0001
type*hum.	1	0.25824189	0.25824189	3.90	0.0557
tension*speed	2	0.14010612	0.07005306	1.06	0.3571
type*tension	1	0.00393668	0.00393668	0.06	0.8086
type*speed	2	0.12190517	0.06095259	0.92	0.4069
hum.*tension	1	0.00272640	0.00272640	0.04	0.8402
hum.*speed	2	0.12562691	0.06281346	0.95	0.3961

Table 6.26. Type III ANOVA for Decay Time

Source	DF	Type I SS	Mean Square	F-value	Pr > F
type	1	0.51282847	0.51282847	7.75	0.0084
humidity	1	0.06421369	0.06421369	0.97	0.3309
tension	1	0.29903374	0.29903374	4.52	0.0402
speed	2	7.20106974	3.60053487	54.43	<.0001
type*hum.	1	0.24926664	0.24926664	3.77	0.0599
tension*speed	2	0.14296614	0.07148307	1.08	0.3498
type*tension	1	0.00493072	0.00493072	0.07	0.7864
type*speed	2	0.13198230	0.06599115	1.00	0.3785
hum.*tension	1	0.00384467	0.00384467	0.06	0.8108
hum.*speed	2	0.12562691	0.06281346	0.95	0.3961

As a further investigation, ANOVA was conducted separately on multifilament and monofilament yarns. For multifilament yarns, relative humidity, yarn tension, and speed were all significant for static generation (Table 6.27, Table 6.28, and Table 6.29), while decay time was influenced only by yarn speed (Table 6.30, Table 6.31, and Table 6.32). For monofilament yarns, the ANOVA model for initial potential was not significant at all (Table 6.33), but the model for decay time was significant (Table 6.36). None of the parameters and interactions appeared to be significant for initial potential model (Table 6.34, and Table 6.35). Decay time model was significant with humidity and yarn speed (Table 6.37, and Table 6.38), but humidity was significant at the low level.

For additional analysis, potential per unit yarn surface area is given in Appendix D-1. Corresponding ANOVA results are in Appendix D-2 for multifilament yarns and Appendix

D-3 for monofilament yarns.

Table 6.27. Overall ANOVA for Initial Potential of Multifilament Yarns

Source	DF	Sum of Squares	Mean Square	F-value	Pr > F
Model	9	2088508.864	232056.540	15.30	<.0001
Error	12	182033.284	15169.440		
Corrected Total	21	2270542.148			

Table 6.28. Type I ANOVA for Initial Potential of Multifilament Yarns

Source	DF	Type I SS	Mean Square	F-value	Pr > F
humidity	**1**	**497805.873**	**497805.873**	**32.82**	**<.0001**
tension	**1**	**397123.585**	**397123.585**	**26.18**	**0.0003**
speed	**2**	**1145091.061**	**572545.530**	**37.74**	**<.0001**
tension*speed	2	30184.134	15092.067	0.99	0.3983
hum.*tension	1	5113.680	5113.680	0.34	0.5722
hum.*speed	2	13190.531	6595.265	0.43	0.6572

Table 6.29. Type III ANOVA for Initial Potential of Multifilament Yarns

Source	DF	Type III SS	Mean Square	F-value	Pr > F
humidity	**1**	**665009.649**	**665009.649**	**43.84**	**<.0001**
tension	**1**	**466686.922**	**466686.922**	**30.76**	**0.0001**
speed	**2**	**1095065.293**	**547532.646**	**36.09**	**<.0001**
tension*speed	2	29545.863	14772.931	0.97	0.4056
hum.*tension	1	3602.576	3602.576	0.24	0.6348
hum.*speed	2	13190.531	6595.265	0.43	0.6572

Table 6.30. Overall ANOVA for Decay Time of Multifilament Yarns

Source	DF	Sum of Squares	Mean Square	F-value	Pr > F
Model	9	4.74540253	0.52726695	9.75	0.0003
Error	12	0.64883098	0.05406925		
Corrected Total	21	5.39423352			

Table 6.31. Type I ANOVA for Decay Time of Multifilament Yarns

Source	DF	Type I SS	Mean Square	F-value	Pr > F
humidity	1	0.01078195	0.01078195	0.20	0.6631
tension	1	0.17681529	0.17681529	3.27	0.0957
speed	**2**	**4.26012914**	**2.13006457**	**39.40**	**<.0001**
hum.*tension	2	0.08204588	0.04102294	0.76	0.4895
hum.*speed	1	0.12743661	0.12743661	2.36	0.1507
tension*speed	2	0.08819366	0.04409683	0.82	0.4655

Table 6.32. Type III ANOVA for Decay Time of Multifilament Yarns

Source	DF	Type III SS	Mean Square	F-value	Pr > F
humidity	1	0.01854640	0.01854640	0.34	0.5689
tension	1	0.11327906	0.11327906	2.10	0.1734
speed	**2**	**3.84258145**	**1.92129072**	**35.53**	**<.0001**
hum.*tension	2	0.11731128	0.05865564	1.08	0.3689
hum.*speed	1	0.12675633	0.12675633	2.34	0.1517
tension*speed	2	0.08819366	0.04409683	0.82	0.4655

Table 6.33. Overall ANOVA for Initial Potential on Monofilament Yarns

Source	DF	Sum of Squares	Mean Square	F-value	Pr > F
Model	9	257812.383	28645.820	0.16	0.9963
Error	20	3615133.619	180756.681		
Corrected Total	29	3872946.002			

Table 6.34. Type I ANOVA for Initial Potential of Monofilament Yarns

Source	DF	Type I SS	Mean Square	F-value	Pr > F
humidity	1	148235.5014	148235.5014	0.82	0.3759
tension	1	41225.5470	41225.5470	0.23	0.6381
speed	2	18204.6247	9102.3123	0.05	0.9510
tension*speed	2	3376.9580	1688.4790	0.01	0.9907
hum*tension	1	23194.8605	23194.8605	0.13	0.7239
hum*speed	2	23574.8914	11787.4457	0.07	0.9371

Table 6.35. Type III ANOVA for Initial Potential of Monofilament Yarns

Source	DF	Type III SS	Mean Square	F-value	Pr > F
humidity	1	148235.5014	148235.5014	0.82	0.3759
tension	1	52623.5405	52623.5405	0.29	0.5955
speed	2	11215.4381	5607.7191	0.03	0.9695
tension*speed	2	3376.9580	1688.4790	0.01	0.9907
hum.*tension	1	23194.8605	23194.8605	0.13	0.7239
hum.*speed	2	23574.8914	11787.4457	0.07	0.9371

Table 6.36. Overall ANOVA for Decay Time on Monofilament Yarns

Source	DF	Sum of Squares	Mean Square	F-value	Pr > F
Model	9	4.34961374	0.48329042	6.42	0.0003
Error	20	1.50536381	0.07526819		
Corrected Total	29	5.85497755			

Table 6.37. Type I ANOVA for Decay Time of Monofilament Yarns

Source	DF	Type I SS	Mean Square	F-value	Pr > F
humidity	**1**	**0.33395617**	**0.33395617**	**4.44**	**0.0480**
tension	1	0.22510806	0.22510806	2.99	0.0991
speed	**2**	**3.53645921**	**1.76822960**	**23.49**	**<.0001**
tension*speed	2	0.06834235	0.03417118	0.45	0.6415
hum.*tension	1	0.05708105	0.05708105	0.76	0.3942
hum.*speed	2	0.12866691	0.06433345	0.85	0.4404

Table 6.38. Type III ANOVA for Decay Time of Monofilament Yarns

Source	DF	Type III SS	Mean Square	F-value	Pr > F
humidity	**1**	**0.33395617**	**0.33395617**	**4.44**	**0.0480**
tension	1	0.17396099	0.17396099	2.31	0.1441
speed	**2**	**3.15156893**	**1.57578447**	**20.94**	**<.0001**
tension*speed	2	0.06834235	0.03417118	0.45	0.6415
hum.*tension	1	0.05708105	0.05708105	0.76	0.3942
hum.*speed	2	0.12866691	0.06433345	0.85	0.4404

6.4.2. Effect of Humidity

Effect of humidity on static generation was significant on multifilament yarns, but not on monofilament yarns. Potential fell down as humidity increased (Figure 6.17), which meant moist atmosphere reduced charge generation on multifilament yarns. The fact that monofilament yarns did not show significant difference in potential with humidity change indicated that air inside of the yarn structure had dominant effect on charge generation. For static dissipation, effect of humidity on static generation was not significant on multifilament yarns. The significance appeared on monofilament yarns.

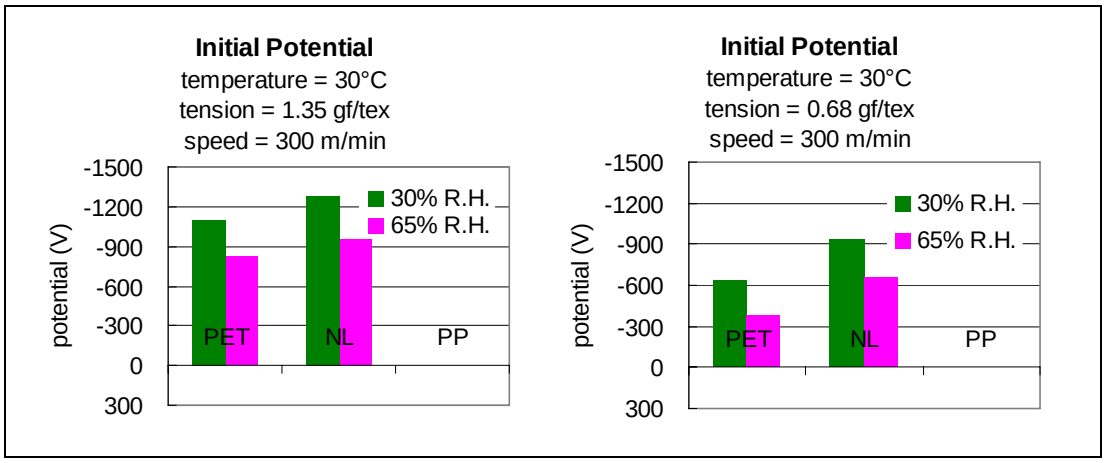

Figure 6.17. Effect of Humidity on Initial Potential of Multifilament Yarns

6.4.3. Effect of Yarn Tension

Yarn tension had a significant effect on static generation on multifilament yarns, but not on monofilament yarns. Potentials increased under higher yarn tension (Figure 6.18) because of enlarged contact area between the yarn and a charge pin due to filament spread as discussed in section 6.1.3. However, higher yarn tension would not significantly influence the contact area of monofilament yarns (one filament may flatten but insignificantly). Yarn

tension did not have an effect on the static dissipation both in multifilament and monofilament yarns.

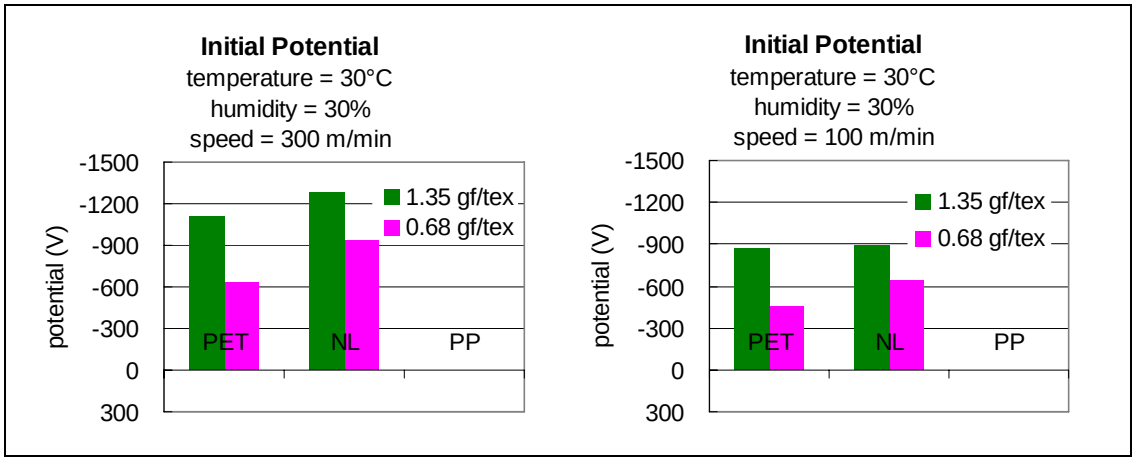

Figure 6.18. Effect of Yarn Tension on Initial Potential of Multifilament Yarns

6.4.4. Effect of Yarn Speed

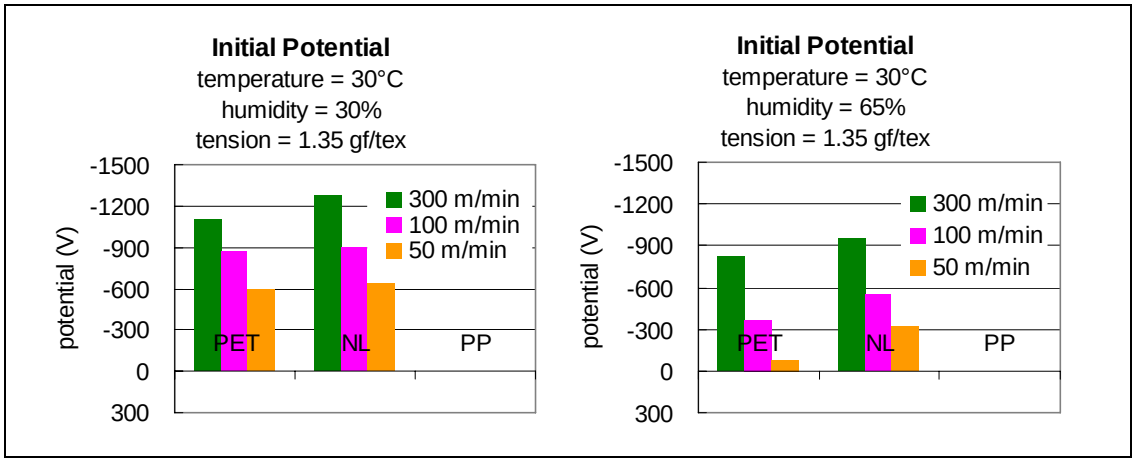

Figure 6.19. Effect of Yarn Speed on Initial Potential of Multifilament Yarns

Static generation on multifilament yarns was affected by yarn speed. More charge was observed on the multifilament yarns under higher yarn speed (Figure 6.19). However, the effect of yarn speed was not significant on the monofilament yarns. For both

multifilament and monofilament yarns, static decay was influenced by yarn speed. Decay time was shorter with high yarn speed (Figure 6.20 and Figure 6.21). This indicated that static charge was diffused effectively throughout the air as the yarn ran faster, but investigating the reason behind the effect of yarn contact with air on static behavior is beyond the scope of the current thesis.

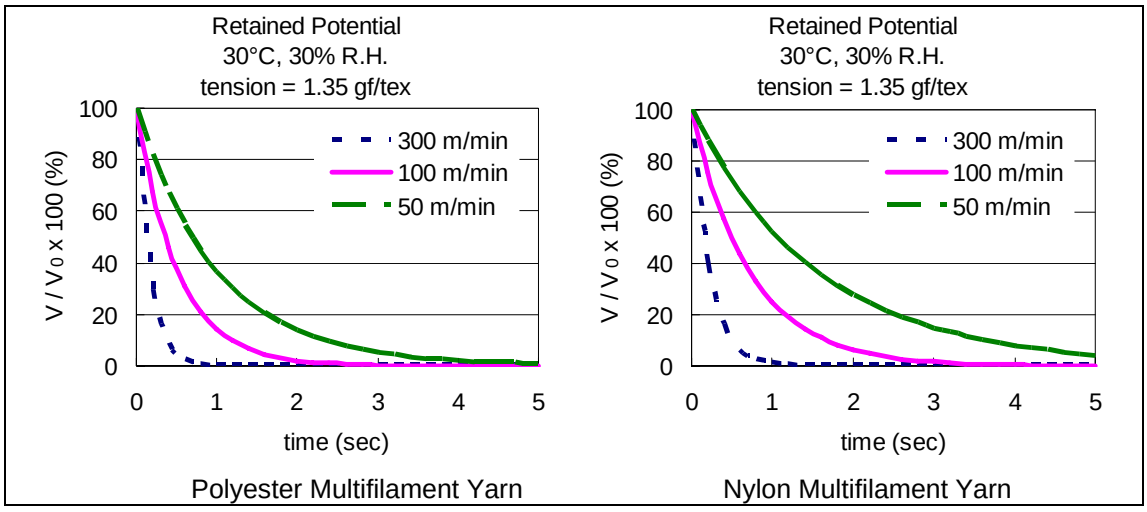

Figure 6.20. Effect of Yarn Speed on Decay Time of Multifilament Yarns

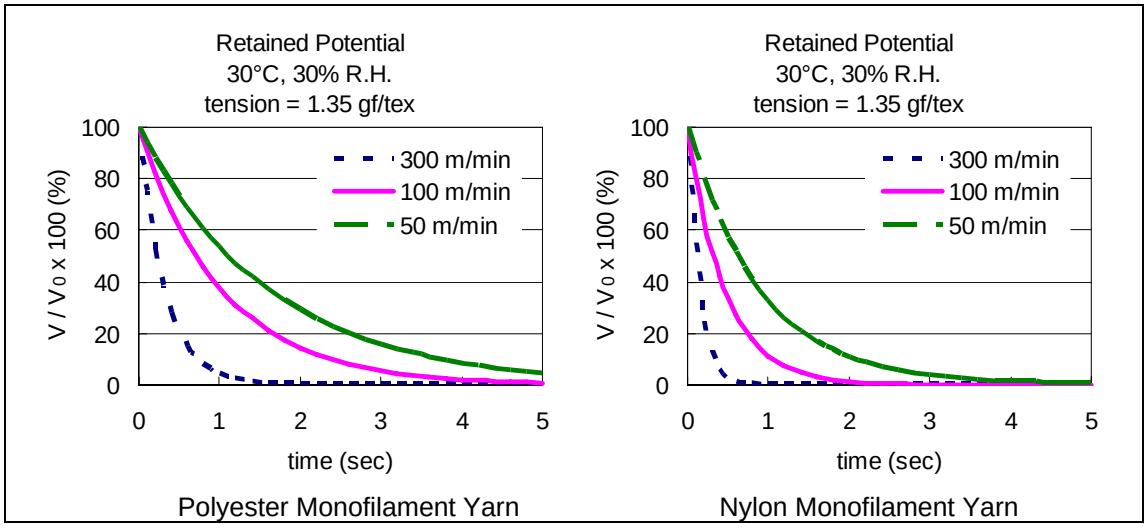

Figure 6.21. Effect of Yarn Speed on Decay Time of Monofilament Yarns

VII. CONCLUSION

7.1. Experimental Design I

Polyester multifilament (1000/140) yarns were rubbed against a stainless steel charge pin in order to investigate static generation and dissipation on dynamic yarns. Linear Tester enabled to make potential measurements at two different points so that initial potential and characteristic decay time can be calculated. Statistical analyses (ANOVA and Scheffe's multiple mean comparison) were conducted on initial potential and decay time for studying effect of temperature, relative humidity, yarn tension, and speed and their first order interactions.

For static generation, temperature, humidity, yarn tension, and speed had significant effects on initial potential. Higher temperature and humidity led to less charge generation, while higher yarn tension and speed caused more charge generation. The effect of yarn tension was caused by the increased contact area between the sample yarn and a charge pin. As yarn speed went up, more static charge was created due to increased friction coefficients between the yarn and charge pin.

For static dissipation, temperature, humidity, and yarn speed were proved to have significant effects on decay time. Longer decay time was observed in the middle level of temperature (25°C) and humidity (40 R.H. and 50% R.H.). Unexpectedly, yarns experienced negative decay times (charge at the second probe is higher than the charge at the first probe) at 35°C. This implies that high temperature around 35°C should be avoided. Generally, 35°C is high temperature as an industrial condition, but it can be in the practical range to reach when taking the heat generated by the machinery into consideration. Yarn speed affected

static dissipation, and this effect is due to the contact between the yarn and surrounding air. More investigation would be necessary for exact explanation, but this gives an implication for industry. If we let the yarns run through the air enough between processes, static charge on the yarn would be dissipated efficiently. It is recommended that long yarn bath between guides, rollers, etc. should be avoided and discharge at different contact points may be considered.

7.2. Experimental Design II

Polyester multifilament (1000/140) yarns were rubbed against different kind of charge pins made of stainless steel, nylon, polyester, polypropylene, and Teflon. As the former experiment, Linear Tester made potential measurements at two different points so that initial potential and characteristic decay time can be calculated. Analysis of variance was conducted for comparing each charge pin's effect on static generation and dissipation. The result indicated that charge pin material affected static generation, but not static dissipation.

Polymer pins caused smaller charges on the yarn compared to stainless steel. Polyester yarns got charged negatively by stainless steel, while the charge was positive with nylon and polyester pins. Polypropylene and Teflon created little charge. This is supported by Scheffe's multiple mean comparison. Different charge pins could be divided into three groups of 1) stainless steel, 2) nylon and polyester, and 3) polypropylene and Teflon. Each group was characterized by 1) strong negative charge, 2) moderate positive charge, and 3) slightly positive charge almost 0, respectively. Static polarity did not coincide with tribo-electric series. This may be attributed to the effect of the finishes on the yarn which changes

the surface characteristics and consequently the static behavior as a result of contact with charge pins. Experimental design III was structured to nullify the effect of finish on the yarn.

7.3. Experimental Design III

In order to remove the finish effect on the yarn on the static behavior, finish-free yarns made of polyester, nylon, and polypropylene were rubbed against a stainless steel charge pin. The rollers and guides of the Linear Tester were cleaned with alcohol thoroughly before experiments in order to avoid any contamination on finish-free surface. This cleaning step is important when starting the test of new yarn (when switching from yarn to another). Gradient adaptors were must to use since the charges generated by such yarns are higher than the voltmeter capacity (voltmeters used are of capacity of 3,000 volts). The gradient adaptor was adjusted to increase the capacity of the voltmeter to 10 times.

Static generation was remarked as negative charges on the polyester and polypropylene yarns, and as positive charges on the nylon yarn against the stainless steel charge pin. Compared to polyester and nylon, polypropylene always had the lowest charge generation. Distinction between the yarns is agreed with Scheffe's multiple comparison. This tendency coincides with the tribo-electric series in literatures. Fiber material of finish-free yarns did not affect static dissipation. The characteristic time considering all fiber materials ranged from 0.03~1.20 seconds.

7.4. Experimental Design IV

Six different sample yarns (multifilament and monofilament yarns made of polyester,

nylon, and polypropylene) were tested against a stainless steel charge pin to compare static generation/dissipation on multifilament and monofilament yarns. Initial potential and decay time were calculated and compared in terms of the effect of humidity, yarn tension, and speed.

Static generation on multifilament yarns was affected by relative humidity, yarn tension, and speed, while none of them affected the monofilament yarns. The fact that relative humidity influenced initial potential on multifilament yarns, but not on monofilament yarns indicated that the air (loaded with moisture) inside the yarn structure had dominant effect on static generation. Yarn tension did not influence the initial potential on monofilament yarns because tension failed to change the contact area between the monofilament yarn and a charge pin significantly.

For static dissipation, only yarn speed had significant effect on both multifilament and monofilament yarns. Static charge was diffused effectively under higher yarn speed. As we discussed in experimental design I, the effect of yarn speed on decay time is due to the contact between the yarn and surrounding air.

VIII. SUGGESTIONS FOR FUTURE STUDIES

The results of this research indicated that the air play an important role in static generation and dissipation as was seen above from the effect of speed and the effect of temperature at 35° C. The reasons behind such behavior need further investigations which are beyond the scope of this work. There are few investigations studied the effect of air contact on static charges. Previous workers studied the static charge behavior in vacuum to nullify the effect of air. Since in real situations air exists, it is suggested that studies need be under taken to investigate the reasons that cause static generation or dissipation by air.

Increasing potentials observed at 35°C needs further investigations, as well. The reason caused static charge increase under the temperature as high as 35°C is a problem awaiting solution. In addition, charge increase behavior is challengeable to be studied. Exponential decay of static charge is no more valid for the increasing potential experienced by the yarns. Measuring potentials at more than two different positions would provide important information about how the charge increased.

For the analysis of charge dissipation, characteristic decay time was discussed here, which is the time required to get 1/e times of initial potential. This enabled to make fair comparisons between experimental runs having different initial potential. However, in order to reduce electrostatic risk, potential level is also important. It is recommended to undertake an investigation to study decay in terms of a critical charge (fixed value) at which problem may be encountered. The corresponding time to reach the critical charge is a measure of decay with longer time indicating poor dissipation.

IX. REFERENCES

1. Adams, C.K. (1987). *Nature's Electricity*. Pennsylvania; Tab Books, Blue Ridge Summit.
2. Akande, A.R. (2005). Contact Charging of Solution-cast Polymers by Metals, *Journal of Electrostatics*, 63(11), pp. 1025-1033.
3. Akande, A.R. and Adedoyin, J.A. (2001). Correlation of Charge Transfer in Metal/Polymer Contact with Contact Potential, *Journal of Electrostatics*, vol. 51-52, pp. 105-110.
4. American Association of Textile Chemists and Colorists (2000). Electrical Surface Resistivity of Fabrics, *AATCC Technical manual,* vol. AATCC Test Method 76, pp. 101-102.
5. American Association of Textile Chemists and Colorists (2000). Electrical Resistance of Yarns, *AATCC Technical Manual,* vol. AATCC Test Method 84, pp. 110-111.
6. American Association of Textile Chemists and Colorists (1996). Electrostatic Propensity of Carpets, *AATCC Technical Manual,* vol. AATCC Test Method 134, pp. 227-229.
7. American Society of Testing and Materials (2005). Standard Test Methods for DC Resistance or Conductance of Insulating Materials, *ASTM International,* vol. D257-99, pp. 1-18.
8. American Society of Testing and Materials (2004). Standard Test Method for Static Electrification, *ASTM International,* vol. D4470-97, pp. 1-10.
9. Bailey, A.G. (2001). The Charging of Insulator Surfaces, *Journal of Electrostatics*, 51-52, pp. 82-90.
10. Berberi, P. (2003). Effect of Processing on Electrical Resistivity of Textile Fibers,

Journal of Electrostatics, 51-52, pp. 538-544.

11. Cai, Y., Seyam, A.M., Kim, Y.K. (2007), Formation of Fiberwebs From Staple Fibers With Controlled Fiber Orientation Using Electrostatic Forces: Theoretical Analysis, *Journal of Engineered Fibers and Fabrics*, 2(2), pp. 17-24.
12. Castle, G.S.P. (1997). Contact Charging Between Insulators, *Journal of Electrostatics*, vol. 40-41, Proceedings of the 8th International Conference on Electrostatics, pp. 13-20.
13. Chubb, J. (2004). Comments on Methods for Charge Decay Measurement, *Journal of Electrostatics,* 62(1), pp. 73-80.
14. Chubb, J. (2002). New approaches for electrostatic testing of materials, *Journal of Electrostatics,* 54(3-4), pp. 233-244.
15. Chubb, J. (1990). Instrumentation and Standards for Testing Static Control Materials, *IEEE Transactions on Industry Applications,* 26(6), pp. 1182-1187.
16. Coehn, A. (1898). Triboelectricity, *Annals of Physics*, 64, pp. 217.
17. Coletti G., Guatavino, F., Dardano, A., and Torello, E. (2003). A Comparison between the static performances of two different families of composite dielectric fabrics used in ESD protective clothing, *Conference on Electrical Insulation and Dielectric Phenomena,* vol. 2003 Annual Report, pp. 100-103.
18. Diaz, A.F., and Felix-Navarro, R.M. (2004). A Semi-quantitative Tribo-electric Series for Polymeric Materials: the Influence of Chemical Structure and Properties, Journal of Electrostatics, 62(4), pp. 277-290.
19. Electrostatic Discharge Association (2001), Surface Resistance measurement of Static Dissipative Planar Materials, *ESD association standard test method,* vol. ANSI/ESD

STM11.11, pp. 1-7.

20. Electrostatic Discharge Association (2000), Volume Resistance Measurements of Static Dissipative Planar Materials, *ESD association standard test method,* vol. ANSI/ESD STM11.12, pp. 1-10.
21. Electrostatic Discharge Association (1995), Triboelectric Charge Accumulation Testing, *ESD association standard test method,* vol. ESD ADV. 11.2, pp. 1-60.
22. Elsdon, R. and Mitchell, F. R. G. (1976). Contact Electrification of Polymers, *Journal of Physics D. Applied Physics*, vol. 9, 1445-1460.
23. Federal Test Standard (1980), Electrostatic Properties of Materials, *Federal Test Method Standard 101C*, Method 4046.
24. Gompf, R., Holdstock, P., and Chubb, J. (1999). Electrostatic Test Methods Compared. *Electrical Overstress / Electrostatic Discharge Symposium, 1999 Proceedings*, 49-53.
25. Gompf, R. (1984). Triboelectric Testing for Electrostatic Charges on Materials at Kennedy Space Center, *Electrical Overstress / Electrostatic Discharge Symposium,* vol. 1984 Proceedings, pp. 58-63.
26. Guastavino, F., Coletti, G., Dardano, A. and Torello, E. (2004), Some Experiments about the Triboelectric Performances of Composite Textiles, *Conference on Electrical Insulation and Dielectric Phenomena,* vol. 2004 Annual Report, pp. 85-88.
27. Henniker, J. (1962). Triboelectricity in Polymers, *Nature*, 196, pp. 474.
28. Henry, P. S. H., Livesey, R. G., and Wood, A. M. (1967). Test for Liability to Electrostatic Charging, *Journal of Textile Institute*, 58(2), 55-77.
29. Hersh, S.P., and Montgomery, D.J. (1955). Static Electrification of Filaments:

Experimental Techniques and Results**,** *Textile Research Journal*, 25(4), pp. 279-295.

30. Hersh, S.P. (1954). *Static Electrification of Fibrous Materials*, Department of Chemistry, Princeton University, Ann Arbor.
31. Holdstock, P., and Wilson, N. (1996) The Effect of Static Charge generated on Hospital Bedding, El*ectrical Overstress / Electrostatic Discharge Symposium, 1996 Proceedings*, 356-364.
32. Holme, I., MchIntyre, J.E., and Shen, Z.J. (1998) Electrostatic Charging of Textiles, *Textile Progress*, 28(1), The Textile Institute.
33. International Standard Organization (2000) Textile Floor Coverings – Assessment of Static Electrical Propensity – Walking Test, *International Standard*, vol. ISO-6356:2000.
34. Joachim, G., Wiggins, R. E., and Arthur, J. B. (1965). *Static Electricity Generation, Measurement, and Its Effects on Textiles*, Department of Textiles, School of Textiles, North Carolina State University, Raleigh.
35. Jonassen, N., Hansson, I., and Aielsen, A. R. (1979). On the Correlation between Decay of Charge and Resistance Parameters of Sheet Materials, *Journal of Physics; Conference Series*, vol. 48, pp. 215-224.
36. Morton, W. E. and Hearle, J. W. S. (1997), *Physical Properties of Textile Fibres*, Bath: The Textile Institute.
37. Nikonova, E.A., Pakshver, A.B., and Yagudina, R.S. (1971). The Frictional and Electrostatic Properties of Synthetic Fibres, Fibre Chemistry, 2(3), pp. 253-256.
38. Ohara, K., Nakamura, I., and Kinoshita, M. (2001). Frictional Electrification between Flat Surfaces of Polymers and of Langmuir-Blodgett Layers, *Journal of Electrostatics*,

51-52, 351-358.

39. Paasi, J., Kalliohaka, S.T., Coletti, G., Guastavino, F., Fast, L., Nilsson, A., Lemaire, P., Laperre, J., Vogel, C., Haase, J., Peltoniemi, T., Reina, G., Borjesson, A., Smallwood, J. (2004). Electrostatic Testing of ESD-protective Clothing for Electronics Industry, *Electrostatics 2003 Conference*, 178, 239-246.
40. Seyam, A.M., Cai, Y., and Oxenham, W. (2007). Devices for Measuring Electrostatic Generation and Dissipation on the Surfaces of Polymeric Materials, Journal of Textile Institute, in Press.
41. Seyam, A.M., Cai, Y., Wendisch, B., and Kim, Y.K. (2007), Disc-Shaped Fiberweb Formation with Controlled Fiber Orientation Using Electrostatic Forces: Theoretical Analysis and Experimental Verification, Journal of Textile Institute, in Press.
42. Seyam, A.M., Oxenham, W. and Castle, P. (2005). Static Generation and Control in Textile Systems, *National Textile Center Annual Report.*
43. Shumway, R.H., and Stoffer, D.S. (2006). *Time Series Analysis and Its Applications with R Examples*, New York: Springer.
44. Sweeney, J. (1955). Evaluation of Antistatic Agents on Nylon Parachute Cloth, *Wright Air Development Center Technical Report*, 54-513, 1-64.
45. Tabata, Y. (1988). Electrostatic Properties of Antistatic Cloth Woven Partly with Electrically conductive Fibers, *IEEE Transactions on Industry Applications,* 24(2), pp. 245-249.
46. Taylor, D. M., and Secker, P. E. (1994). *Industrial Electrostatics: Fundamentals and Measurements*, New York: John Wiley & Sons.

47. Ukraintseva, S. V., Nikitin, A. A., Akopova, V. V., Biryukove, T. N., and Rodionov, V. V. (1992), Electro Physical Properties of Antistatic Yarns, *Fibre Chemistry*, 23(3), 224-226.

48. Wilson, N. (1985). The Nature and Incendiary Behavior of Spark Discharges from Textile Surfaces, *Journal of Electrostatics,*16(2-3), pp. 231-245.

X. APPENDICES

APPENDIX A-1: Responses of Experimental Design I

Experimental Response for Experimental Design I

Temperature	Humidity	Tension	Speed	Initial Potential		Decay Time	
				Average	St. Dev.	Average	St. Dev.
(°C)	(%)	(gf)	(m/min)	(volts)	(volts)	(sec)	(sec)
21	40	150	300	-1668.3	132.3217	0.3006	0.0542
21	40	150	100	-1475.3	180.6903	0.8419	0.3253
21	40	150	50	-1176.4	180.6785	1.7527	2.9924
21	40	100	300	-1155.2	96.8310	0.3149	0.0641
21	40	100	100	-1030.0	156.9819	0.9870	1.6862
21	40	100	50	-756.0	141.5465	1.9175	3.0229
21	40	75	300	-833.9	81.0465	0.3663	0.0973
21	40	75	100	-721.6	119.4783	1.0816	2.3596
21	40	75	50	-514.0	103.4595	2.2887	5.3152
21	40	50	300	-512.6	64.2882	0.4988	0.3703
21	40	50	100	-427.4	93.4785	1.1333	2.2203
21	40	50	50	-272.8	71.9636	2.2131	3.8517
21	50	150	300	-1098.1	97.9421	0.3678	0.4713
21	50	150	100	-897.9	129.9420	1.1760	4.1092
21	50	150	50	-627.3	110.8068	1.5814	6.3131
21	50	100	300	-524.3	54.7957	0.4608	1.8562
21	50	100	100	-493.0	87.3509	0.4600	3.9525
21	50	100	50	-321.2	70.8339	1.2701	5.5301
21	50	75	300	-619.2	62.0244	0.3599	0.8307
21	50	75	100	-549.4	100.3531	0.9351	2.9639
21	50	75	50	-350.4	81.7791	1.0898	5.1815
21	50	50	300	-376.4	47.7341	0.3550	0.7290
21	50	50	100	-298.2	65.3102	0.6413	2.4968
21	50	50	50	-179.2	51.3916	0.8662	3.4891
21	65	150	300	-1413.9	133.7601	0.7018	1.8983
21	65	150	100	-919.6	148.6003	1.4503	3.8982
21	65	150	50	-383.6	115.1039	1.3147	5.5900
21	65	100	300	-961.4	91.3494	0.6295	1.2808
21	65	100	100	-613.9	107.3026	1.2667	3.4167
21	65	100	50	-205.9	72.4988	1.1720	3.9758
21	65	75	300	-688.1	75.0024	0.4807	1.1344
21	65	75	100	-448.6	93.5720	1.1517	2.8928
21	65	75	50	-163.8	61.5612	1.4331	3.0529
21	65	50	300	-409.8	46.5299	0.4520	0.8266
21	65	50	100	-246.2	57.2764	1.0957	2.0036
21	65	50	50	-78.8	31.7561	1.0482	1.3450

Experimental Response for Experimental Design I [continued]

Temperature	Humidity	Tension	Speed	Initial Potential		Decay Time	
				Average	St. Dev.	Average	St. Dev.
(°C)	(%)	(gf)	(m/min)	(volts)	(volts)	(sec)	(sec)
25	40	150	300	-1621.9	169.6032	0.5661	1.7471
25	40	150	100	-1633.8	377.5889	0.8907	1.2537
25	40	150	50	-1003.7	182.2573	2.0610	3.5660
25	40	100	300	-1137.2	105.4204	0.6065	1.6517
25	40	100	100	-1175.9	258.7228	0.8404	2.3636
25	40	100	50	-738.4	142.1776	2.3575	4.1298
25	40	75	300	-815.6	73.4123	0.5047	1.3727
25	40	75	100	-739.7	120.2498	1.2156	3.7528
25	40	75	50	-566.6	123.2972	2.3034	4.8264
25	40	50	300	-470.9	49.9897	0.5154	1.6105
25	40	50	100	-413.6	81.4382	1.2642	3.3521
25	40	50	50	-279.7	64.9336	2.4551	5.1079
25	50	150	300	-1436.0	126.0557	0.6983	1.5477
25	50	150	100	-1348.6	288.6825	1.0278	2.5980
25	50	150	50	-722.9	202.8076	2.3608	5.4805
25	50	100	300	-1213.9	267.4446	0.4625	1.3591
25	50	100	100	-829.9	122.5396	1.4729	3.5616
25	50	100	50	-583.9	158.6067	1.6882	4.7521
25	50	75	300	-690.0	64.6747	0.6038	1.3440
25	50	75	100	-678.6	148.9474	0.9853	2.7299
25	50	75	50	-350.2	80.2225	2.2462	5.8487
25	50	50	300	-419.8	94.4572	0.4451	1.4800
25	50	50	100	-346.6	76.7682	1.1768	3.0142
25	50	50	50	-203.0	69.8837	1.5810	4.0392
25	65	150	300	-1265.3	227.1918	0.6453	2.3104
25	65	150	100	-773.2	213.2320	1.0305	3.0024
25	65	150	50	-179.0	58.6964	1.4612	3.7880
25	65	100	300	-684.0	58.9250	-0.0433	3.2353
25	65	100	100	-620.9	167.2076	1.0579	2.9281
25	65	100	50	-177.3	56.1863	1.3709	3.5054
25	65	75	300	-542.8	54.5931	0.7513	1.7068
25	65	75	100	-384.4	71.5495	1.3507	3.3666
25	65	75	50	-92.5	42.0106	1.0549	2.1417
25	65	50	300	-331.4	42.0287	0.4854	1.3480
25	65	50	100	-210.4	59.5976	0.8388	1.8354
25	65	50	50	-43.9	21.4012	0.6345	0.8548

Experimental Response for Experimental Design I [continued]

Temperature	Humidity	Tension	Speed	Initial Potential		Decay Time	
				Average	St. Dev.	Average	St. Dev.
(°C)	(%)	(gf)	(m/min)	(volts)	(volts)	(sec)	(sec)
30	30	150	300	-1107.1	78.6149	0.1652	0.0287
30	30	150	100	-868.2	86.5438	0.5167	0.0941
30	30	150	50	-597.7	80.3077	1.0022	0.1792
30	30	100	300	-846.5	74.4290	0.1530	0.0304
30	30	100	100	-638.0	76.1401	0.5277	0.1101
30	30	100	50	-421.3	70.0625	1.0481	0.2468
30	30	75	300	-639.8	80.8209	0.1490	0.0523
30	30	75	100	-460.9	59.9011	0.5812	0.1769
30	30	75	50	-299.4	49.7097	1.1058	0.3630
30	30	50	300	-386.3	45.9998	0.1602	0.0408
30	30	50	100	-284.5	36.1095	0.5664	0.1586
30	30	50	50	-176.8	34.0721	1.1688	0.5592
30	40	150	300	-940.5	61.5216	0.2444	0.0600
30	40	150	100	-727.4	81.8521	0.6735	0.1606
30	40	150	50	-459.2	63.0212	1.2613	0.3006
30	40	100	300	-715.7	67.2790	0.1996	0.0553
30	40	100	100	-531.6	62.2433	0.6991	0.1993
30	40	100	50	-330.4	51.0234	1.3513	0.4662
30	40	75	300	-529.3	61.8401	0.1952	0.0594
30	40	75	100	-358.7	52.8782	0.6975	0.2512
30	40	75	50	-220.8	40.2870	1.3655	0.5217
30	40	50	300	-335.6	55.0656	0.1965	0.0849
30	40	50	100	-220.7	36.3483	0.7435	0.4329
30	40	50	50	-112.5	25.0097	1.3237	0.7701
30	50	150	300	-899.9	70.7023	0.2679	0.0669
30	50	150	100	-642.8	65.4052	0.7765	0.2015
30	50	150	50	-327.2	55.3370	1.6663	1.0374
30	50	100	300	-635.2	65.6260	0.2928	0.1526
30	50	100	100	-423.6	54.4741	1.1268	0.9515
30	50	100	50	-213.8	43.2580	2.0108	1.9709
30	50	75	300	-473.8	68.4535	0.3466	0.3730
30	50	75	100	-299.3	44.0668	1.4326	1.5966
30	50	75	50	-133.3	30.7781	2.2803	2.7893
30	50	50	300	-283.1	35.8089	0.4184	0.4648
30	50	50	100	-178.5	27.6206	1.3384	1.5479
30	50	50	50	-78.0	22.0926	2.1098	2.4008

Experimental Response for Experimental Design I [continued]

Temperature	Humidity	Tension	Speed	Initial Potential		Decay Time	
				Average	St. Dev.	Average	St. Dev.
(°C)	(%)	(gf)	(m/min)	(volts)	(volts)	(sec)	(sec)
30	65	150	300	-818.3	76.5267	0.2299	0.0638
30	65	150	100	-366.0	58.5188	0.8802	0.7235
30	65	150	50	-76.4	34.0481	1.3127	1.4608
30	65	100	300	-531.6	58.4255	0.2472	0.0839
30	65	100	100	-244.8	50.8479	0.8260	0.5837
30	65	100	50	-34.6	17.0154	0.7376	0.6670
30	65	75	300	-379.8	45.2412	0.2794	0.1281
30	65	75	100	-176.9	36.4150	0.8538	0.5714
30	65	75	50	-31.4	17.4729	0.6932	0.7329
30	65	50	300	-227.4	33.1777	0.2855	0.1537
30	65	50	100	-82.9	20.2219	0.8390	0.8355
30	65	50	50	N/A	N/A	N/A	N/A
35	30	150	300	-1080.9	74.4478	0.4673	4.9939
35	30	150	100	-844.2	84.3608	0.3715	13.3875
35	30	150	50	-484.7	76.2120	0.7989	18.2806
35	30	100	300	-801.7	52.5897	-0.8909	3.1035
35	30	100	100	-579.3	71.6147	-1.6238	8.4626
35	30	100	50	-356.9	55.7521	-2.1068	14.5447
35	30	75	300	-621.7	44.0698	-0.6830	2.5697
35	30	75	100	-455.2	60.6837	-0.4698	5.9554
35	30	75	50	-240.3	44.8197	-2.5486	11.0344
35	30	50	300	-379.4	31.9074	-0.7001	1.6762
35	30	50	100	-260.6	37.0866	-1.7354	4.8093
35	30	50	50	-133.9	29.3997	-2.5258	7.0344
35	40	150	300	-1033.4	63.4535	-0.8432	2.3196
35	40	150	100	-753.6	81.5284	-2.3777	6.2516
35	40	150	50	-409.0	81.3558	-3.5921	8.7449
35	40	100	300	-726.4	51.1228	-0.7734	1.5939
35	40	100	100	-517.3	71.3428	-2.3459	6.3835
35	40	100	50	-263.6	47.0057	-2.4558	11.2920
35	40	75	300	-539.0	37.8527	-0.6258	2.0244
35	40	75	100	-369.9	58.3786	-1.9853	4.6150
35	40	75	50	-169.1	37.0251	-2.7843	8.3067
35	40	50	300	-344.9	31.0322	-0.5498	1.7236
35	40	50	100	-189.3	31.1368	-1.7220	3.1080
35	40	50	50	-81.6	24.5641	-2.1819	4.7221

Experimental Response for Experimental Design I [continued]

Temperature	Humidity	Tension	Speed	Initial Potential		Decay Time	
				Average	St. Dev.	Average	St. Dev.
(°C)	(%)	(gf)	(m/min)	(volts)	(volts)	(sec)	(sec)
35	50	150	300	-1047.4	77.5804	-0.5296	1.4464
35	50	150	100	-578.2	74.1955	-1.7588	3.7135
35	50	150	50	-215.6	52.4685	-2.4859	8.3237
35	50	100	300	-690.8	49.8005	-0.3256	0.1341
35	50	100	100	-385.1	59.8809	-1.3424	1.8363
35	50	100	50	-134.9	35.2484	-2.2975	6.3287
35	50	75	300	-525.0	40.1390	-0.2996	0.5019
35	50	75	100	-292.1	42.3747	-1.2375	1.3838
35	50	75	50	-96.9	29.1526	-1.8124	5.1634
35	50	50	300	-321.1	43.7371	-0.3934	1.0192
35	50	50	100	-162.8	28.8702	-1.3055	1.4457
35	50	50	50	-42.3	20.3595	-0.9289	2.8532
35	65	150	300	-794.5	58.6058	-0.2576	0.0566
35	65	150	100	-268.0	66.6632	-1.2322	2.2737
35	65	150	50	-30.2	21.6650	-0.3687	2.1261
35	65	100	300	-563.3	48.2710	-0.2744	0.0985
35	65	100	100	-156.2	39.7045	-1.2944	1.9280
35	65	100	50	N/A	N/A	N/A	N/A
35	65	75	300	-415.6	40.9135	-0.2753	0.2796
35	65	75	100	-109.2	35.7679	-1.0704	1.8371
35	65	75	50	N/A	N/A	N/A	N/A
35	65	50	300	-238.1	25.5399	-0.2521	0.1214
35	65	50	100	-48.0	18.2662	-0.8266	1.2371
35	65	50	50	N/A	N/A	N/A	N/A

APPENDIX A-2: Responses of Experimental Design II

Experimental Response for Experimental Design II

Charge Pin Material	Humidity (%)	Tension (gf)	Speed (m/min)	Initial Potential Average (volts)	Initial Potential St. Dev. (volts)	Decay Time Average (sec)	Decay Time St. Dev. (sec)
Stainless Steel	30	150	300	-1107.1	78.6149	0.1652	0.0287
Stainless Steel	30	150	100	-868.2	86.5438	0.5167	0.0941
Stainless Steel	30	150	50	-597.7	80.3077	1.0022	0.1792
Stainless Steel	30	75	300	-639.8	80.8209	0.1490	0.0523
Stainless Steel	30	75	100	-460.9	59.9011	0.5812	0.1769
Stainless Steel	30	75	50	-299.4	49.7097	1.1058	0.3630
Stainless Steel	65	150	300	-818.3	76.5267	0.2299	0.0638
Stainless Steel	65	150	100	-366.0	58.5188	0.8802	0.7235
Stainless Steel	65	150	50	-76.4	34.0481	1.3127	1.4608
Stainless Steel	65	75	300	-379.8	45.2412	0.2794	0.1281
Stainless Steel	65	75	100	-176.9	36.4150	0.8538	0.5714
Stainless Steel	65	75	50	-31.4	17.4729	0.6932	0.7329
Nylon	30	150	300	N/A	N/A	N/A	N/A
Nylon	30	150	100	205.1	113.8951	0.2106	3.0465
Nylon	30	150	50	496.0	154.9037	0.9043	8.3491
Nylon	30	75	300	-215.3	46.2541	0.1123	0.0466
Nylon	30	75	100	N/A	N/A	N/A	N/A
Nylon	30	75	50	187.1	90.8765	0.5243	3.8498
Nylon	65	150	300	439.4	66.9656	0.6037	1.6154
Nylon	65	150	100	494.4	114.8209	1.2492	5.4950
Nylon	65	150	50	286.0	97.6087	0.8932	8.8349
Nylon	65	75	300	212.9	42.3004	0.4648	0.5096
Nylon	65	75	100	242.9	63.5589	1.0696	4.3055
Nylon	65	75	50	147.3	48.7478	-0.1748	6.9666
Polyester	30	150	300	-160.8	66.5336	0.1094	0.0626
Polyester	30	150	100	127.8	57.8558	0.0040	2.8206
Polyester	30	150	50	376.4	110.2842	0.3655	8.2508
Polyester	30	75	300	-215.5	51.9994	0.1638	0.1886
Polyester	30	75	100	N/A	N/A	N/A	N/A
Polyester	30	75	50	170.8	72.4929	0.2457	5.8011
Polyester	65	150	300	163.9	36.6153	0.3628	1.0408
Polyester	65	150	100	371.3	77.6853	0.9795	5.2092
Polyester	65	150	50	314.8	90.4621	0.7386	9.3763
Polyester	65	75	300	58.8	20.4908	0.0494	0.7362
Polyester	65	75	100	177.0	44.0021	0.3719	3.7736
Polyester	65	75	50	131.0	45.0656	0.5903	5.8419

Experimental Response for Experimental Design II [continued]

Charge Pin Material	Humidity (%)	Tension (gf)	Speed (m/min)	Initial Potential Average (volts)	Initial Potential St. Dev. (volts)	Decay Time Average (sec)	Decay Time St. Dev. (sec)
Polypropylene	30	150	300	-132.8	42.1525	0.1270	0.1513
Polypropylene	30	150	100	-29.1	109.2870	0.4071	0.4922
Polypropylene	30	150	50	34.6	137.7701	0.3862	0.9275
Polypropylene	30	75	300	-147.9	38.5563	0.1725	0.2341
Polypropylene	30	75	100	-78.7	42.9749	0.4482	0.7439
Polypropylene	30	75	50	-46.6	62.7812	0.3308	0.9454
Polypropylene	65	150	300	0.0	N/A	N/A	N/A
Polypropylene	65	150	100	0.0	N/A	N/A	N/A
Polypropylene	65	150	50	0.0	N/A	N/A	N/A
Polypropylene	65	75	300	0.0	N/A	N/A	N/A
Polypropylene	65	75	100	0.0	N/A	N/A	N/A
Polypropylene	65	75	50	0.0	N/A	N/A	N/A
Teflon	30	150	300	-112.2	46.6687	0.1280	0.0522
Teflon	30	150	100	-130.5	125.8540	0.2138	0.6039
Teflon	30	150	50	-106.0	128.0963	0.3734	1.2707
Teflon	30	75	300	-160.1	41.4091	0.1440	0.0246
Teflon	30	75	100	-123.5	95.1925	0.2964	0.6865
Teflon	30	75	50	-113.6	96.1186	0.3949	1.4593
Teflon	65	150	300	0.0	N/A	N/A	N/A
Teflon	65	150	100	0.0	N/A	N/A	N/A
Teflon	65	150	50	0.0	N/A	N/A	N/A
Teflon	65	75	300	0.0	N/A	N/A	N/A
Teflon	65	75	100	0.0	N/A	N/A	N/A
Teflon	65	75	50	0.0	N/A	N/A	N/A

APPENDIX A-3: Responses of Experimental Design III

Experimental Response for Experimental Design III

Charge Pin	Humidity	Tension	Speed	Initial Potential		Decay Time	
				Average	St. Dev.	Average	St. Dev.
Material	(%)	(gf)	(m/min)	(volts)	(volts)	(sec)	(sec)
Polyester	30	45	300	-851.8	58.6187	0.0333	0.0023
Polyester	30	45	100	-812.1	103.7771	0.1119	0.0115
Polyester	30	45	50	-649.9	136.6728	0.2274	0.0362
Polyester	30	30	300	-663.6	59.3498	0.0317	0.0026
Polyester	30	30	100	-649.8	93.2508	0.1096	0.0126
Polyester	30	30	50	-541.9	127.9068	0.2232	0.0426
Polyester	65	45	300	-468.7	70.9307	0.0395	0.0041
Polyester	65	45	100	-440.3	84.4515	0.1093	0.0132
Polyester	65	45	50	-417.6	84.9077	0.1992	0.0310
Polyester	65	30	300	-600.7	81.0584	0.0354	0.0030
Polyester	65	30	100	-447.8	108.5404	0.1020	0.0159
Polyester	65	30	50	N/A	N/A	N/A	N/A
Nylon	30	45	300	199.5	40.6521	0.0738	0.0086
Nylon	30	45	100	220.4	64.8225	0.2683	0.0833
Nylon	30	45	50	135.8	60.5294	0.6977	0.4712
Nylon	30	30	300	145.5	44.0585	0.1223	0.0646
Nylon	30	30	100	117.9	29.9928	0.3988	0.2158
Nylon	30	30	50	94.4	28.4312	1.1966	1.1142
Nylon	65	45	300	587.2	71.0936	0.0573	0.0045
Nylon	65	45	100	485.2	65.8836	0.1246	0.0164
Nylon	65	45	50	474.5	64.1834	0.2315	0.0333
Nylon	65	30	300	354.2	54.0353	0.0716	0.0112
Nylon	65	30	100	98.3	65.3868	0.2194	0.2365
Nylon	65	30	50	N/A	N/A	N/A	N/A
Polypropylene	30	45	300	-71.5	21.9802	0.0621	0.0423
Polypropylene	30	45	100	-66.0	28.5818	0.1941	0.2423
Polypropylene	30	45	50	-60.4	31.3211	0.4290	0.6267
Polypropylene	30	30	300	-58.0	23.2244	0.0546	0.0424
Polypropylene	30	30	100	-62.9	30.0774	0.1548	0.1560
Polypropylene	30	30	50	-62.9	32.8905	0.3325	0.3884
Polypropylene	65	45	300	-335.8	38.5344	0.0440	0.0038
Polypropylene	65	45	100	-296.8	49.5243	0.1107	0.0221
Polypropylene	65	45	50	-272.9	59.5283	0.1739	0.0477
Polypropylene	65	30	300	-375.5	30.0718	0.0316	0.0041
Polypropylene	65	30	100	-333.6	50.3530	0.0838	0.0166
Polypropylene	65	30	50	-301.6	61.0047	0.1700	0.0400

APPENDIX A-4: Responses of Experimental Design IV

Experimental Response for Experimental Design IV

Fiber	Yarn	Humidity	Tension	Speed	Initial Potential		Decay Time	
					Average	St. Dev.	Average	St. Dev.
Type		(%)	(gf/tex)	(m/min)	(volts)	(volts)	(sec)	(sec)
Polyester	Multi	30	1.35	300	-1107.1	78.6149	0.1652	0.0287
Polyester	Multi	30	1.35	100	-868.2	86.5438	0.5167	0.0941
Polyester	Multi	30	1.35	50	-597.7	80.3077	1.0022	0.1792
Polyester	Multi	30	0.68	300	-639.8	80.8209	0.1490	0.0523
Polyester	Multi	30	0.68	100	-460.9	59.9011	0.5812	0.1769
Polyester	Multi	30	0.68	50	-299.4	49.7097	1.1058	0.3630
Polyester	Multi	65	1.35	300	-818.3	76.5267	0.2299	0.0638
Polyester	Multi	65	1.35	100	-366.0	58.5188	0.8802	0.7235
Polyester	Multi	65	1.35	50	-76.4	34.0481	1.3127	1.4608
Polyester	Multi	65	0.68	300	-379.8	45.2412	0.2794	0.1281
Polyester	Multi	65	0.68	100	-176.9	36.4150	0.8538	0.5714
Polyester	Multi	65	0.68	50	-31.4	17.4729	0.6932	0.7329
Nylon	Multi	30	1.35	300	-1279.1	84.3164	0.2199	0.0483
Nylon	Multi	30	1.35	100	-897.7	97.7107	0.7256	0.2034
Nylon	Multi	30	1.35	50	-636.4	98.4690	1.5616	0.8338
Nylon	Multi	30	0.68	300	-939.8	74.2754	0.2126	0.0420
Nylon	Multi	30	0.68	100	-639.0	69.2755	0.6551	0.1571
Nylon	Multi	30	0.68	50	-451.9	72.3348	1.5387	0.8857
Nylon	Multi	65	1.35	300	-955.2	79.5660	0.3348	0.1115
Nylon	Multi	65	1.35	100	-551.8	60.7462	0.8854	0.3145
Nylon	Multi	65	1.35	50	-314.9	47.2625	1.8433	2.1634
Nylon	Multi	65	0.68	300	-655.8	79.0437	0.1599	1.5083
Nylon	Multi	65	0.68	100	-298.1	37.0966	-1.2746	7.9200
Nylon	Multi	65	0.68	50	-179.1	28.2166	-2.4259	9.4794
Polypropylene	Multi	30	1.35	300	0.0	N/A	N/A	N/A
Polypropylene	Multi	30	1.35	100	0.0	N/A	N/A	N/A
Polypropylene	Multi	30	1.35	50	0.0	N/A	N/A	N/A
Polypropylene	Multi	30	0.68	300	0.0	N/A	N/A	N/A
Polypropylene	Multi	30	0.68	100	0.0	N/A	N/A	N/A
Polypropylene	Multi	30	0.68	50	0.0	N/A	N/A	N/A
Polypropylene	Multi	65	1.35	300	0.0	N/A	N/A	N/A
Polypropylene	Multi	65	1.35	100	0.0	N/A	N/A	N/A
Polypropylene	Multi	65	1.35	50	0.0	N/A	N/A	N/A
Polypropylene	Multi	65	0.68	300	0.0	N/A	N/A	N/A
Polypropylene	Multi	65	0.68	100	0.0	N/A	N/A	N/A
Polypropylene	Multi	65	0.68	50	0.0	N/A	N/A	N/A

Experimental Response for Experimental Design IV [continued]

Fiber	Yarn	Humidity	Tension	Speed	Initial Potential		Decay Time	
					Average	St. Dev.	Average	St. Dev.
Type		(%)	(gf/tex)	(m/min)	(volts)	(volts)	(sec)	(sec)
Polyester	Mono	30	1.35	300	-206.9	21.4721	0.3162	0.1675
Polyester	Mono	30	1.35	100	-126.4	35.4117	1.0352	0.7255
Polyester	Mono	30	1.35	50	-133.7	33.6377	1.6120	0.8667
Polyester	Mono	30	0.68	300	-196.8	19.0026	0.2573	0.0476
Polyester	Mono	30	0.68	100	-127.6	25.9695	0.7191	0.3579
Polyester	Mono	30	0.68	50	-116.0	36.4383	1.4417	1.0992
Polyester	Mono	65	1.35	300	-59.6	13.8270	0.2388	0.6146
Polyester	Mono	65	1.35	100	-29.2	14.0554	0.5277	0.6326
Polyester	Mono	65	1.35	50	-35.2	16.6435	1.1390	1.5070
Polyester	Mono	65	0.68	300	-64.1	13.1118	0.1846	0.0764
Polyester	Mono	65	0.68	100	-25.5	8.6532	0.3717	0.2827
Polyester	Mono	65	0.68	50	-38.7	25.0078	1.0172	2.3704
Nylon	Mono	30	1.35	300	-109.0	24.9424	0.1441	0.0209
Nylon	Mono	30	1.35	100	-88.7	45.7630	0.4624	0.1368
Nylon	Mono	30	1.35	50	-74.8	68.8705	0.8997	0.5085
Nylon	Mono	30	0.68	300	-61.1	15.7782	0.0602	0.0152
Nylon	Mono	30	0.68	100	-48.1	25.7845	0.2425	0.1263
Nylon	Mono	30	0.68	50	-39.9	23.5736	0.4793	0.2798
Nylon	Mono	65	1.35	300	0.0	N/A	N/A	N/A
Nylon	Mono	65	1.35	100	0.0	N/A	N/A	N/A
Nylon	Mono	65	1.35	50	0.0	N/A	N/A	N/A
Nylon	Mono	65	0.68	300	0.0	N/A	N/A	N/A
Nylon	Mono	65	0.68	100	0.0	N/A	N/A	N/A
Nylon	Mono	65	0.68	50	0.0	N/A	N/A	N/A
Polypropylene	Mono	30	1.35	300	451.7	219.8374	0.1662	0.5085
Polypropylene	Mono	30	1.35	100	580.4	127.1253	0.7265	0.4818
Polypropylene	Mono	30	1.35	50	808.6	235.7609	1.5046	3.9919
Polypropylene	Mono	30	0.68	300	587.1	87.9736	0.1347	0.0271
Polypropylene	Mono	30	0.68	100	665.6	116.2914	0.4147	0.0883
Polypropylene	Mono	30	0.68	50	696.6	176.2448	0.9171	1.7390
Polypropylene	Mono	65	1.35	300	598.3	158.4109	0.0775	0.0474
Polypropylene	Mono	65	1.35	100	434.8	123.7693	0.2332	0.0724
Polypropylene	Mono	65	1.35	50	345.4	95.1489	0.5353	0.1156
Polypropylene	Mono	65	0.68	300	660.4	184.6605	0.0802	0.0953
Polypropylene	Mono	65	0.68	100	815.4	165.4183	0.2352	0.0245
Polypropylene	Mono	65	0.68	50	760.5	162.0681	0.4642	0.2115

APPENDIX B: Voltmeter Calibration Results

Manufacturer recommends calibrating voltmeters every year for making accurate measurements. Calibration procedure for Monroe Electronics ISOPROBE® Electrostatic Voltmeter 244A is described. Instruments include High Voltage Pulse Generator, Oscilloscope, High Voltage Probe for Oscilloscope, Metal Plate, Probe, and Voltmeter to be calibrated. The probe and the voltmeter should be calibrated together.

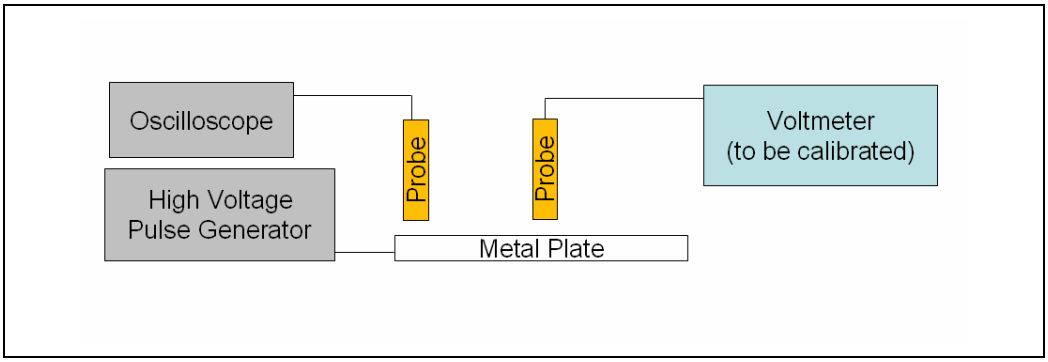

Instruments for Calibration

Calibration procedures consist of:

1. Turn on the devices.
2. Zero the voltmeter as described in section 4.5.
3. Position the probe to the metal plate at a distance of 0.005 inches.
4. Supply 1,000 volts to the metal plate using a high voltage pulse generator.
5. Record the voltage detected by the voltmeter.
6. Increase supply voltage gradually to 2,000 or 3,000 volts, and record the readings on the voltmeter.
7. Turn off the devices.

Voltmeter Calibration Result

Test No.	Generated Potential (volts)	Measured Potential (volts)	Difference (volts)	% Difference (%)
1	117	108	9	7.7
2	210	190	20	9.5
3	485	442	43	8.8
4	732	665	67	9.1
5	1003	909	94	9.3
6	1255	1140	115	9.1
7	1533	1392	141	9.2
8	1833	1667	166	9.0
9	1955	1777	178	9.1
10	2292	2083	209	9.1
11	2534	2180	354	14.0
12	2903	2640	263	9.0
13	3147	2851	296	9.4

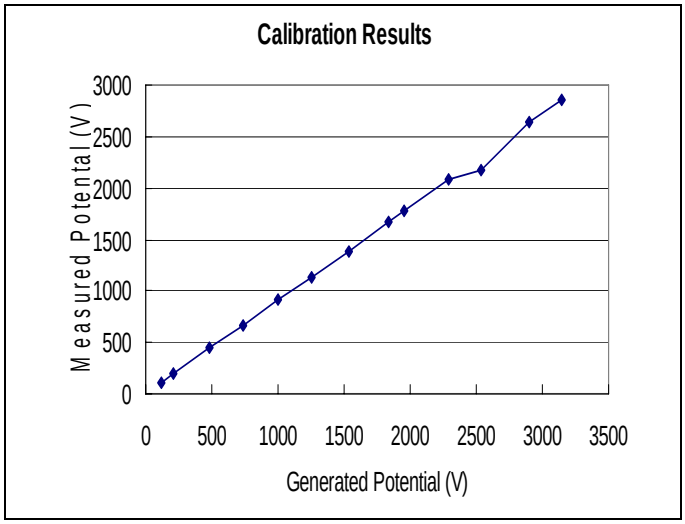

Voltmeter Calibration Results

Calibration data on the voltmeter are shown above. The difference between the generated potential and the measured potential was within acceptable level (10%).

APPENDIX C-1: Potential per Surface Area of Finish-free Yarns in Experimental Design III

Potential per Surface Area unit: volt/cm^2

		30°C, 30% R.H.		30°C, 65% R.H	
Yarn	Speed (m/min)	2.00 gf/tex	1.35 gf/tex	2.00 gf/tex	1.35 gf/tex
Polyester	300	-5466.9	-4259.0	-3008.2	-3855.3
	100	-5212.1	-4170.5	-2825.9	-2874.0
	50	-4171.1	-3478.0	-2680.2	0.0
Nylon	300	1163.6	848.6	3424.9	2065.9
	100	1285.5	687.7	2830.0	573.3
	50	792.1	550.6	2416.4	0.0
Polypropylene	300	-370.6	-300.6	-1740.4	-1946.2
	100	-342.1	-326.0	-1538.3	-1729.0
	50	-313.1	-326.0	-1414.4	-1563.2

APPENDIX C-2: ANOVA Results for Potential per Surface Area in Experimental Design III

Overall ANOVA for Initial Potential per Surface Area

Source	DF	Sum of Squares	Mean Square	F-value	Pr > F
Model	2	156500844.9	78250422.4	98.46	<.0001
Error	31	24637026.4	794742.8		
Corrected Total	33	181137871.3			

Type I and Type III ANOVA for Initial Potential per Surface Area

Source	DF	Type I SS	Mean Square	F-value	Pr > F
Yarn Material	2	156500844.9	78250422.4	98.46	<.0001

APPENDIX D-1: Potential per Surface Area of Yarns in Experimental Design IV

Potential per Surface Area of Multifilament Yarns unit: volt/cm^2

		30°C, 30% R.H.		30°C, 65% R.H	
Yarn	Speed (m/min)	1.35 gf/tex	0.68 gf/tex	1.35 gf/tex	0.68 gf/tex
Polyester	300	-208.0	-120.2	-153.7	-71.4
	100	-163.1	-86.6	-68.8	-33.2
	50	-112.3	-56.2	-14.4	-5.9
Nylon	300	-470.0	-345.3	-351.0	-241.0
	100	-329.8	-234.8	-202.7	-109.5
	50	-233.8	-166.0	-115.7	-65.8
Polypropylene	300	0.0	0.0	0.0	0.0
	100	0.0	0.0	0.0	0.0
	50	0.0	0.0	0.0	0.0

Potential per Surface Area of Monofilament Yarns unit: volt/cm^2

		30°C, 30% R.H.		30°C, 65% R.H	
Yarn	Speed (m/min)	1.35 gf/tex	0.68 gf/tex	1.35 gf/tex	0.68 gf/tex
Polyester	300	-22.0	-20.9	-6.3	-6.8
	100	-13.4	-13.5	-3.1	-2.7
	50	-14.2	-12.3	-3.7	-4.1
Nylon	300	-17.3	-9.7	0.0	0.0
	100	-14.1	-7.7	0.0	0.0
	50	-11.9	-6.4	0.0	0.0
Polypropylene	300	28.8	37.4	38.1	42.0
	100	36.9	42.4	27.7	51.9
	50	51.5	44.3	22.0	48.4

APPENDIX D-2: ANOVA Results for Potential per Surface Area (Multifilament) in Experimental Design IV

Overall ANOVA for Initial Potential per Surface Area of Multifilament Yarns

Source	DF	Sum of Squares	Mean Square	F-value	Pr > F
Model	9	167524.0352	18613.7817	1.53	0.2421
Error	12	146050.1943	12170.8495		
Corrected Total	21	313574.2295			

Type I ANOVA for Initial Potential per Surface Area of Multifilament Yarns

Source	DF	Type I SS	Mean Square	F-value	Pr > F
humidity	1	39157.58438	39157.58438	3.22	0.0981
tension	1	30460.56017	30460.56017	2.50	0.1396
speed	2	95002.45829	47501.22915	3.90	0.0495
tension*speed	2	1643.99525	821.99763	0.07	0.9350
hum.*tension	1	8.14074	8.14074	0.00	0.9798
hum.*speed	2	1251.29641	625.64820	0.05	0.9501

Type III ANOVA for Initial Potential per Surface Area of Multifilament Yarns

Source	DF	Type III SS	Mean Square	F-value	Pr > F
humidity	1	54095.36014	54095.36014	4.44	0.0567
tension	1	37447.69969	37447.69969	3.08	0.1049
speed	2	92118.63641	46059.31820	3.78	0.0532
tension*speed	2	1577.87474	788.93737	0.06	0.9376
hum.*tension	1	0.23269	0.23269	0.00	0.9966
hum.*speed	2	1251.29641	625.64820	0.05	0.9501

APPENDIX D-3: ANOVA Results for Potential per Surface Area (Monofilament) in Experimental Design IV

Overall ANOVA for Initial Potential per Surface Area of Monofilament Yarns

Source	DF	Sum of Squares	Mean Square	F-value	Pr > F
Model	9	1721.12189	191.23577	0.22	0.9887
Error	20	17749.53178	887.47659		
Corrected Total	29	19470.65367			

Type I ANOVA for Initial Potential per Surface Area of Monofilament Yarns

Source	DF	Type I SS	Mean Square	F-value	Pr > F
humidity	1	1147.107556	1147.107556	1.29	0.2690
tension	1	231.296333	231.296333	0.26	0.6153
speed	2	143.464667	71.732333	0.08	0.9227
tension*speed	2	12.692667	6.346333	0.01	0.9929
hum.*tension	1	59.397556	59.397556	0.07	0.7985
hum.*speed	2	127.163111	63.581556	0.07	0.9311

Type III ANOVA for Initial Potential per Surface Area of Monofilament Yarns

Source	DF	Type III SS	Mean Square	F-value	Pr > F
humidity	1	1147.107556	1147.107556	1.29	0.2690
tension	1	270.357556	270.357556	0.30	0.5871
speed	2	95.707111	47.853556	0.05	0.9476
tension*speed	2	12.692667	6.346333	0.01	0.9929
hum.*tension	1	59.397556	59.397556	0.07	0.7985
hum.*speed	2	127.163111	63.581556	0.07	0.9311

APPENDIX E: Correlation between Friction Coefficient and Potential

tension (gf)	yarn speed (m/min)	friction coefficient	potential (volt)	correlation coefficient
50	50	0.2137	-78.8	0.9928
75	50	0.2054	-163.8	
100	50	0.1937	-205.9	
150	50	0.1657	-383.6	
50	100	0.2287	-246.2	0.9767
75	100	0.2169	-448.6	
100	100	0.1981	-613.9	
150	100	0.1871	-919.6	
50	300	0.2591	-409.8	0.9837
75	300	0.2482	-688.1	
100	300	0.2308	-961.4	
150	300	0.1884	-1413.9	

The polyester (1000/140) yarn was rubbed against a stainless steel charge pin at 21°C temperature and 65% relative humidity.

APPENDIX F: Correlation between Resistance and Decay Time

Fiber type	Number of Filament	Resistance (Ω)	Decay time (sec)
Polyester	140	3.89E+12	0.1652
Nylon	72	3.30E+13	0.2199
Polypropylene	144	1.64E+12	N/A
Polyester	60	2.26E+16	0.3162
Nylon	60	9.41E+15	0.1441
Polypropylene	60	2.24E+16	0.1662
Polyester	1	1.28E+17	0.0333
Nylon	1	N/A	0.0738
Polypropylene	1	4.59E+17	0.0621
Correlation coefficient		-0.5904	

The yarns were rubbed against a stainless steel charge pin at 30°C temperature, 30% relative humidity, 1.35 gf/tex yarn tension, and 300 m/min yarn speed.

APPENDIX G-1: Analytical Result on Extract of 420/72 Nylon Yarn

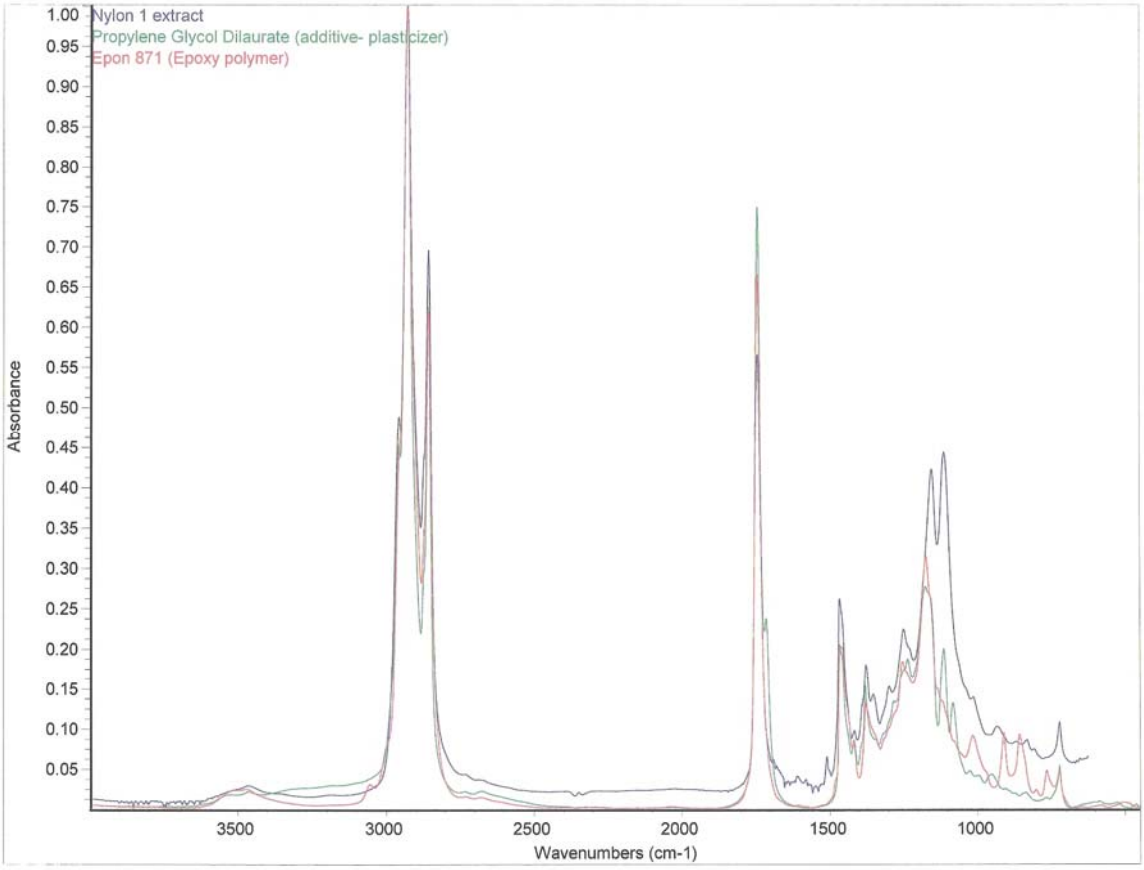

Propylene Glycol Dilaurate is 94.37% matched to the yarn extract.

Epon 871 is 94.13% matched to the yarn extract.

APPENDIX G-2: Analytical Result on Extract of 300/144 Polypropylene Yarn

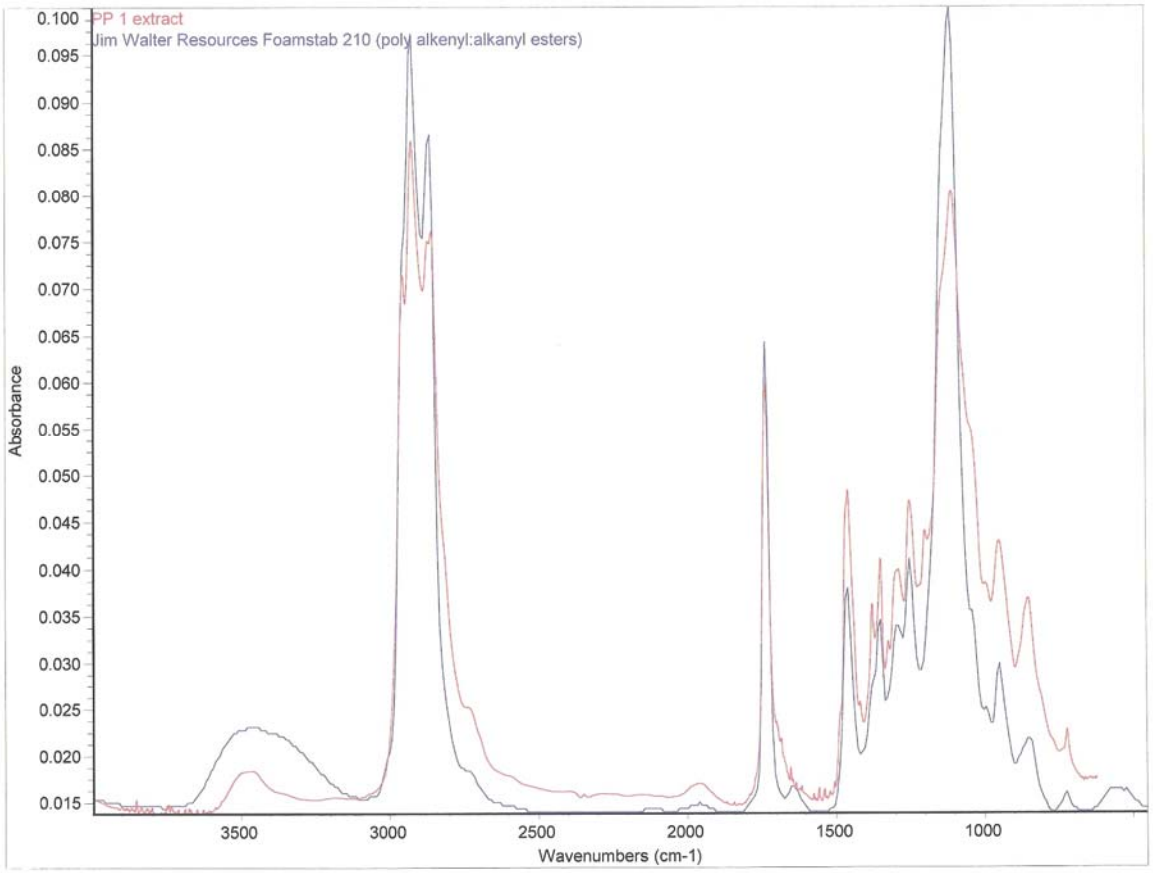

Jim Walter Resources Foamstab 210 is 91.48% matched to the yarn extract.

APPENDIX G-3: Analytical Result on Extract of Polyester Finish-free Yarn

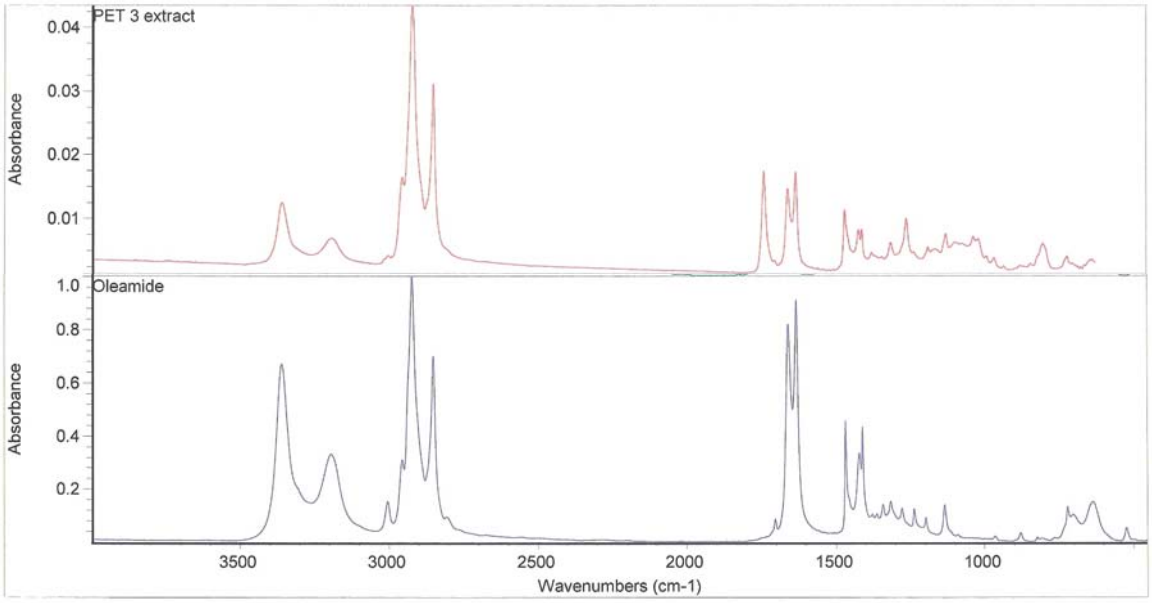

Oleamide is 98.48% matched to the yarn extract.

APPENDIX G-4: Analytical Result on Extract of Polypropylene Finish-free Yarn

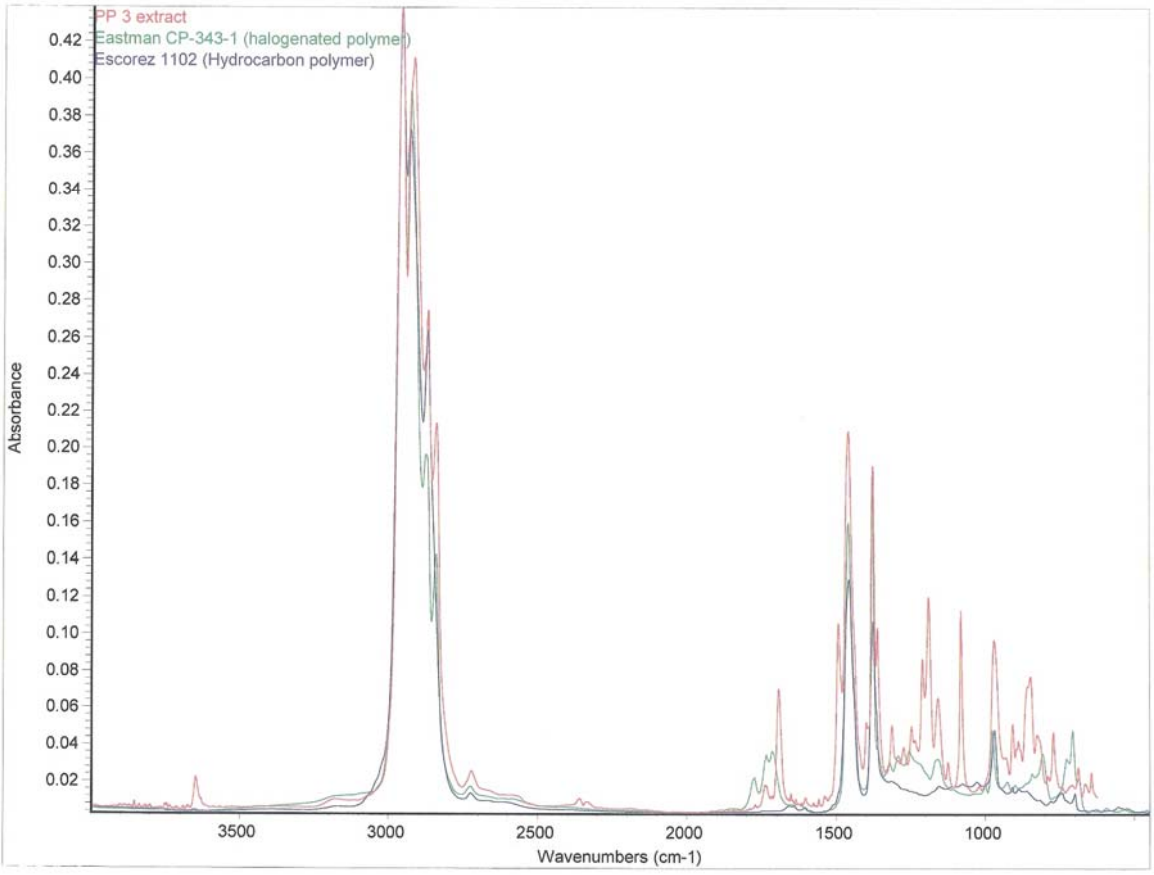

Eastman CP-343-1 is 81.38% matched to the yarn extract.

Escorez 1102 is 73.85% matched to the yarn extract.

APPENDIX G-5: Analytical Result on Extract of Nylon Monofilament Yarn

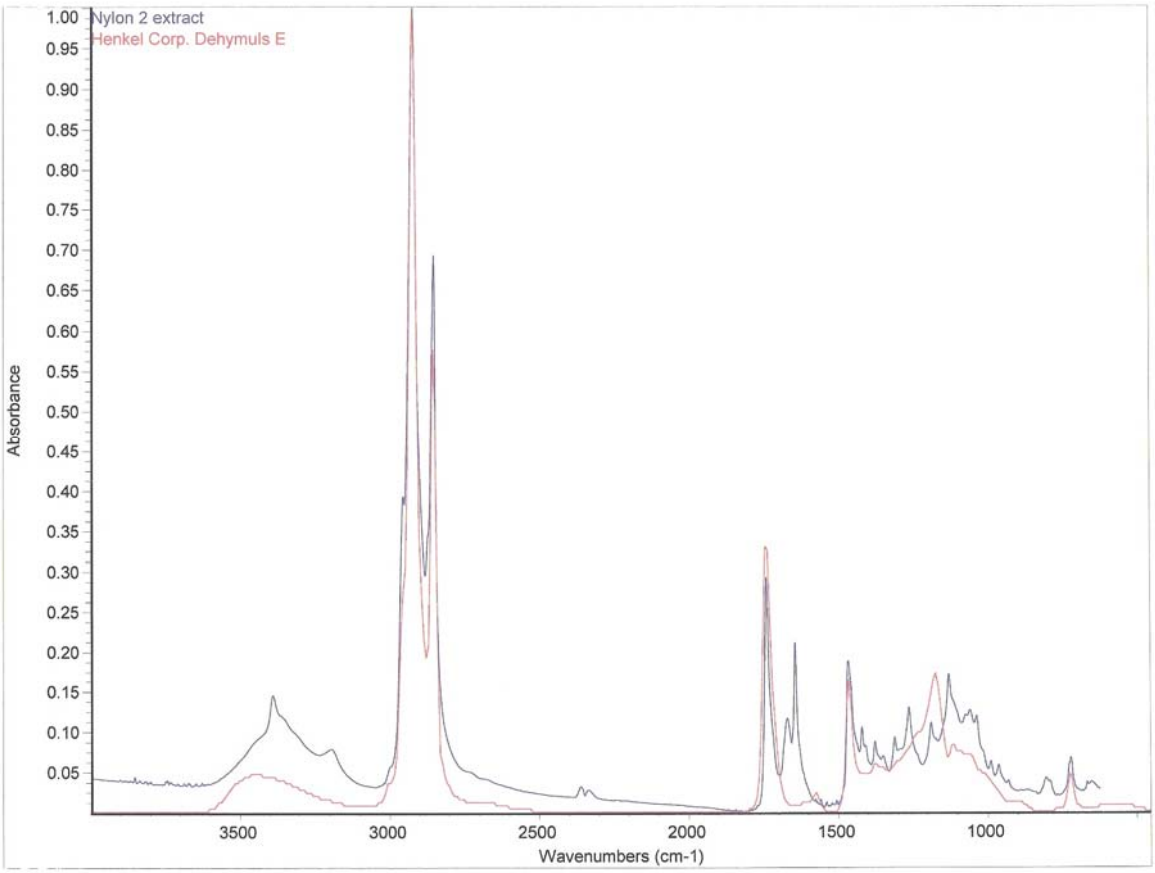

Henkel Corp. Dehymuls E is 94.76% matched to the yarn extract.

APPENDIX G-6: Analytical Result on Extract of Polypropylene Monofilament Yarn

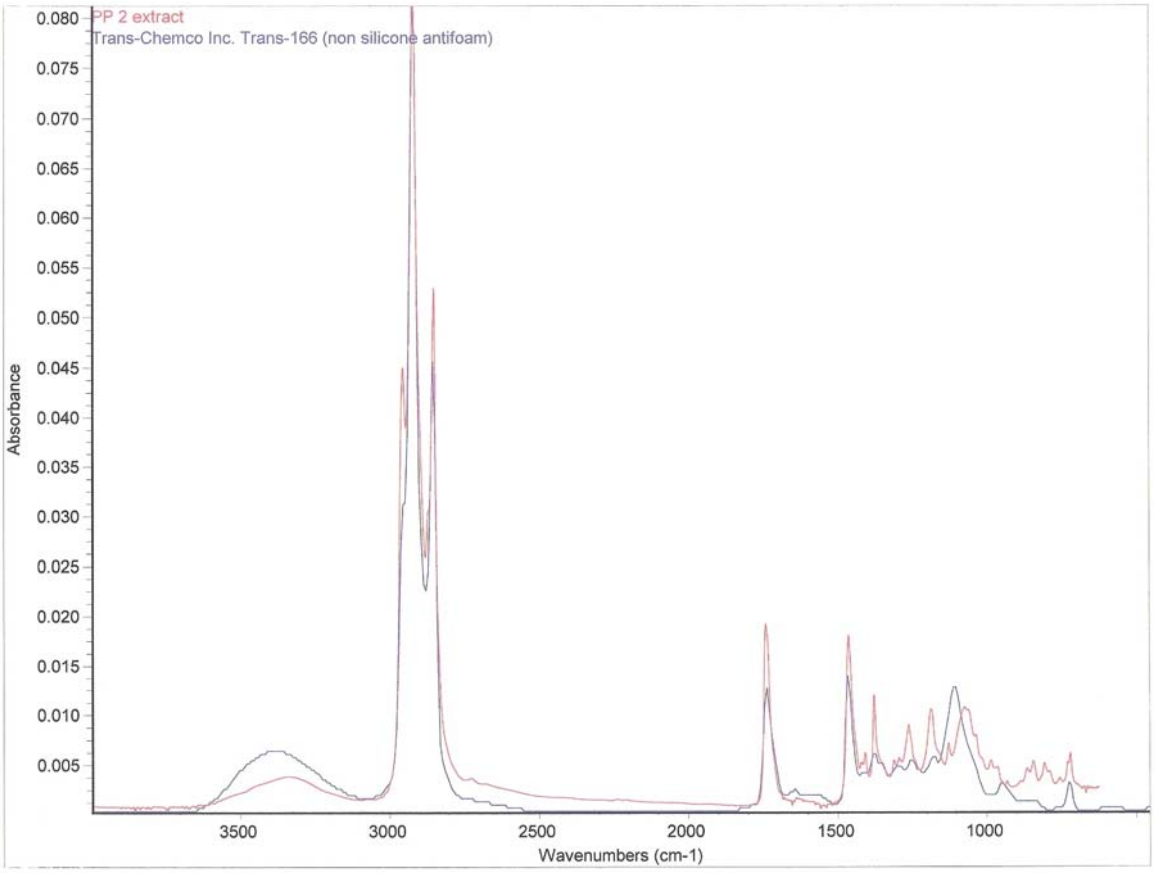

Trans-Chemco Inc. Tans-166 is 95.01% matched to the yarn extract.